AD-A127 663 INTEGRALLY CAST LOW-COST COMPRESSOR(U) AVCO LYCOMING 1/2
DIV STRATFORD CT B H HESSLER ET AL. 03 JAN 83
TACOM-TR-1273 DAAK30-78-C-0039

UNCLASSIFIED F/G 11/6 NL

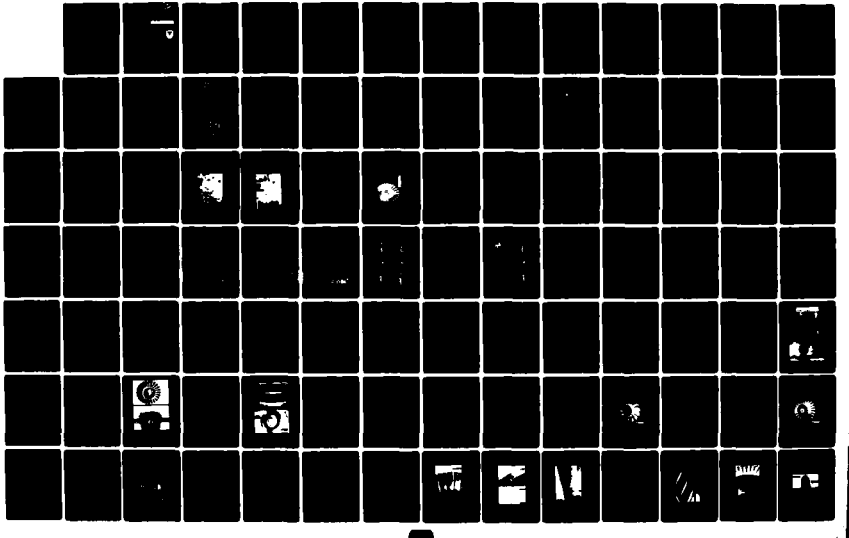

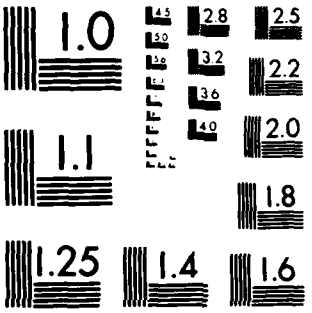

12

R and D CENTER LABORATORY

TECHNICAL REPORT

NO. 12673

INTEGRALLY CAST LOW-COST COMPRESSOR

Department of Army Project Number T785097

MARCH 1983

by M.S. Muntner
B.H. Hessler
AVCO LYCOMING DIVISION

Approved for public release, distribution unlimited.

U.S. ARMY TANK-AUTOMOTIVE COMMAND
RESEARCH AND DEVELOPMENT CENTER
Warren, Michigan 48090

NOTICES

The findings in this report are not to be construed as an official Department of the Army position.

Mention of any trade names or manufacturers in this report shall not be construed as advertising nor as an official indorsement or approval of such products or companies by the U.S. Government.

Destroy this report when it is no longer needed. Do not return to the originator.

UNCLASSIFIED

SECURITY CLASSIFICATION OF THIS PAGE (When Data Entered)

REPORT DOCUMENTATION PAGE		READ INSTRUCTIONS BEFORE COMPLETING FORM
1. REPORT NUMBER 1973	2. GOVT ACCESSION NO. AD-A127663	3. RECIPIENT'S CATALOG NUMBER
4. TITLE (and Subtitle) Integrally Cast Low Cost Compressor		5. TYPE OF REPORT & PERIOD COVERED Final Technical Report 26 May 78 – 25 Mar 82
		6. PERFORMING ORG. REPORT NUMBER
7. AUTHOR(s) Barton H. Hessler – AVCO Michael S. Muntner – AVCO Don Cargo – TACOM Dr. B. Roopchand – TACOM		8. CONTRACT OR GRANT NUMBER(s) DAAK30-78-C-0039
9. PERFORMING ORGANIZATION NAME AND ADDRESS AVCO Lycoming Division 550 South Main Street Stratford, CT 06497		10. PROGRAM ELEMENT, PROJECT, TASK AREA & WORK UNIT NUMBERS MM&T Project No. T785097
11. CONTROLLING OFFICE NAME AND ADDRESS US Army Tank – Automotive Command ATTN: DRSTA-RCKM Warren, MI 48090		12. REPORT DATE 3 Jan 83
		13. NUMBER OF PAGES
14. MONITORING AGENCY NAME & ADDRESS(if different from Controlling Office)		15. SECURITY CLASS. (of this report) Unclassified
		15a. DECLASSIFICATION/DOWNGRADING SCHEDULE

16. DISTRIBUTION STATEMENT (of this Report)

DISTRIBUTION STATEMENT A
Approved for public release;
Distribution Unlimited

17. DISTRIBUTION STATEMENT (of the abstract entered in Block 20, if different from Report)

18. SUPPLEMENTARY NOTES

19. KEY WORDS (Continue on reverse side if necessary and identify by block number)

Axial Compressor Stages
Investment Castings
Custom 450 Alloy
Integrally Cast Rotors
Hot Isostatically Pressed
Surface Integrity

20. ABSTRACT (Continue on reverse side if necessary and identify by block number)

The low pressure compressor stages of the AGT-1500 engine are designed as separately bladed assemblies requiring extensive precision machining and grinding. Cost savings could be achieved if the compressor stages were integrally cast in order to eliminate many machining operations. The casting of precision parts involving very thin leading and trailing edges was achieved in a multi-phased effort; acceptable product yields were achieved with the first and second stage wheels and not with the fifth stage. A follow-on effort will be required in order to support implementation of program results.

DD FORM 1 JAN 73 1473 EDITION OF 1 NOV 65 IS OBSOLETE

Unclassified

SECURITY CLASSIFICATION OF THIS PAGE (When Data Entered)

ABSTRACT

The low-pressure compressor stages of the AGT-1500 engine are designed as separately bladed assemblies requiring extensive precision machining and grinding. Cost savings could be achieved if the compressor stages were integrally cast in order to eliminate many machining operations. The casting of precision parts involving very thin leading and trailing edges was achieved in a multi-phased effort; acceptable product yields were achieved with the first and second stage wheels and not with the fifth stage. A follow-on effort will be required in order to support implementation of program results.

FOREWORD

This final Technical Report covering work performed for MM & T Project No. T785097 under Contract DAAK30-78- C-0039 from May 26, 1978 through March 25, 1982 is submitted in compliance with Exhibit A, Item A003 of the contract.

Subject contract with Avco Lycoming Division, Stratford, Connecticut was sponsored by the U.S. Army Tank-Automotive Command, Warren, MI, 48090. Messrs. D. Cargo and Dr. B. Roopchand were the program managers.

The program was conducted by the Materials and Processing Technology Laboratories under the technical direction of Messers. M.S. Muntner (Principal Engineer) and B. Hessler (Program Manager).

Subcontract efforts were conducted by HOWMET Turbine Components Corp., Austenal Div., La Porte, IN., who produced the first and the fifth-stage integral castings, and by Aerocast, Inc., Miami, FL, who produced the second-stage integral castings.

TABLE OF CONTENTS

LIST OF ILLUSTRATIONS

LIST OF TABLES

1.0 INTRODUCTION

The axial compressor stages of the AGT 1500 engine are designed as separately bladed assemblies requiring electrochemically machined airfoils with precision ground roots and related precision broached slots in the disks. Figure 1 shows the location of the first, second, and fifth-stages within the AGT 1500 engine. Cost savings can be achieved in the AGT 1500 engine by integrally casting axial compressor stages, thereby eliminating many costly machining operations. However, a manufacturing technology program was required to develop the special casting parameters necessary to produce airfoils with very thin leading and trailing edges and to develop post-casting thermomechanical treatments to maximize the mechanical properties (particularly fatigue strength of the cast alloy). Since casting of the first stage required elimination of a mid-span shroud, a design effort leading to the program scope defined below was required.

This program was conceived as three phases of effort:

1. Phase I
   - A. Preliminary Redesign of the Low-Pressure Compressor Incorporating Cast First- and Second-Stage Rotors
   - B. Performance Analyses of Cast First- and Second-Stage Rotors
   - C. Tooling Construction for Fifth-Stage Rotor Castings
2. Phase II
   - A. Tooling Construction for First- and Second-Stage Rotor Castings
   - B. Casting Process Parameter Development
   - C. Production of "Engine Runable" Castings
3. Phase III
   - A. Final Design of Related Compressor Components
   - B. Component Testing
   - C. Engine Testing

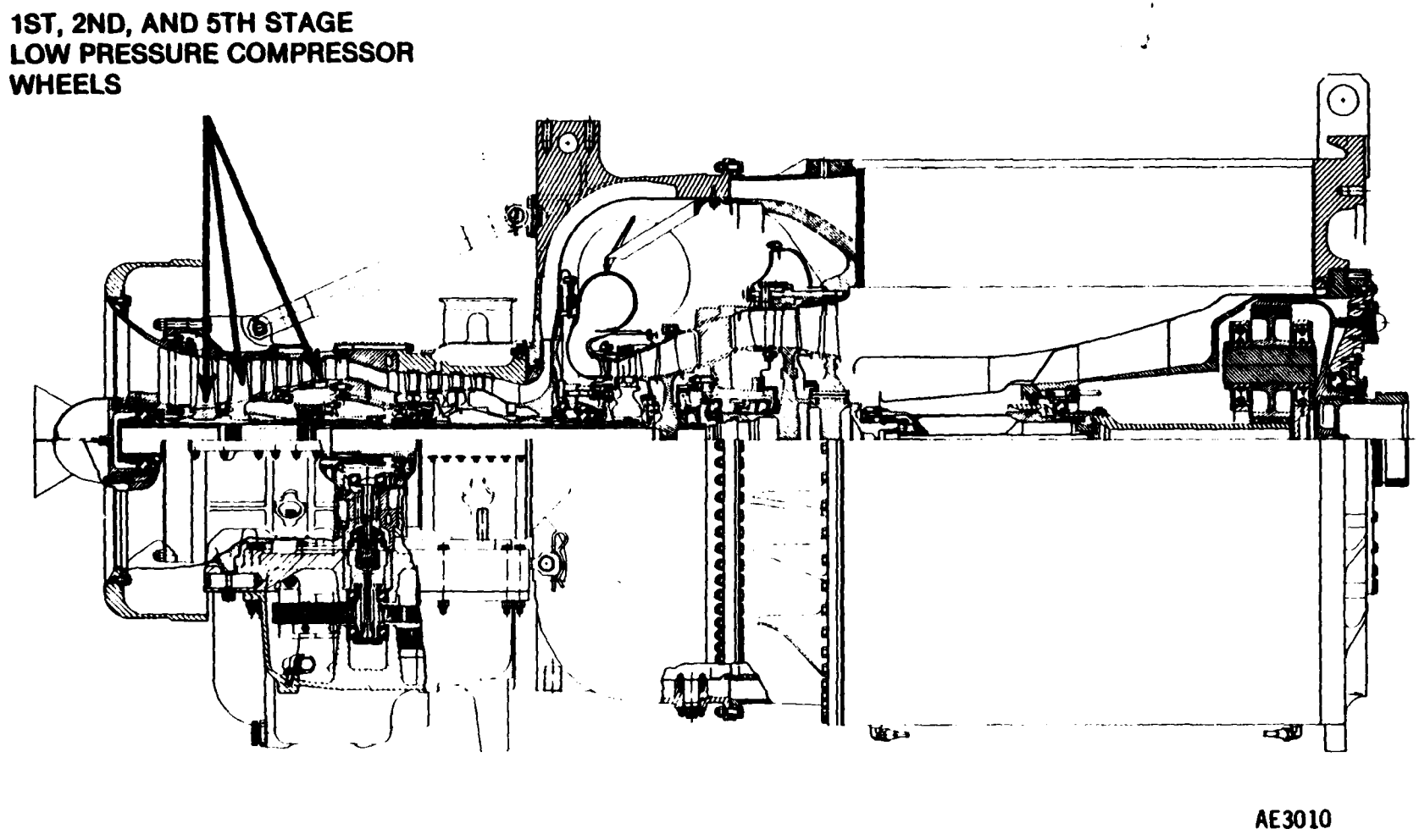

Figure 1. AGT 1500 Engine Schematic

2.0 SUMMARY AND CONCLUSIONS

2.1 PHASE I DESIGN AND PERFORMANCE STUDIES

In order to cast the first-stage rotor, the design had to be modified to accomplish elimination of the mid-span shroud. Aerodynamic effects from this change also influenced the second stage. A preliminary design was developed for the low-pressure compressor which incorporated the first- and second-stages as castings. A detailed design and performance analysis of the first- and the second-stage rotors as investment castings was also conducted. Aerodynamic analysis optimized final airfoil geometry. Stress and vibration analyses determined that the operating stresses of the first- and the second-stage rotors should be well below the mechanical property capabilities of the selected alloy, Custom 450.

The current "Bill of Material", separately bladed fifth-stage low-pressure rotor assembly, was redrawn as an integral casting. Although this stage did not require a redesigned airfoil, analytical studies were conducted to confirm that the Custom 450 properties exceeded fifth-stage rotor operating requirements.

2.2 PHASES I AND II TOOLING CONSTRUCTION

Howmet Turbine Components Corp., Austenal Div., La Porte, Ind., was selected as the casting source for both the first- and the fifth-stage rotors. Aerocast, Inc., Miami, Fla., was selected to produce the second-stage rotors.

Investment casting tooling to produce the three rotor stages was constructed. The tooling for the fifth-stage rotors was completed within Phase I of the program, while the first- and second-stage tools were built during Phase II of the contract.

Dimensional layouts of the product from the first-, second-, and fifth-stage investment casting tooling confirmed that the tools could produce integral components to blueprint requirements. Subsequent to the layouts, fifth-stage casting process changes (required to improve the yield of acceptable castings) affected rotor dimensions. Tool rework will be required prior to the casting of "Engine Runable" fifth-stage rotors in any follow-on qualification program.

Special gaging fixtures for the second- and fifth-stage rotors were designed and fabricated for the dimensional inspection and in-situ correction of rotor airfoils.

2.3 PHASE II CASTING PARAMETER DEVELOPMENT

Casting parameter studies were conducted and casting processes for all three stages were defined to produce the thin-bladed integral rotors. These processes were subsequently used to produce rotors for the mechanical properties evaluation portion of the program.

First- and second-stage casting processes were able to achieve product yields of approximately 75 percent, based on conventional NDT acceptance criteria. However, subsurfce defects found on second-stage airfoils late in the program will require further refinement of melting and/or heat-treating practice. The process initially developed for fifth-stage rotor production exhibited a product yield of only approximately 10 percent. This initial process was used to cast fifth-stage rotors for mechanical testing while fifth-stage rotor casting development continued.

Towards the end of the program, a modified process was developed that increased the product yield of the fifth-stage to approximately 50 percent. This yield estimate is based on a small sample of 10 pieces, and additional castings will have to be conducted to determine if in fact, a viable production process is achievable.

2.4 PHASE II MECHANICAL PROPERTIES EVALUATION

Initial mechanical property testing indicated that rotors hot isostatically pressed (HIP'd) at 2165°F (1185°C) had slightly better fatigue properties than rotors HIP'd at 2050°F (1121°C). The 2165°F temperature was, therefore, selected to produce the remaining rotors required for the program testing and evaluation
efforts.

Mechanical property testing was completed. All of the tested Custom 450 rotors exhibited acceptable low cycle fatigue (LCF) and tensile properties after HIP and heat treatment, except those cast from one particular heat; these rotors had low tensile ductility and poor LCF life (this heat had a higher than normal columbium content). High-cycle fatigue (HCF) testing of airfoils showed the second-stage to have lower fatigue life than the fifth-stage. The lower life was caused by subsurface defects and metallurgical anomalies which might be related to alloy chemistry, melting practice, or heat treatment.

2.5 PHASE II PRODUCTION OF "ENGINE RUNABLE" CASTINGS

Tooling and casting processes were adequately developed to produce dimensionally acceptble first- and second-stage rotors. "Engine Runable" castings were produced for the first-stage. Second-stage castings were also produced, but metallurgical anomalies found late in the program caused concern regarding the fatigue capability of these wheels in an engine environment.

Some of the fifth-stage castings produced exhibited acceptable quality levels. However, the process modifications necessary to improve fifth-stage product yields resulted in castings that now deviate from blueprint dimensions. Therefore, the investment casting tooling will have to be corrected prior to producing "Engine Runable" hardware.

2.6 PHASE III FUTURE EFFORTS

Based upon the satisfactory results of Phases I and II, a follow-on effort should be funded. This effort was originally conceived as a third phase to the current contract. However, current concepts are to include the three cast low-pressure compressor rotors within the planned TACOM Support Cost Reduction Program (SCORE), improved compressor program. This program should include as part of its objectives:

1. Eliminating second-stage rotor defects
2. Producing dimensionally acceptable fifth-stage rotor castings
3. Completing the redesign of the low-pressure compressor section to accept first- and second-stage integrally cast rotors
4. Performing component test of the first- and second-stages
5. Conducting engine performance tests of all three stages.

3.0 APPROACH

3.1 PHASE I DESIGN AND PERFORMANCE STUDIES

3.1.1 Initial Design

As previously mentioned, to incorporte integrally cast compressor rotors, a manufacturing technology program was required to develop the special casting parameters necessary to produce airfoils with very thin leading (LE) and trailing (TE) edges (0.001-0.003 in. or 0.025-0.0076 mm) and the post-casting thermomechanical treatments to maximize the mechanical properties (particularly fatigue strength) of the cast alloy.

At the initiation of the program, a cost estimate was made of the savings to be realized from the use of integrally cast wheels in the low-pressure compressor. This estimate is shown in Table 1. The high savings shown for the first two stages is attributable in a large part to the fact that the wrought version of the first-stage blade has a mid-span shroud. This is a major cost driver of the first blade adding close to $100 to the cost of the blade (in comparison with a similar blade without a shroud). A requirement for the redesigned integral wheel was the elimination of the mid-span shroud. This shroud was considered to be extremely difficult to cast and would have an adverse effect on cost and productivity. The aerodynamic aspects of replacing the current wrought configuration with a wide-chord, cast airfoil influenced the second-stage stator and blade, the preceding variable inlet guide vanes, and the bearing arrangement.

Accordingly, a low-pressure compressor preliminary design was conceived with a wide-chord, unshrouded first stage, and the second-stage rotor was configured as an integral casting with the airfoil aerodynamically compatible with the first stage. Simultaneously, the first- and second-stage rotor changes allowed the elimination of the variable inlet guide vanes (the cost savings from this change are substantial, but are not included in the Table 1 estimate). This program covered the detailed design of the first- and second-stage rotors, but not the detailed design of the related components. The conceptual redesign of the low-pressure compressor is shown in Figure 2.

Initially, the high-pressure compressor impeller had been selected as the third casting for development under this program. This component offered a configuration which would not require extensive redesign to allow its early development within Phase I of the program. However, since the impeller had been identified as a candidate for a separate high-pressure compressor improvement program, and because the impeller was not thought to represent a high degree of casting difficulty, the fifth-stage low-pressure rotor was substituted for the impeller as part of this program.

TABLE 1. ESTIMATE OF THE RELATIVE CASTABILITY FOR EACH OF THE LOW-PRESSURE (LP) COMPRESSOR STAGES AND THE ESTIMATED SAVINGS AS INTEGRALLY CAST ROTORS

LP Stage	Estimated Savings ($)	Casting Risk
1 & 2*	1700	Low
3	150	Very High
4	200	Very High
5	250	High

*The first and second stages had to be redesigned as a matching set for aerodynamic compatibility (estimated savings does not include elimination of inlet guide vane assembly).

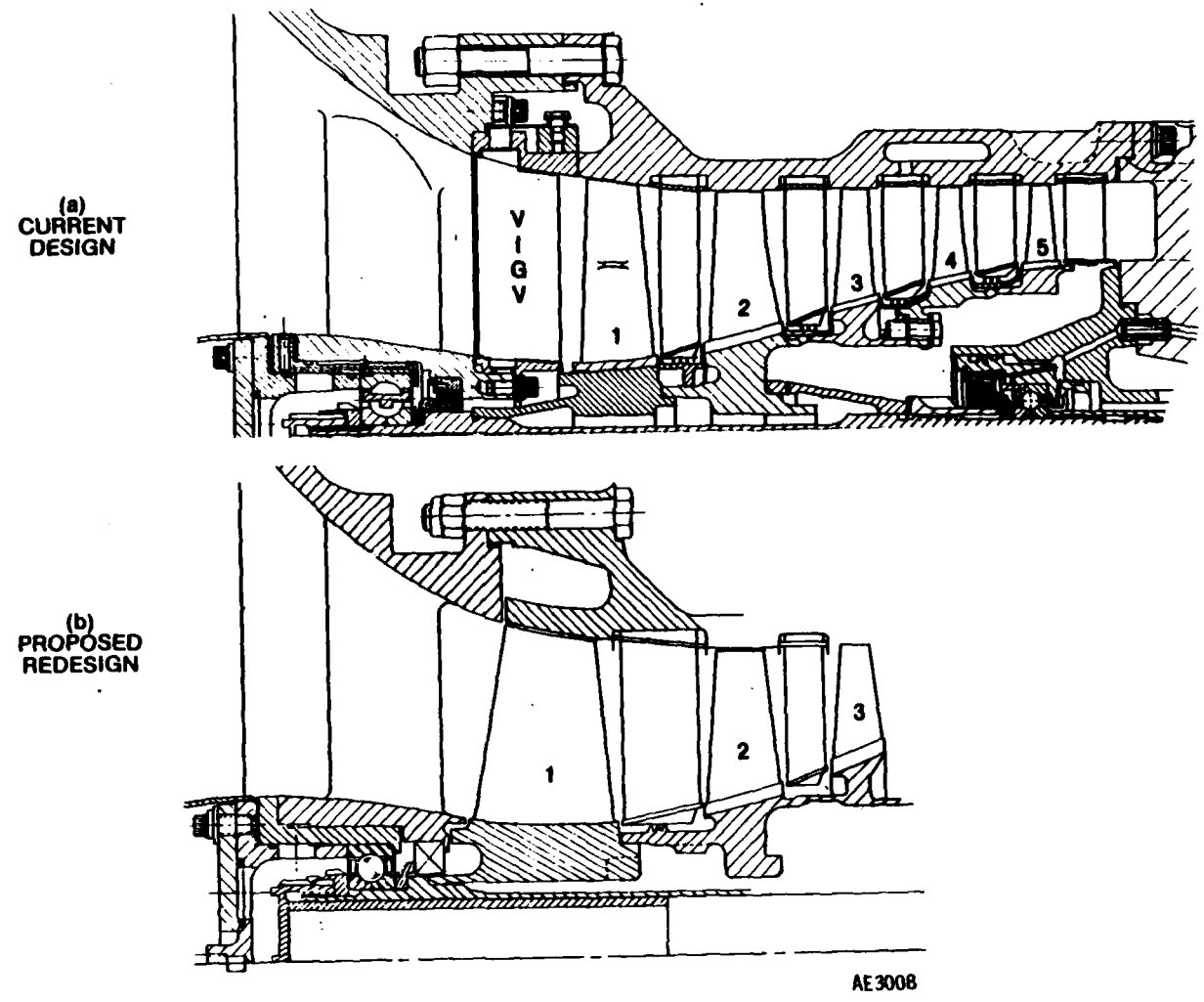

Figure 2. AGT 1500 Low Pressure Compressor Section Redesign

Of the three stages finally selected, the fifth-stage rotor was the most technically challenging because its extremely thin airfoils (0.021-0.33 in. or 0.553-0.838 mm range of maximum thickness) would be difficult to cast. The third- and the fourth-stage low-pressure compressor rotors had also been considered as candidates for the effort; but, since these stages had airfoils with length-to-width ratios greater than those of the fifth-stage rotor, they would have been even more difficult to cast than the fifth stage. A decision to attempt third- and fourth-stage integrally cast rotors was, therefore, postponed pending experience with fifth-stage casting development. Table 1 compares the early estimates of the relative risks associated with the casting of the various low-pressure compressor stages versus their estimated cost savings.

Selection of Custom 450 as the casting alloy was based upon the results of past Lycoming evaluation efforts. For the past several years, Lycoming had been involved in the evaluation of cast compressor alloys. These studies were conducted primarily with IRAD sponsorship and investigated the mechanical properties and stress corrosion cracking resistance of iron and nickel-based compressor alloys. Also evaluated was the effect of hot isostatic pressing (HIP) of castings to improve mechanical properties. These studies had shown that Custom 450 alloy (a precipitation hardening martensitic stainless steel) had properties which approach those of the forged materials currently used in the low-pressure compressor assemblies (AM350 for blades and AM355 for discs). Figures 3 through 6 summarize cast Custom 450 properties compared with wrought AM350 and 355 and cast 17-4PH (a common compressor casting alloy).

3.1.2 Performance Analyses

Aerodynamic modeling was performed on the first- and second-stage rotor configuration in order to finalize the design of the components. The model considered the elimination of both the variable inlet guide vane and the first-stage mid-span shroud.

Lateral vibration analysis of the low-pressure compressor section was performed using computer program D103. This program employed a lumped mass, transfer matrix technique for obtaining critical speeds. This technique of analysis was used to determine the difference between the dynamic response (at critical speed) of the proposed rotor designs and the current wrought configuration.

Vibratory excitation analysis of the first- and the second-stage rotor airfoils was conducted to insure that dynamic characteristics of the proposed cast rotor airfoils were similar to the current wrought blades. Vibratory excitation diagrams for each of the airfoils could then be plotted with respect to airfoil geometry and the vibratory stresses assigned with the assistance of finite-element analysis. The model used a fine mesh of triangular elements with an aspect ratio of 1:1 and a MSC/NASTRAN program. The results of these analyses could then be used to modify blade geometries (as required) to adjust the blade natural frequencies to bring the associated stresses in line with the expected material properties. Figure 7 is a NASTRAN 2-D plot of the first-stage redesigned airfoil.

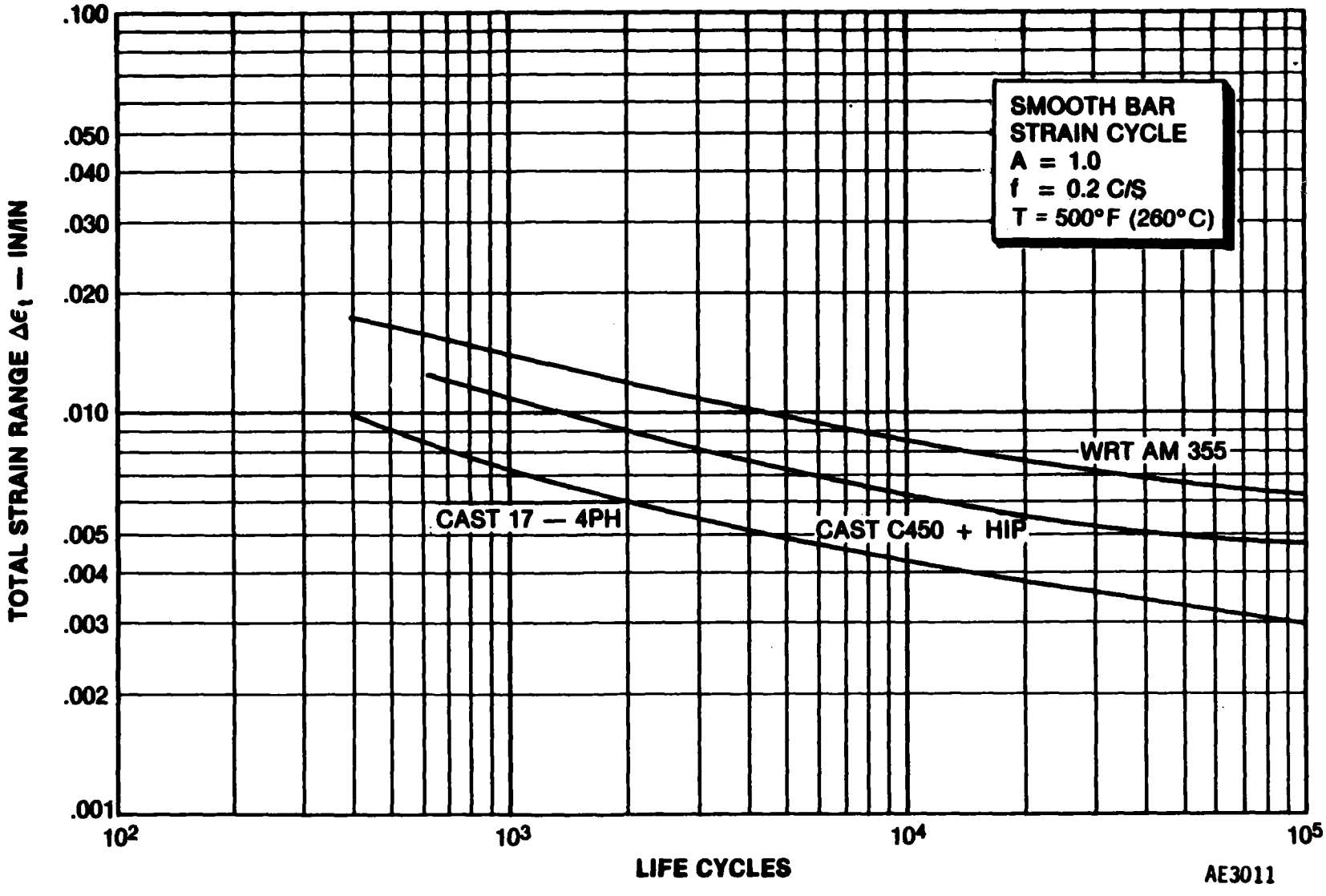

Figure 3. Typical Low-Cycle Fatigue Properties for Common Compressor Alloys

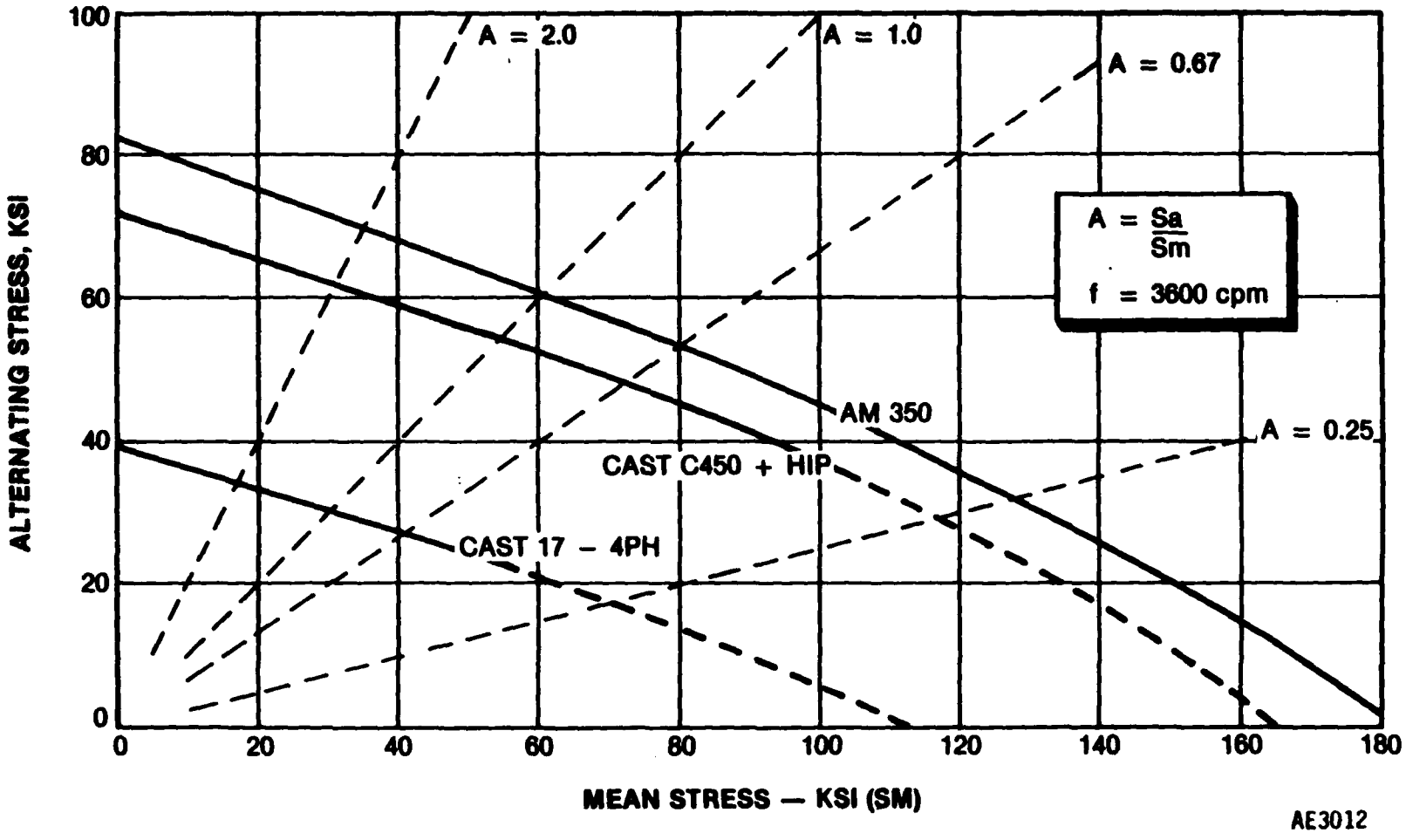

Figure 4. Typical High-Cycle Fatigue Properties for Common Compressor Alloys

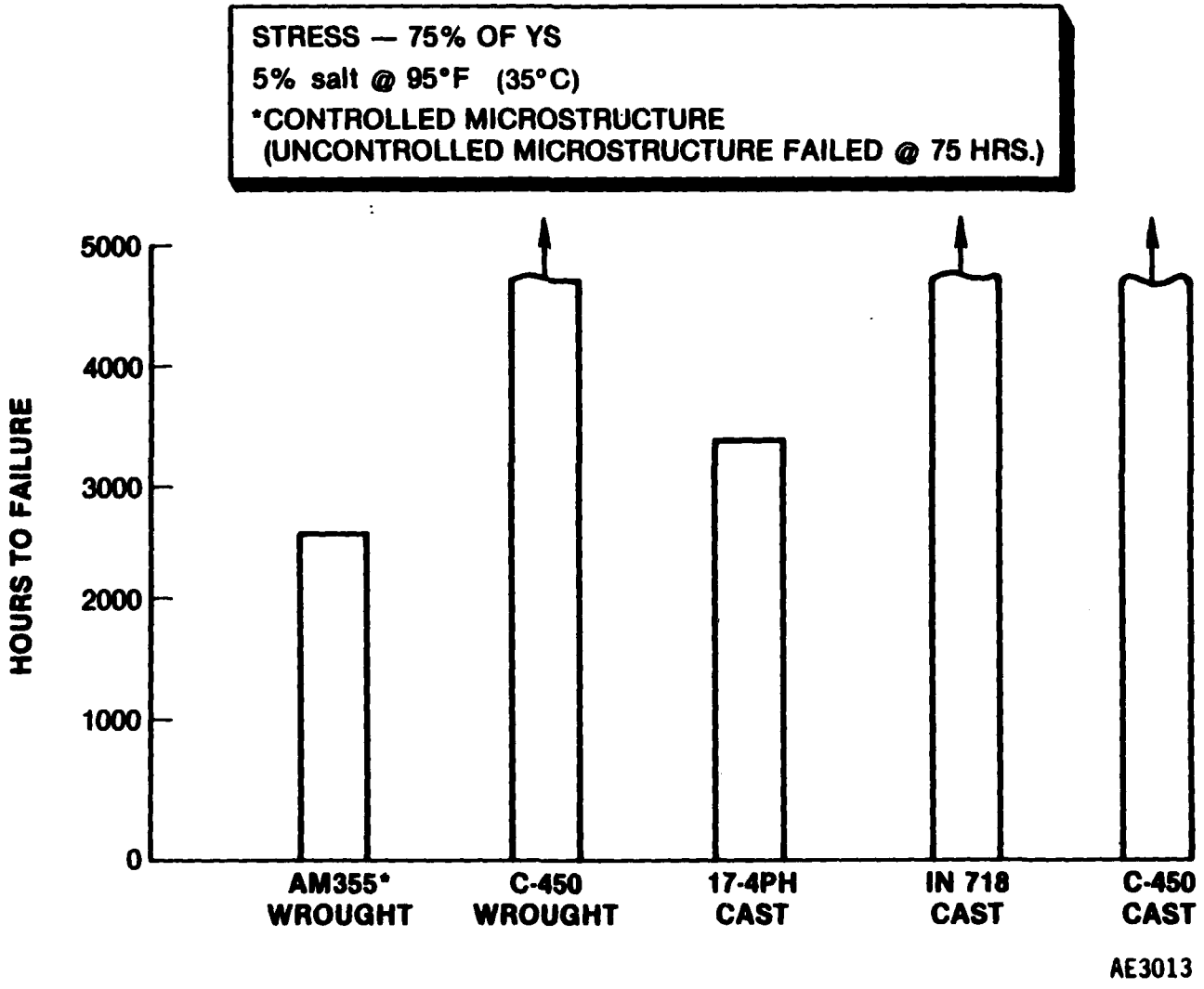

Figure 5. Comparative Stress Corrosion Resistance of Compressor Materials

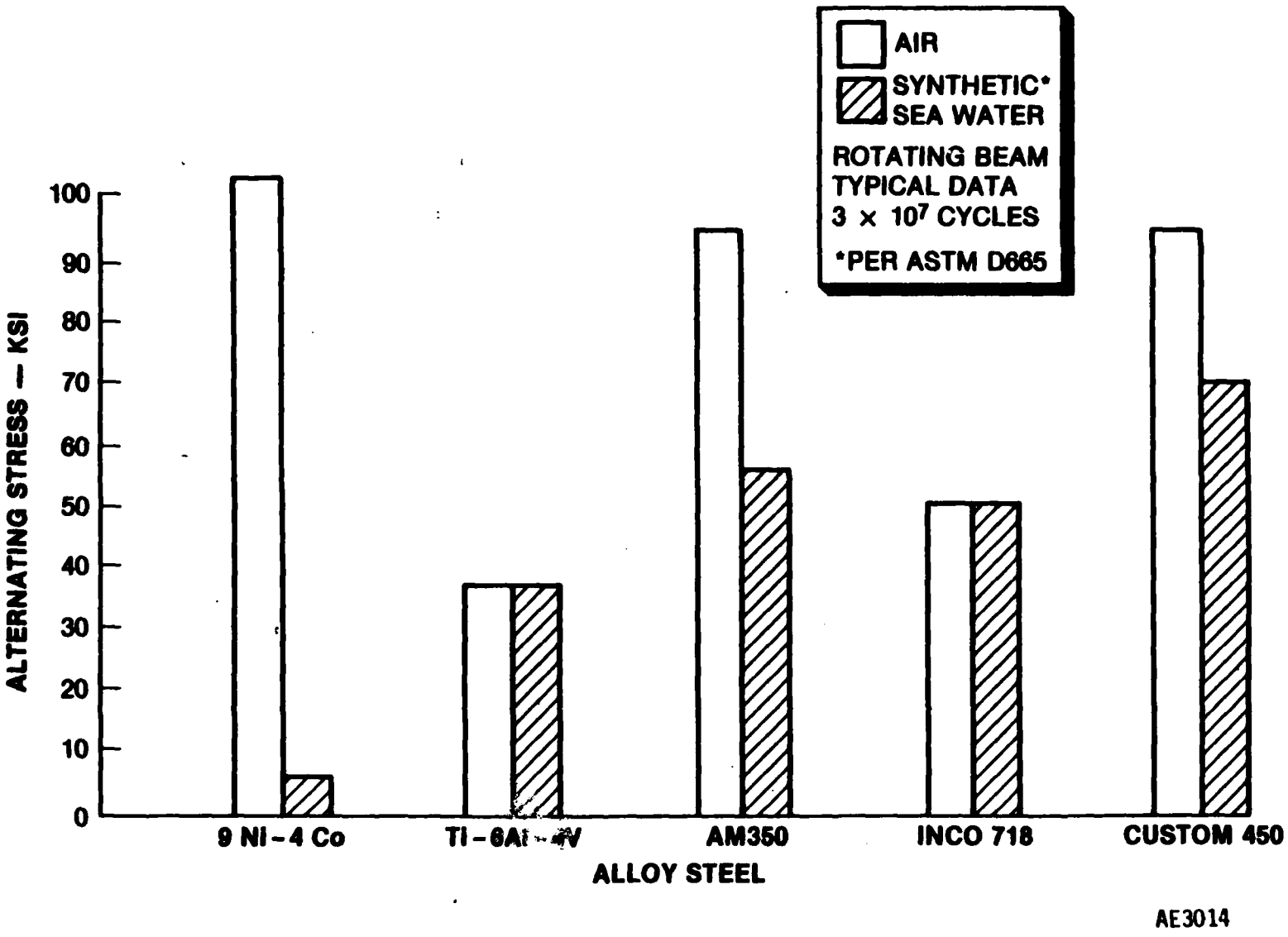

Figure 6. Corrosion Fatigue Behavior of Compressor Alloys

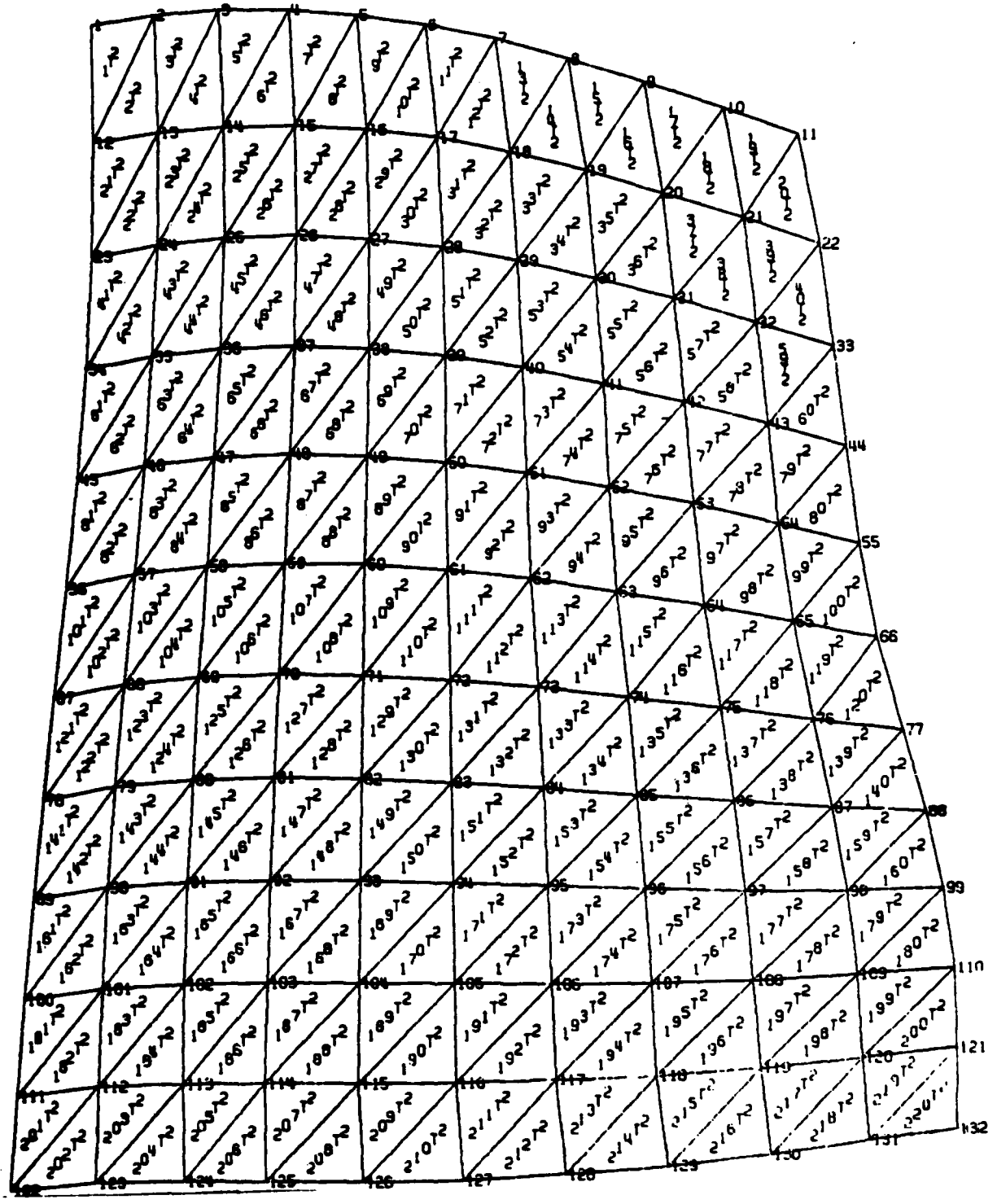

AE3015

Figure 7. Nastran Finite-Element Net Used for First-Stage Airfoil Stress Analyses

In addition, finite-element analyses of maximum operating stresses were conducted to aid designers in equalizing the steady-state stress levels at the concave and convex surfaces of the rotors' airfoils. This approach serves to minimize the bending stresses induced under high centrifugal loads. These stresses are typically introduced by blade twist and axial or tangential lean.

Also, to assure that the fifth-stage low-pressure rotor assembly had an airfoil geometry adequate for direct incorporation as an integrally cast rotor, performance studies (similar to those used for the first and the second stage) were conducted.

3.2 PHASE I AND II TOOLING CONSTRUCTION

As noted previously, the inclusion of the fifth-stage low-pressure rotor in the program enabled the Phase I initiation of investment casting tool construction. The first- and second-stage rotor tooling was fabricated during the Phase II portion of the contract. First article layouts (L/O) were performed using the cast product of each of the tools. This was necessary to determine whether the tooling was capable of producing integrally cast rotors to blueprint dimensions. Based on the results of these layouts, the tools could then be reworked as required. Implicit in this procedure of casting/tooling dimensional control was the fact that a fixed casting process had to be established prior to the final L/O and tooling corrections.

The investment casting tooling for all stages was constructed using separate plastic airfoil injection dies, wax hub injection dies, and assembly fixtures. Plastic was selected as the preferred airfoil pattern material because compared with the wax, plastic patterns were capable of holding closer dimensional tolerances in thin airfoil designs. The use of plastic minimizes the classic problems of wax breakage and geometric instabilities. The addition of plastic to a wax pattern, however, can aggravate the stresses which develop between pattern and mold during mold fabrication and dewaxing. In spite of this disadvantage, the requirement for dimensional control was deemed of paramount importance.

Special gaging fixtures were designed and constructed for the second- and fifth-stage rotors' dimensional inspection, and in-situ dimensional adjustment of airfoils. These fixtures allow inspection of the rotor airfoils for position (i.e., the blade-to-blade spacing), contour, tangent angle, tangenital lean, and axial lean. The fifth-stage gage is shown in Figures 8 and 9. Each fixture was designed with a pneumatic chuck to secure a rotor in a "timed" sequence. Since each consecutive airfoil was indexed, guillotine slides were used to check airfoil contour and position. When a deviation was found, the airfoils were carefully "tweaked" (while still locked in the gage) in order to correct the observed dimensional discrepancy.

The first-stage airfoils were too rigid to allow easy, in-situ corrections, and, therefore, a special gaging fixture was not built for this stage.

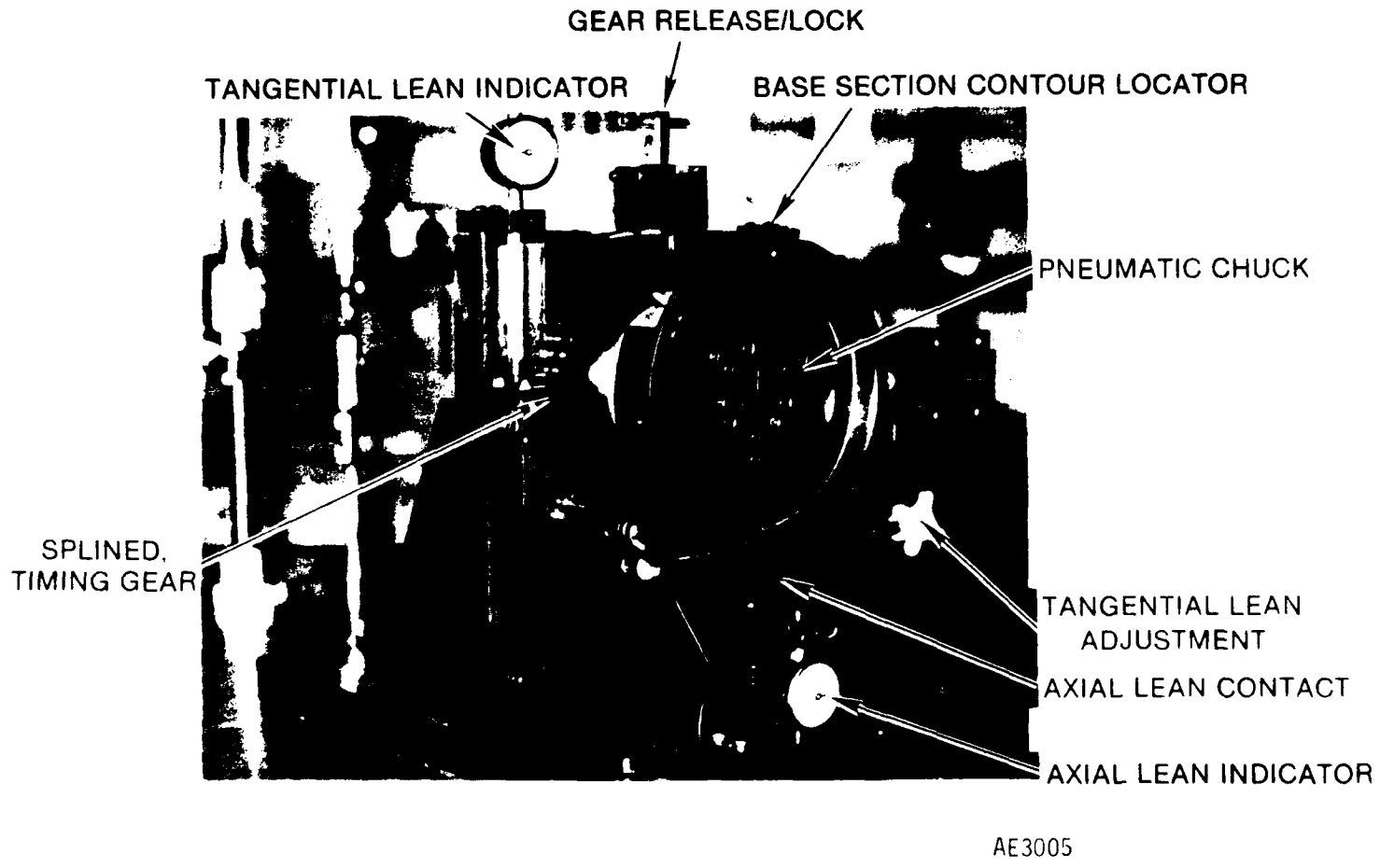

Figure 8. Left View of Special Airfoil Gaging Fixture

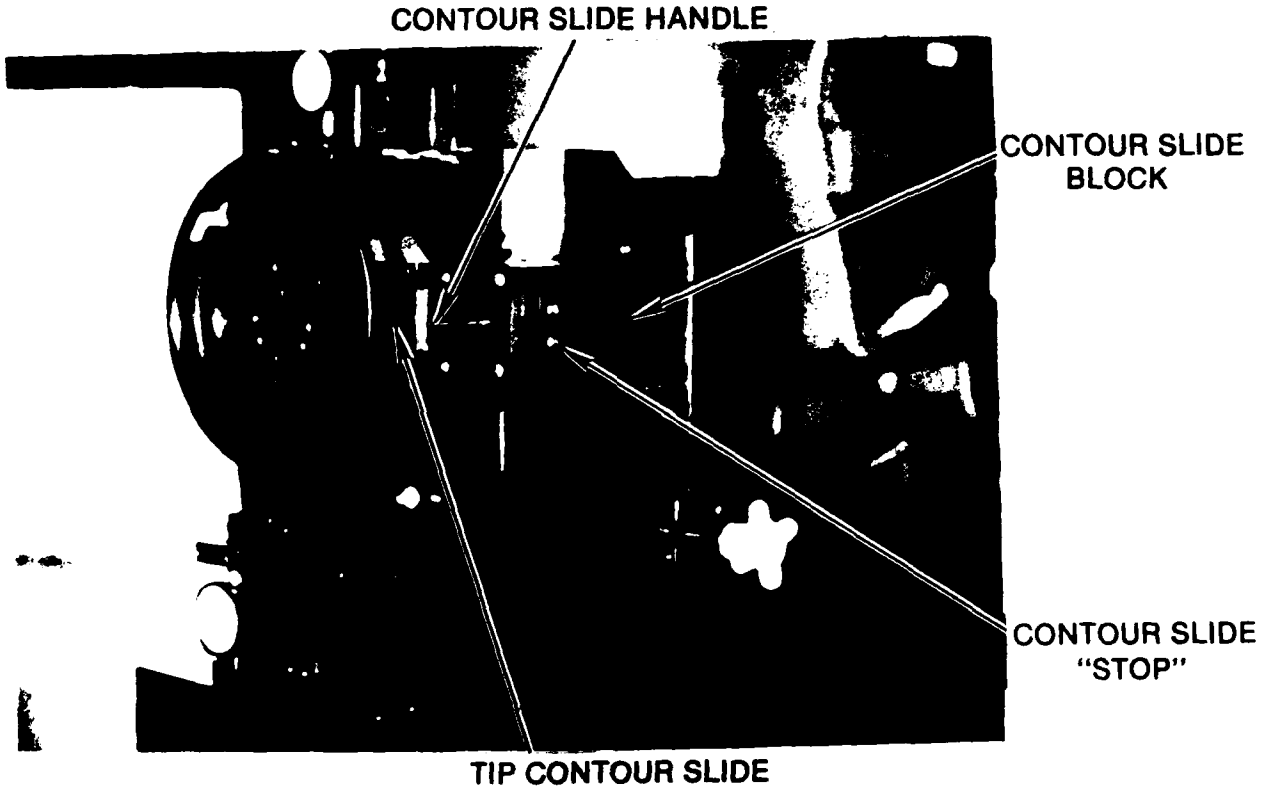

Figure 9. Right View of Special Airfoil Gaging Fixture

3.3 PHASE II CASTING PARAMETER DEVELOPMENT

Although previously developed Custom 450 mechanical property data showed much promise, Lycoming had had only limited Custom 450 casting experience. This experience consisted of one compressor impeller and one axial rotor in the LT101 engine series. Neither of these applications, however, required the casting of ultra-thin leading and trailing edges (the LT101 compressor rotor shown in Figure 10 has LE and TE radii averaging 0.005 in. or 0.127 mm). The current program was required to better understand how to select and optimize casting parameters with respect to component geometry. Also, relatively little data were available regarding the influence of Custom 450 casting parameter variations on the microstructure, mechanical properties, and product yield of Custom 450 castings.

In order to fill this experience gap, first-, second-, and fifth-stage casting parameter studies were conducted. The specific objective of this study was to develop viable casting processes to produce the three rotor configurations at an acceptable quality and with high product yield.

The casting parameter studies investigated the influences of casting variables such as pattern gating, mold type, insulation wrap, mold preheat temperatures, and metal pouring temperatures on casting defects. The defects of prime concern were: airfoil misruns, mold splits, hot-tear cracking, and surface pitting. Internal shrinkage was not of major concern since all rotors were to be hot isostatically pressed (HIP'd) after casting.

The parametric study, therefore, evaluated the effects of casting variables on the overall quality of the cast product. The evaluation of casting quality was grouped into two general categories for the purpose of this investigation, namely, mold fill and surface integrity.

Mold fill was defined as the ability of the casting process to totally fill the very narrow airfoil mold passages. Failure to fill this cavity is called a misrun and is commonly found at thin airfoil edges and tips. The principal technique used to detect misruns is visual inspection. Experience has shown that mold fill is related to the fluidity of the alloy being poured, the thermal characteristics of the mold, and the mold/metal surface tension and reactions.

Surface integrity was defined as the lack of occurrence of surfce defects such as: hot-tear cracking, mold-split effects, and anomalous surface reactions (especially pitting). Surface integrity of a casting is degraded by variables which favor the thermodynamics and kinetics of undesirable mold/metal reactions; in other words, casting parameters which foster longer times at elevated temperature and the reduction of protective or desirable surface oxides. Visual and penetrant inspection were the principal tools for evaluating surface integrity.

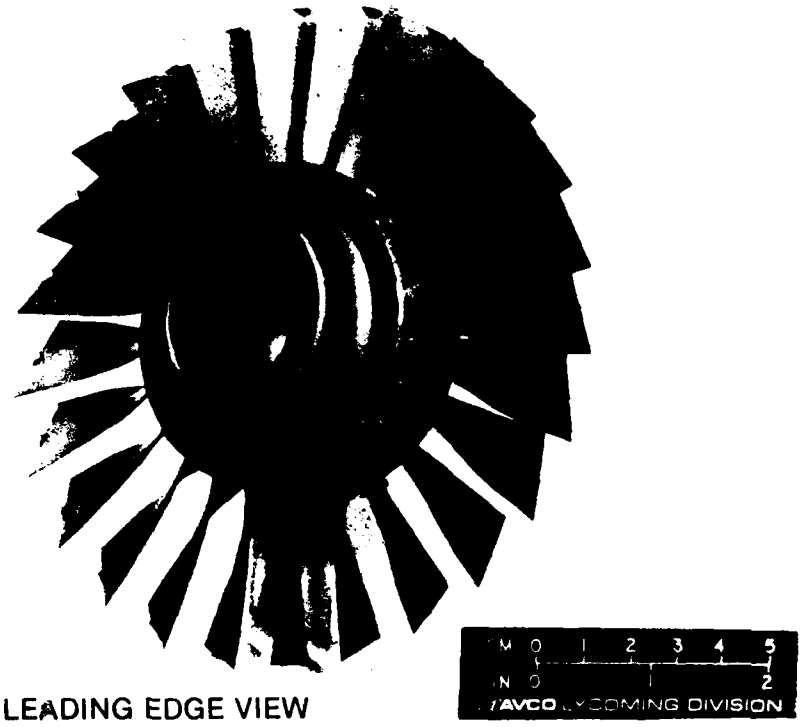

Figure 10. LTS 101 Integrally Cast Axial Compressor Rotor

The basic plan of action in developing casting processes for the three rotors involved: 1) identifying a functional gating system, 2) developing a mold system, and 3) defining the thermal parameters (mold preheat, alloy pouring temperature, and the thickness and location of mold insulation). All melting and pouring was done in vacuum, since the thin airfoil edges could not be filled by conventional air casting.

The technical approach was to establish the gating system early in the casting development effort because changes to the gating system at a later date in the program could markedly affect final casting dimensions (requiring further investment casting tooling rework). Of course, changes to the mold system or the thermal parameters could also affect casting geometry, but experience had shown that these effects were not as dramatic. After the selection of a gating system which seemed to allow reasonably rapid and uniform filling of the investment casting mold with molten alloy, the effort concentrated on defining the mold system and the thermal variables.

Mold composition has been found to be able to influence: a) the solidification and cooling rates of castings (through its thermal mass and heat-transfer characteristics), b) the alloy fluidity (due to mold/metal surface tension and reactions), c) hot-tear cracking (a result of mold strength versus metal strength at high temperatures), and d) the casting surface integrity (mold/metal reactions at elevated temperatures). Mold compositions are considered proprietary by casting vendors. Therefore, the types of mold systems used to produce rotors in this program have been designated in this report as "A", "B", "C", etc.

Investment molds were built-up of several layers of refractory grain and binder. The "facecoats" which were immediately adjacent to the wax pattern (or casting), used refractories of 120 mesh. The "back-up" or "stucco" sands were of 90 mesh. The refractories in this casting parameter effort consisted of combinations of alumina, zircon, and silica.

The initial thermal parameters were based upon prior experience with the casting of other Custom 450 alloy and 17-4PH alloy components. Although higher casting and mold temperatures normally assist alloy fluidity, these same higher temperatures also encourage surface/metal interactions which could impair mold fill and surface integrity. Thus, it was expected that the final (optimum) values of the thermal parameters would represent a compromise between alloy fluidity and mold/metal reactivity.

The processes developed were to be used to supply hardware for the balance of the program. The rotors produced for the Phase II mechanical property evaluation were to be cast from the best available casting process (provided it was at least capable of producing rotors with sufficient metallurgical quality to warrant testing) existing at the time test rotors were required by the contract schedule. Assuming the development of viable production processes, rotors of each stage were to be produced for subsequent engine testing under Phase III.

3.4 PHASE II MECHANICAL PROPERTIES EVALUATION

Based upon the ability to produce rotors of acceptable metallurgical quality, the best process for each rotor was selected to cast samples for the program's mechanical properties evaluation.

The mechanical properties evaluation included hub low-cycle fatigue (LCF), airfoil high-cycle fatigue (HCF), and tensile properties. Six first-, six second-, and eight fifth-stage rotors were cast, HIP'd and heat treated for this effort.

Rotor LCF tests were conducted using test specimens (Figure 11) machined from the hub section of the rotors. All specimens were tested at 500°F and at a strain range of 0.006 inch. A sine wave form with a cyclic frequency of 0.4 Hz and an "A" ratio of 1:1 was employed.

Airfoil HCF testing was performed using the "beehive" method by which the airfoils are excited by a stream of air. Tip deflections are controlled through the regulation of air pressure. Blade tip deflections were related to the stress at the failure locations by strain gaging techniques. All HCF testing was done at room temperature. First-stage airfoil HCF testing could not be performed because of the rigidity of the airfoils.

All tensile tests were conducted using mechanical test specimens (Figure 12) machined from the hub section of the rotors. All testing was done at room temperature.

The results of these tests were used to:

1. Optimize Custom 450 HIP parameters
2. Determine the extent of Custom 450 property variance from heat to heat
3. Assess the effects of rotor configuration on mechanical properties.

The first castings available for testing were the fifth-stage rotors. The tool fabrication of fifth-stage rotors had been initiated in Phase I; this resulted in a three-month lead in casting development and availability (compared with first- and second-stage rotors). The fifth-stage rotors were, therefore, used to optimize HIP parameters for the program.

Lycoming has had previous experience in the HIP processing of Custom 450 castings. Most of the hardware which had been HIP'd before the time of this evaluation had been processed at temperatures between 2165° and 2200°F (1185°C and 1204°C). This study investigated the effects of HIP at 2050°F (1121°C) compared with the standard 2165°F (1185°C) temperature. The advantage of a 2050°F (1121°C) HIP temperature was that it would tend to extend autoclave life and is a temperature commonly used with other alloys and, therefore, would help productivity/economy. The results of the HIP investigation were to be used to specify the optimum HIP parameters for the post-casting processing of the remaining rotors of the mechanical property program (i.e., heat chemistry and configuration effects).

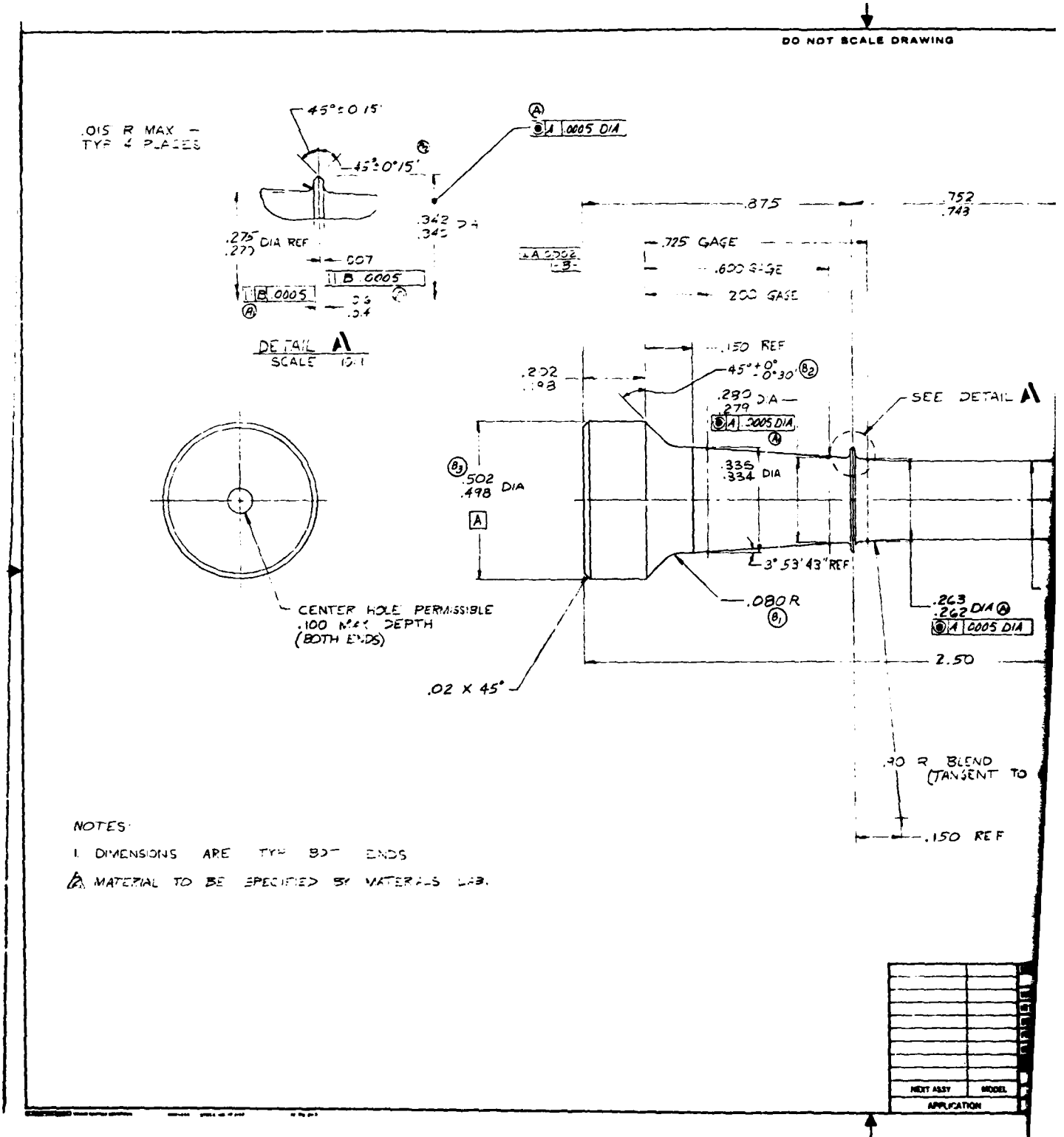

Figure 11. LCF Test Specimen Used for Cast Rotor Mechanical Property Evaluation

DO NOT SCALE DRAWING

REVISIONS

E.O.	ZONE	LTR	DESCRIPTION	DATE	APPROVED
2262		A	1.) ADDED CONCENTRICITY & PARALLEL SYMBOLS 8 PLACES & 2 PLACES RESP 2) ADDED ±0°15'		
72650		B	1) .080 R WAS .08 R 2) ADDED +0° -0°30' 3) .498-.502 WAS .495-.505 4) IN TOL BLOCK CHG .XXX±.010 TO .XXX±.005	5/3/72	

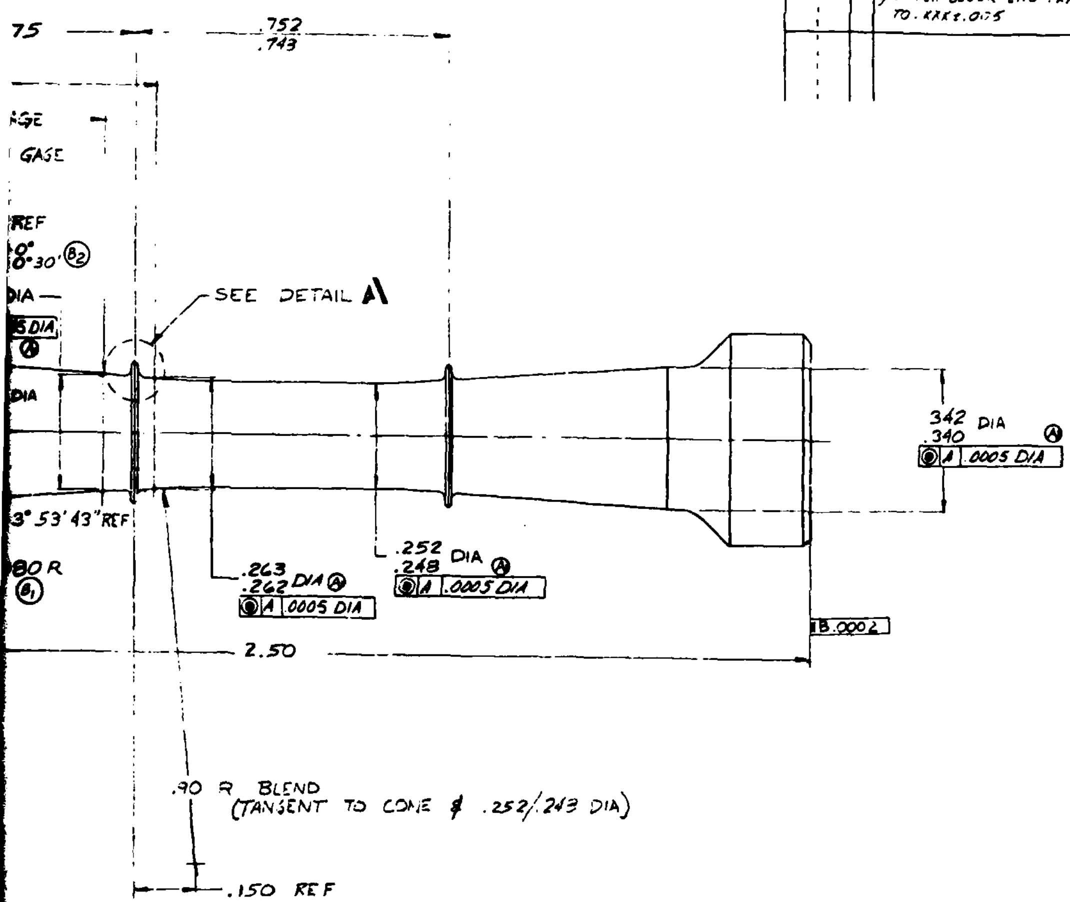

QTY REQD	ITEM NO.	PART OR IDENTIFYING NO.	NOMENCLATURE OR DESCRIPTION	MATERIAL OR NOTE	ZONE
—	1	TE 24322-01	SPECIMEN		

LIST OF MATERIAL

NEXT ASSY	MODEL
APPLICATION	

MATERIAL / HARDNESS: MAT. SPEC; HT TR SPEC; SURF TREAT; PROCESS; INSPECTION; WELDING OR BRAZING

UNLESS OTHERWISE SPECIFIED ALL DIMENSIONS ARE IN INCHES. TOLERANCES .X ± .03 .XX ± .01 .XXX ± .005 ANGLES ± 1°

BREAK SHARP EDGES AND CORNERS .005 TO .015 APPROXIMATE. DIMENSIONS LOCATING TRUE POSITIONS ARE BASIC.

SURFACE ROUGHNESS PER 8/

GEOMETRIC SYMBOLS PER USASI Y14.5. DRAWING INTERPRETATION PER E1000. THREADS PER MIL-STD-9/HANDBOOK H28

LYCOMING DIVISION — STRATFORD, CONNECTICUT

MATERIAL TEST
LOW CYCLE FATIGUE SPECIMEN

SIZE	CODE IDENT NO.	
D	91547	TE 24322

SCALE 4/1 | WT | SHEET 1 OF 1

RELEASED 7.7.71

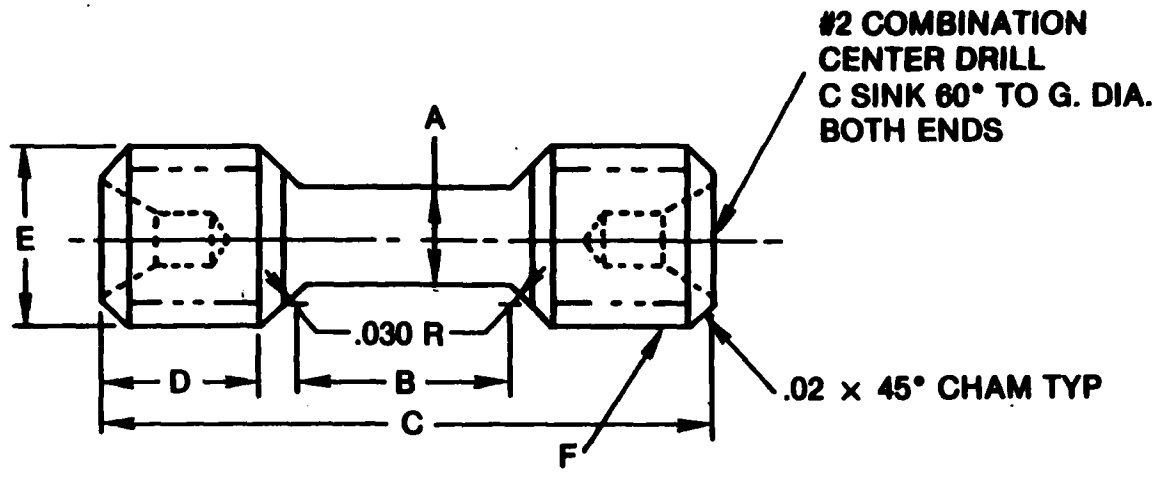

	A	B	C (MIN)	D (MIN)	E	F	G
in.	0.135 ± .001	.750 ± .020	1.25 —	.28 —	.250 $^{+.000}_{-.005}$	.250-20NC-3 —	.10 —
mm	3.429 ‡.025	19.05 ‡.51	31.75	7.11	6.35 $^{+.000}_{-.127}$		2.54

AE3003

Figure 12. Tensile Specimen Utilized for Cast Rotor Mechanical Property Evaluation

The influences of Custom 450 heat chemistry were evaluated using the mechanical property results of multiple heats of second- and fifth-stage rotors. Tests were conducted using second-stage rotors from each of two heats of material and fifth-stage rotors cast from three different Custom 450 heats. As-cast rotor chemistries indicated that one of the heats had a higher than normal columbium content. Second- and fifth-stage test results were evaluated independently of each other to assure that configuration effects did not influence this comparison.

The effects of configuration on Custom 450 rotor mechanical properties were determined using first- and fifth-stage rotors cast from the same heat of material. The first- and the fifth-stage rotors had been selected for the evaluation because they represented the two extremes in low-pressure rotor geometry.

As a minor evaluation (not included in the original scope of the contract), the effect of glass-bead peening on fifth-stage airfoil HCF failure locations was conducted. Airfoil fractures in cast fifth-stage rotors were more randomly located than would have been expected. Prior to HCF testing, two (of six) fifth-stage rotors were glass-bead peened per AMS2430H, using No. 13, 0.0025 inch B glass shot (MIL-G-9954) at an intensity of 2.5N. All airfoils were peened twice (edges were masked to help prevent edge rollover).

3.5 PHASE II PRODUCTION OF "ENGINE RUNABLE" CASTINGS

As discussed previously, the production of "Engine Runable" castings for use within a future follow-on effort was a primary goal of Phase II of the contract. Radiography, visual, and fluorescent penetrant inspection were the principal in- struments used to evaluate the physical soundness of the castings. These in- spection procedures were applied to each individual part. Supplementary metal- lurgical and mechanical testing was used to assure the basic integrity of the casting process.

4.0 RESULTS AND DISCUSSION

4.1 PHASE I DESIGN AND PERFORMANCE STUDIES

To achieve the goal of a lower cost low-pressure compressor through the substitution of integral castings for the current wrought blade and hub assemblies, preliminary design efforts reconfigured the first-stage airfoil as a wide-chord blade and eliminated the mid-span shroud. This mid-span shroud was con- sidered to be extremely difficult to cast and would therefore have an adverse effect on cost and productivity. The aerodynamic aspects of replacing the current wrought configuration with a wide-chord, cast airfoil influenced both the second-stage stator and blade (as well as the preceding variable inlet guide vanes and inlet housing; see Figure 2.) As a result, the low-pressure compressor preliminary design conceived the second-stage rotor as an integral casting which was aerodynamically compatible with the wide-chord first stage. The redesigned first and second stages also allowed the elimination of the variable inlet guide vanes. The absence of this vane assembly will result in significant cost savings over and above the direct substitution of cast rotors for conventionally assembled wheels.

Following the preliminary design, the detailed redesign of the first- (Figure 13) and the second- (Figure 14) stage rotors was conducted based upon the concepts described above. In addition, the low-pressure compressor's fifth-stage rotor assembly was redrawn as an integrally cast rotor (Figure 15). This stage did not require a major redesign study because the integral casting has the same basic geometry of the current, separately bladed wrought assembly.

Performance analyses were conducted that confirmed that the operating stresses of the cast rotors were well within the mechanical property capabilities of cast Custom 450 alloy. The results of these studies were incorporated into the final casting design.

4.1.1 Lateral Vibratory Analysis of the Low-Pressure Compressor

A lateral vibration analysis was made of two alternate front bearing arrangements designated HB-1 and HB-2. As can be seen in Figure 16, the two new front bearing arrangements were designed to be compatible with the first and second stage low-pressure cast compressors. The analysis was used to investigate the effects of front-bearing displacement and rotor redesign on low-pressure compressor dynamic response. The two alternate front-bearing designs investigated were as follows:

1. Design HB-1, with approximately 0.25 in. (6.35 mm) front bearing relocation (forward of its current low-pressure compressor position)

2. Design HB-2, with approximately 1.0 in. (25.4 mm) front bearing relocation (forward of its current low-pressure compressor position).

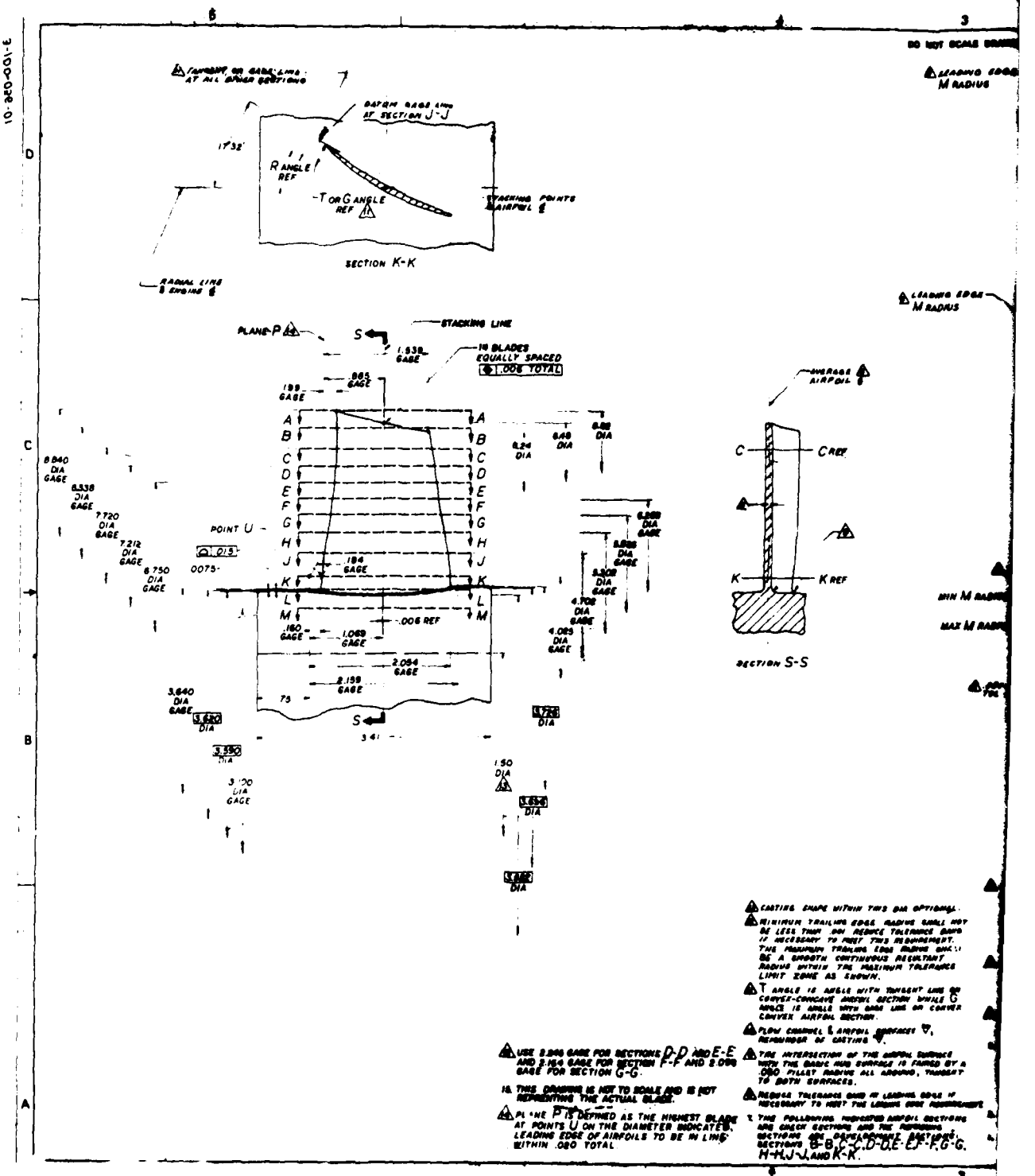

Figure 13. P/N 3-100-056-01, First-Stage Integrally Cast Rotor

PRECEDING PAGE BLANK-NOT FILMED

DO NOT SCALE DRAWING

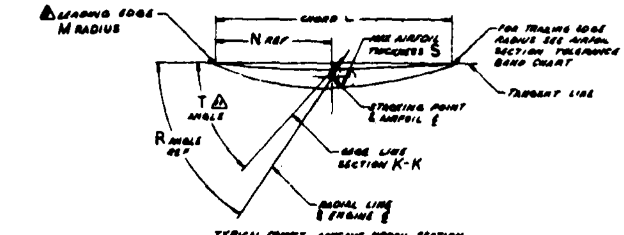

TYPICAL CONVEX-CONCAVE AIRFOIL SECTION
AIRFOIL SECTION A-A, B-B, C-C, J-J, K-K, L-L, AND M-M.
SCALE-NONE

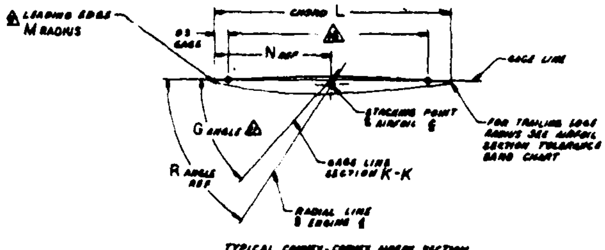

TYPICAL CONVEX-CONVEX AIRFOIL SECTION
AIRFOIL SECTION D-D, E-E, F-F, G-G, AND H-H.
SCALE-NONE

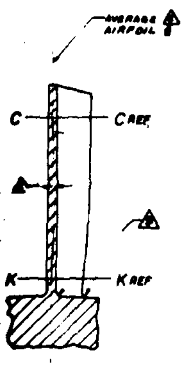

SECTION S-S

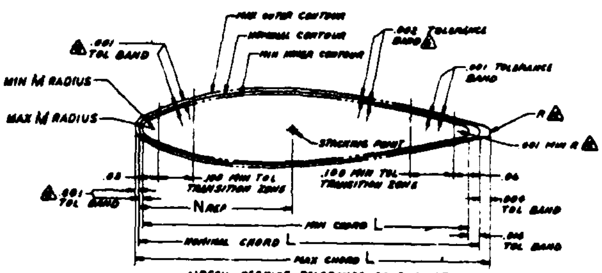

AIRFOIL SECTION TOLERANCE BAND CHART
FOR CONVEX-CONCAVE OR CONVEX-CONVEX AIRFOIL METHOD OF PREPARING MASTER AIRFOIL CHARTS USED IN MANUFACTURING & INSPECTION OF BLADES. TOLERANCE BANDS ARE PARALLEL TO THE NOMINAL CONTOUR EXCEPT FOR TRANSITION ZONES.
SCALE-NONE

SECTION	T 0°30'	G 0°30'	S ±.004	L	N REF	M ±.001	R REF
A-A	41°55'	–	.076	2.492	1.377	.004	59°26'
B-B	39°38'	–	.166	2.469	1.279	.005	57°08'
C-C	37°02'	–	.082	2.440	1.218	.006	54°33'
D-D	–	34°47'	.102	2.392	1.189	.007	52°20'
E-E	–	32°26'	.126	2.337	1.163	.008	50°01'
F-F	–	28°34'	.155	2.283	1.141	.008	47°11'
G-G	–	25°43'	.186	2.220	1.106	.009	43°22'
H-H	–	19°44'	.219	2.161	1.079	.010	37°24'
J-J	11°40'	–	.231	2.073	1.047	.010	29°15'
K-K	0°00'	–	.233	1.966	1.000	.011	17°32'
L-L	-6°04'	–	.231	1.914	.962	.011	9°25'
M-M	-17°01'	–	.224	1.851	.917	.011	-0°33'

⚠ CASTING SHAPE WITHIN THIS DIA OPTIONAL.

⚠ MINIMUM TRAILING EDGE RADIUS SHALL NOT BE LESS THAN .001. REDUCE TOLERANCE BAND IF NECESSARY TO MEET THIS REQUIREMENT. THE MAXIMUM TRAILING EDGE RADIUS SHALL BE A SMOOTH CONTINUOUS RESULTANT RADIUS WITHIN THE MAXIMUM TOLERANCE LIMIT ZONE AS SHOWN.

⚠ T ANGLE IS ANGLE WITH TANGENT LINE ON CONVEX-CONCAVE AIRFOIL SECTION WHILE G ANGLE IS ANGLE WITH GAGE LINE ON CONVEX CONVEX AIRFOIL SECTION.

⚠ FLOW CHANNEL & AIRFOIL SURFACES ▽, REMAINDER OF CASTING ▽.

⚠ THE INTERSECTION OF THE AIRFOIL SURFACE WITH THE BASIC HUB SURFACE IS FAIRED BY A .030 FILLET RADIUS ALL AROUND, TANGENT TO BOTH SURFACES.

⚠ REDUCE TOLERANCE BAND AT LEADING EDGE IF NECESSARY TO MEET THE LEADING EDGE REQUIREMENT.

7. THE FOLLOWING INDICATED AIRFOIL SECTIONS ARE CHECK SECTIONS AND THE REMAINING SECTIONS ARE DEVELOPMENT SECTIONS: SECTIONS B-B, C-C, D-D, E-E, F-F, G-G, H-H, J-J, AND K-K.

⚠ AT EACH AIRFOIL SECTION, CHECKED INDEPENDENTLY NO POINT MAY LIE MORE THAN .002 INSIDE OR .002 OUTSIDE THE NOMINAL AIRFOIL CONTOUR. THE SECTION CONTOUR MAY CHANGE WITHIN THIS TOLERANCE BAND AT A RATE NOT GREATER THAN .002 IN .100 OF LENGTH. THESE REQUIREMENTS ARE EXCLUSIVE OF THE TRASH AT THE ENDS OF THE AIRFOIL SECTIONS.

⚠ PERMISSIBLE BOW IS DEFINED AS A DISPLACEMENT OF ANY AIRFOIL STACKING POINT IN ANY DIRECTION AND IS CALCULATED ON A RATE BASIS OF .006 PER INCH DISTANCE ALONG THE STACKING LINE FROM THE NEAREST SECTION C-C OR K-K.

⚠ THE AVERAGE AIRFOIL ℄ IS DEFINED AS A STRAIGHT LINE PASSING THRU THE STACKING POINT(S) OF AIRFOIL SECTIONS C-C AND K-K.

3. THE AIRFOIL SURFACE IS PRODUCED BY FAIRED LINES CONNECTING THE CORRESPONDING STATIONS OF THE DESIGNATED AIRFOIL SECTIONS. THE SURFACE MUST BE CONTINUOUSLY SMOOTH THROUGHOUT THE BLADE LENGTH. ALL AIRFOIL CHARACTERISTICS, INCLUDING THICKNESS, MUST VARY LINEARLY BETWEEN SUCCESSIVE SECTIONS.

2. FOR AIRFOIL SECTION CONTOUR SEE AIRFOIL SHAPE NUMBER 10306.

1. ALL CAST RADII TO BE .06 UNLESS OTHERWISE SPECIFIED.

3-100-056-01

AVCO LYCOMING DIVISION

COMPRESSOR-ROTOR, AXIAL 1ST STAGE, LOW PRESSURE, CASTING OF

91847 3-100-056-01

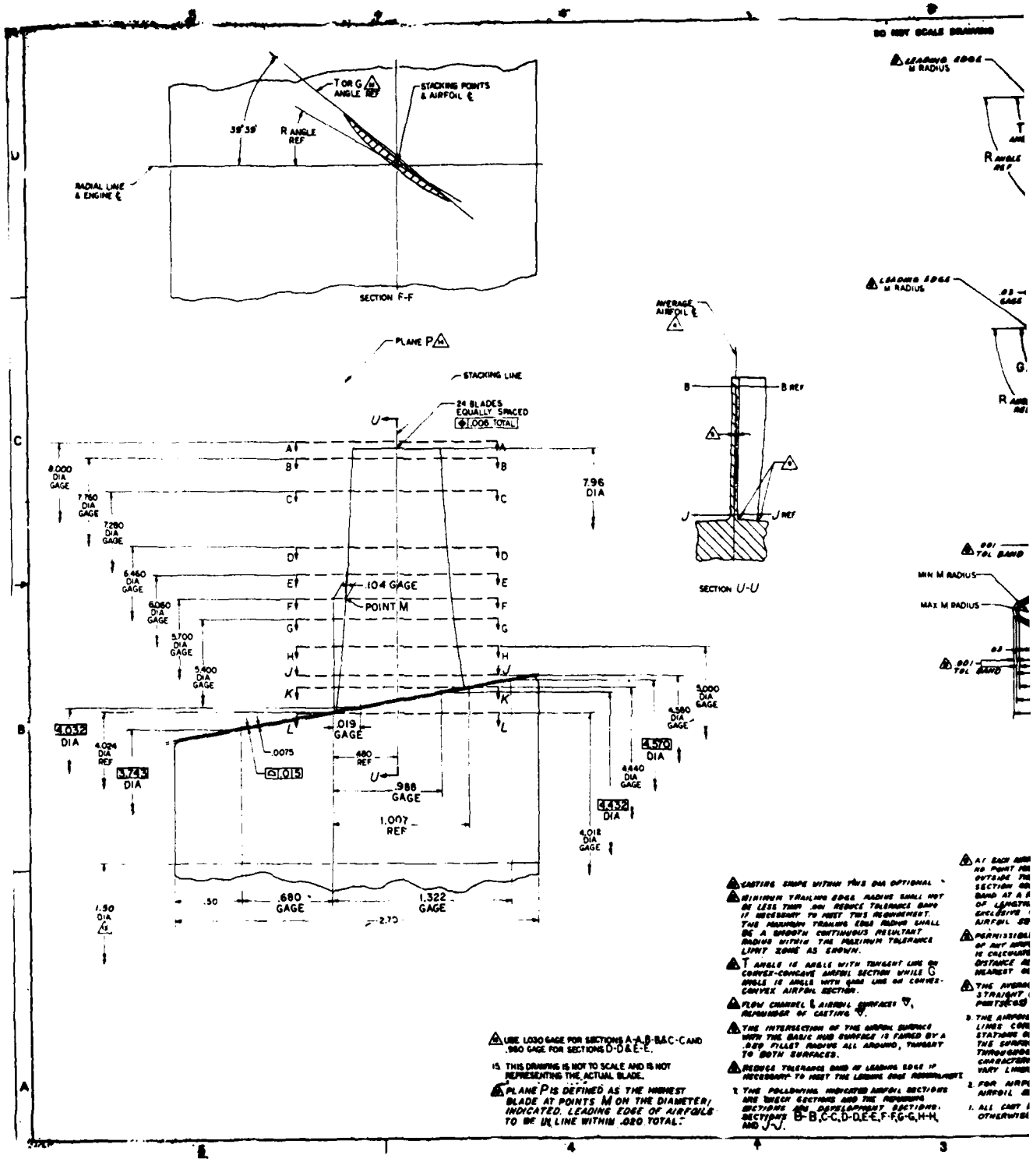

Figure 14. P/N 3-100-057-01, Second-Stage Integrally Cast Rotor

PRECEDING PAGE BLANK-NOT FILMED

DO NOT SCALE DRAWING

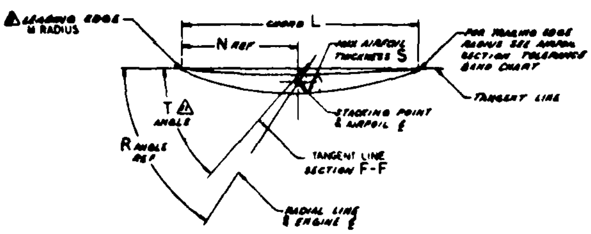

TYPICAL CONVEX-CONCAVE AIRFOIL SECTION
AIRFOIL SECTION F-F,G-G,H-H,J-J,K-K,L-L
SCALE NONE

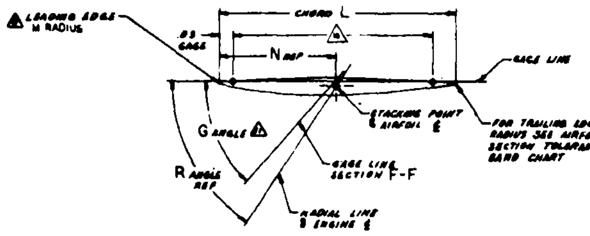

TYPICAL CONVEX-CONVEX AIRFOIL SECTION
AIRFOIL SECTION A-A,B-B,C-C,D-D & E-E
SCALE NONE

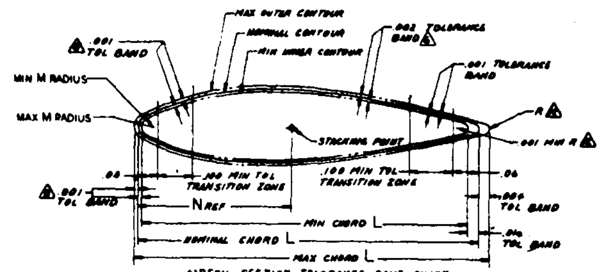

AIRFOIL SECTION TOLERANCE BAND CHART
FOR CONVEX-CONCAVE OR CONVEX-CONVEX AIRFOIL METHOD OF PREPARING MASTER AIRFOIL CHARTS USED IN MANUFACTURING & INSPECTION OF BLADE TOLERANCE BANDS ARE PARALLEL TO THE NOMINAL CONTOUR EXCEPT FOR TRANSITION ZONES.
SCALE NONE

SECTION	T ±0°30'	G ±0°30'	S ±.004	L +.005 -.015	R REF	N REF	M ±.001
A-A	–	15°54'	.029	1.127	55°37'	.560	.003
B-B	–	14°35'	.042	1.114	54°13'	.553	.003
C-C	–	11°44'	.050	1.089	51°24'	.543	.004
D-D	–	6°30'	.064	1.049	46°08'	.524	.005
E-E	–	3°24'	.070	1.030	43°01'	.515	.006
F-F	0°00'	–	.075	1.012	39°39'	.507	.007
G-G	-3°14'	–	.079	.998	36°26'	.501	.007
H-H	-8°40'	–	.085	.989	30°58'	.497	.008
J-J	-16°38'	–	.092	.981	22°55'	.494	.009
K-K	-19°45'	–	.095	.978	19°46'	.492	.009
L-L	-28°52'	–	.108	.978	11°48'	.490	.010

...ING SHAPE WITHIN THIS DIA OPTIONAL

...IMUM TRAILING EDGE RADIUS SHALL NOT LESS THAN .001. REDUCE TOLERANCE BAND NECESSARY TO MEET THIS REQUIREMENT. ... MAXIMUM TRAILING EDGE RADIUS SHALL ... A SMOOTH CONTINUOUS RESULTANT ... WITHIN THE MAXIMUM TOLERANCE ... ZONE AS SHOWN.

... ANGLE IS ANGLE WITH TANGENT LINE ON ...-CONCAVE AIRFOIL SECTION WHILE G ... IS ANGLE WITH GAGE LINE ON CONVEX-... AIRFOIL SECTION.

... CHANNEL & AIRFOIL SURFACES ▽, ... NUMBER OF CASTING ▽.

... INTERSECTION OF THE AIRFOIL SURFACE ... THE BASIC HUB SURFACE IS FAIRED BY A ... FILLET RADIUS ALL AROUND, TANGENT ... BOTH SURFACES.

... TOLERANCE BAND AT LEADING EDGE IF ... TO MEET THE LEADING EDGE REQUIREMENT

... FOLLOWING INDICATED AIRFOIL SECTIONS ... CHECK SECTIONS AND THE REMAINING ... ARE DEVELOPMENT SECTIONS: ... B-B,C-C,D-D,E-E,F-F,G-G,H-H, J-J.

⚠ AT EACH AIRFOIL SECTION, CHECKED INDEPENDENTLY, NO POINT MAY LIE MORE THAN .002 INSIDE OR .002 OUTSIDE THE NOMINAL AIRFOIL CONTOUR. THE SECTION CONTOUR MAY CHANGE WITHIN THIS TOLERANCE BAND AT A RATE NOT GREATER THAN .002 IN .100 OF LENGTH. THESE REQUIREMENTS ARE EXCLUSIVE OF THE RADII AT THE ENDS OF THE AIRFOIL SECTIONS.

⚠ PERMISSIBLE BOW IS DEFINED AS A DISPLACEMENT OF ANY AIRFOIL STACKING POINT IN ANY DIRECTION AND IS CALCULATED ON A RATE BASIS OF .006 PER INCH DISTANCE ALONG THE STACKING LINE FROM THE NEAREST SECTION B-B OR J-J.

⚠ THE AVERAGE AIRFOIL ℄ IS DEFINED AS A STRAIGHT LINE PASSING THRU THE STACKING POINTS(CGS) OF AIRFOIL SECTIONS B-B AND J-J

3. THE AIRFOIL SURFACE IS PRODUCED BY FAIRED LINES CONNECTING THE CORRESPONDING STATIONS OF THE DESIGNATED AIRFOIL SECTIONS. THE SURFACE MUST BE CONTINUOUSLY SMOOTH THROUGHOUT THE BLADE LENGTH. ALL AIRFOIL CHARACTERISTICS, INCLUDING THICKNESS, MUST VARY LINEARLY BETWEEN SUCCESSIVE SECTIONS.

2. FOR AIRFOIL SECTION CONTOUR SEE AIRFOIL SHAPE NUMBER 10307.

1. ALL CAST RADII TO BE .06 UNLESS OTHERWISE SPECIFIED.

3-100-057-01

LYCOMING DIVISION
COMPRESSOR-ROTOR, AXIAL 2ND STAGE, LOW PRESSURE, CASTING 'IN'
3-100-057-01

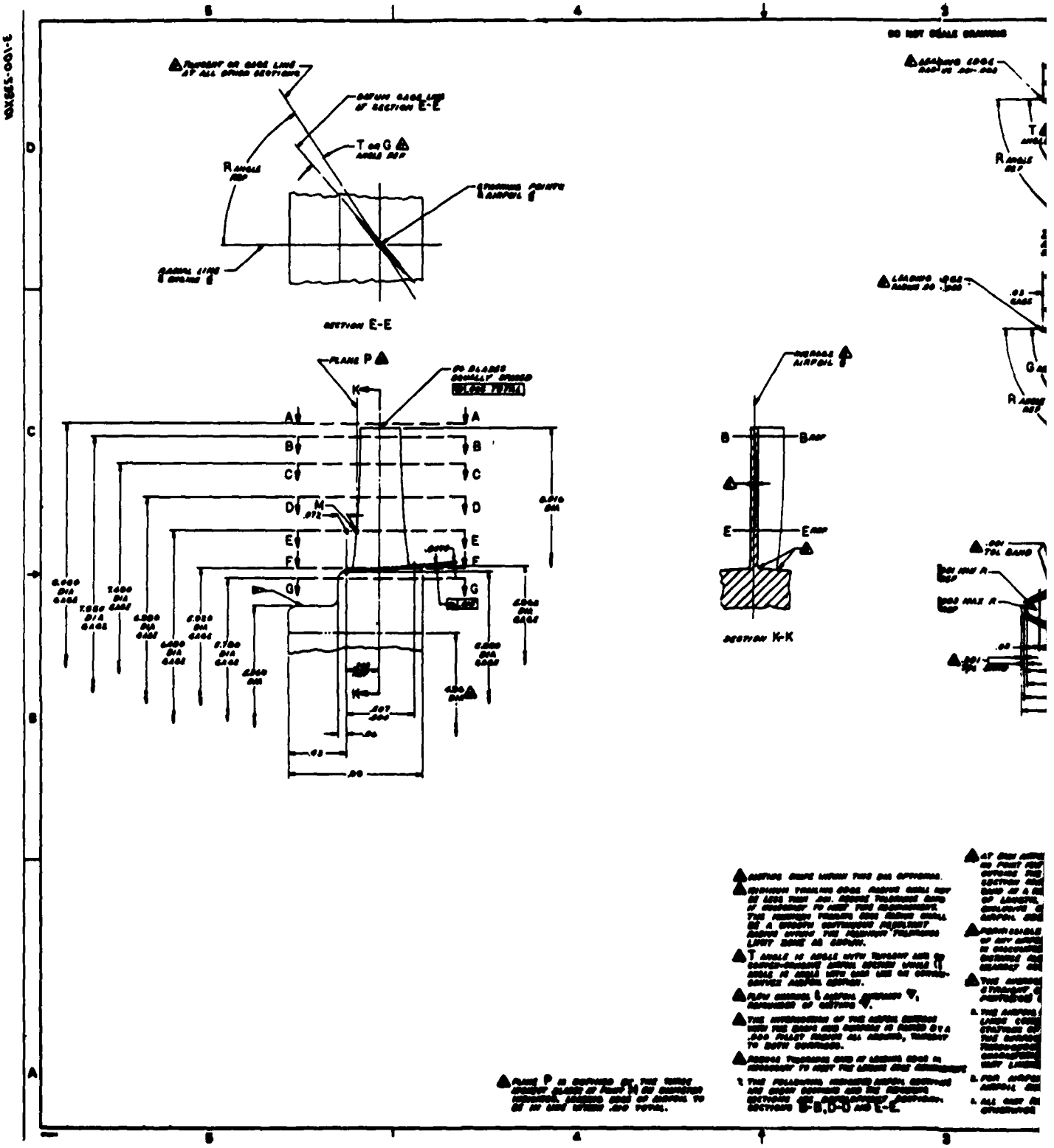

Figure 15. P/N 3-100-233X01, Fifth-Stage Integrally Cast Rotor

PRECEDING PAGE BLANK-NOT FILMED

DO NOT SCALE DRAWING

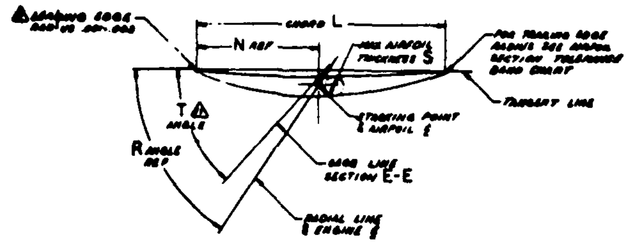

TYPICAL CONVEX-CONCAVE AIRFOIL SECTION
AIRFOIL SECTION F-F & G-G
SCALE: NONE

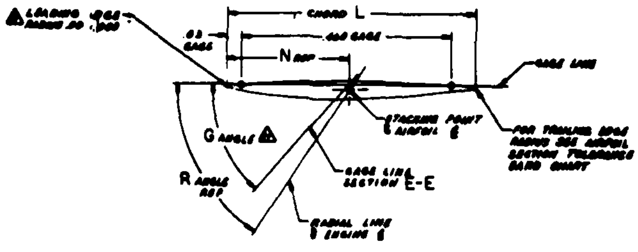

TYPICAL CONVEX-CONVEX AIRFOIL SECTION
AIRFOIL SECTION A-A, B-B, C-C, D-D & E-E
SCALE: NONE

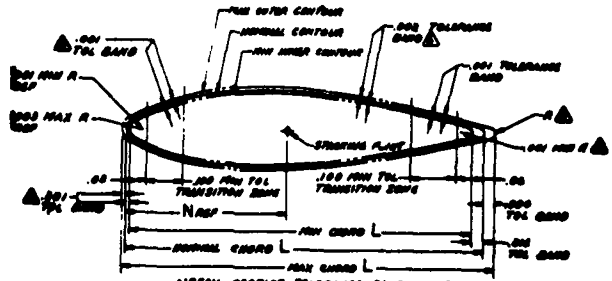

AIRFOIL SECTION TOLERANCE BAND CHART
FOR CONVEX-CONCAVE OR CONVEX-CONVEX AIRFOIL

SECTION	T	G	S	L	N REF	R REF
A-A	—	7°25'	.001	.004	.267	66°05'
B-B	—	7°05'	.003	.004	.267	57°05'
C-C	—	6°05'	.024	.004	.267	65°05'
D-D	—	5°06'	.020	.004	.267	55°06'
E-E	—	0°	.038	.004	.267	45°10'
F-F	-10°07'	—	.060	.004	.266	50°25'
G-G	-16°05'	—	.060	.060	.266	35°05'

COMPRESSOR-ROTOR, AXIAL 5TH STAGE, LOW PRESSURE CASTING OF

3-100-233XD1

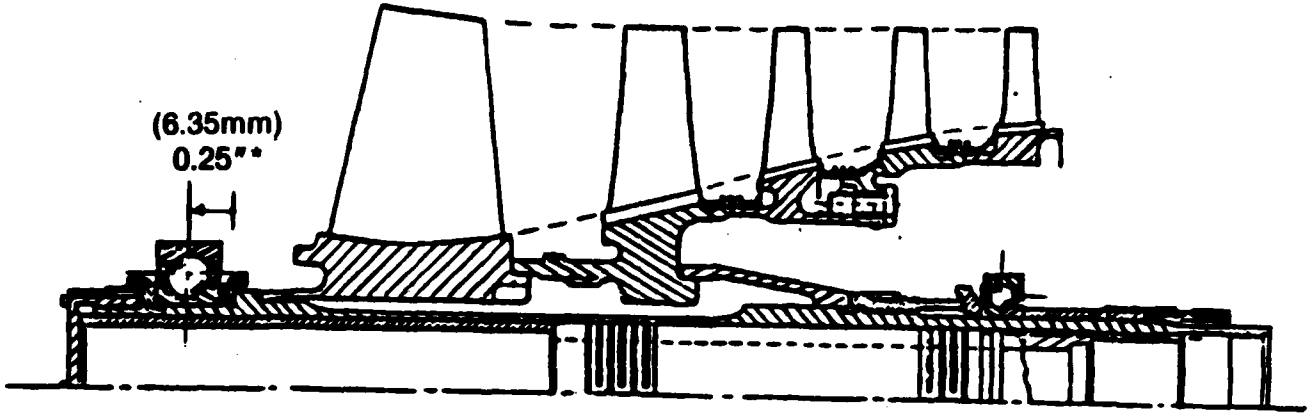

L.P. COMPRESSOR ROTOR
PROPOSED DESIGN HB-1

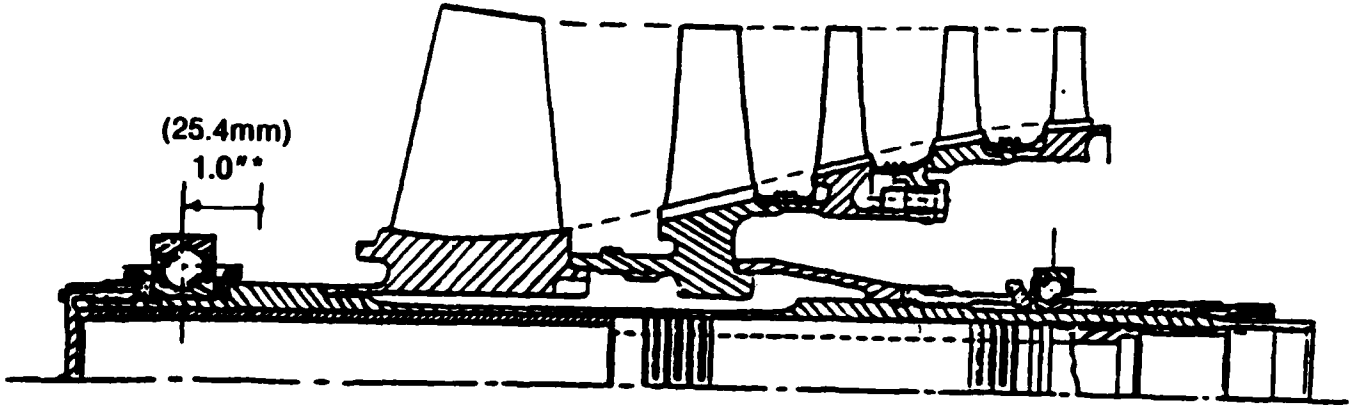

L.P. COMPRESSOR ROTOR
PROPOSED DESIGN HB-2

*INDICATES DISPLACEMENT
FROM CURRENT BEARING LOCATION

AE3007

Figure 16. AGT 1500 LP Compressor Schematic Illustrating Front Bearing Arrangements

The analysis was first performed using the current production low-pressure compressor rotors which were splined to the wrought low-pressure turbine rotor-shaft assembly as illustrated in Figure 17. Subsequent analyses evaluated the proposed cast first-, second-, and fifth-stage integral rotors.

Figure 18 illustrates the lateral vibration model employed in the determination of the natural frequencies of the low-pressure compressor section (i.e., dynamic response) at the design speed of 33,900 rpm. Table 2 summarizes the results of the lateral vibration study. The results of the lateral vibration study indicate that there is minimal difference among the current and the proposed configuration's dynamic responses. Both front bearing arrangements would, therefore, be acceptable from a critical speed/vibration standpoint.

4.1.2 First-Stage Low-Pressure Compressor Rotor Airfoil Development

Analysis of the AGT 1500 low-pressure first-stage compressor blade was performed, and the optimum blade stacking configuration was determined. This optimized airfoil configuration successfully eliminated the blade mid-span shroud and the low-pressure compressor variable inlet guide vane.

The dynamic characteristics of the redesigned blade were matched to the response of the current shrouded, wrought blade (i.e., equivalent first bending mode natural frequencies above the third order). This was accomplished by increasing the blade chordal width and thickness. Figure 19 shows the characteristic excitation diagram for the redesigned first-stage airfoil.

It was also required that the redesigned blade have balanced concave and convex, steady-state operating stresses (i.e., bending from centrifugal and gas loads had to be minimized). This was achieved by shifting or tilting the airfoil sections to produce more efficient radial load paths. A study was conducted to evaluate airfoil stress distributed at various tilts.

Figure 20 shows the steady-state stress distribution for various tilts at approximately 10 percent span from the airfoil base. The optium displacement of the airfoil sections to achieve minimum stresss was attained by tilting the airfoil sections tangentially in the opposite direction to the rotation of the wheel. The required airfoil section tilt for minimum stress was determined to be 0.055 in. at the blade tip.

As can be seen from Figure 20, the maximum steady-state stress level for the basic airfoil shape (without tilt) is 69 KSI (476 MPa) at 53 percent of the chord from the leading edge at the concave surface, while the maximum on the convex surface was 41 KSI (a difference of 28 KSI or 193 MPa). As illustrated in Figure 21, applying the optimized airfoil tilt (0.055 inch or 1.397 mm) results in maximum steady-state stresses of 56.5 (389.5 MPa) and 55.5 KSI (382.7 MPa) for the concave and convex surfaces, respectively. The application of optimized tilt, therefore, not only reduces the airfoil's tendency to bend during operation (concave-convex stress difference was reduced to approximately 1 KSI or 6.9 MPa), but also the magnitude of the maximum steady-state stress in the first blade was reduced by approximately 12.5 KSI (86.2 MPa) at the design speed of 33,900 rpm. The maximum steady-state stress now occurs at the 50 percent of the chordal width, on the concave side of the airfoil.

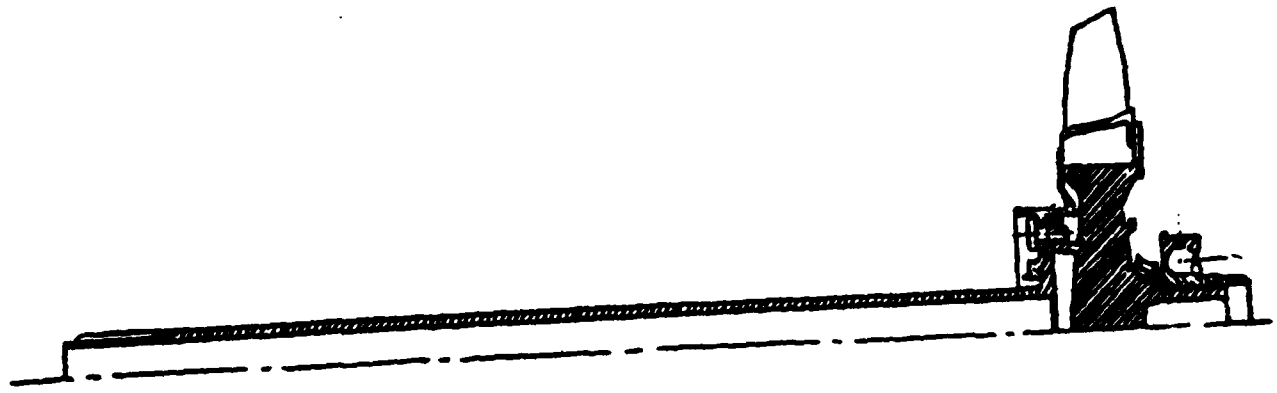

L.P. TURBINE ROTOR

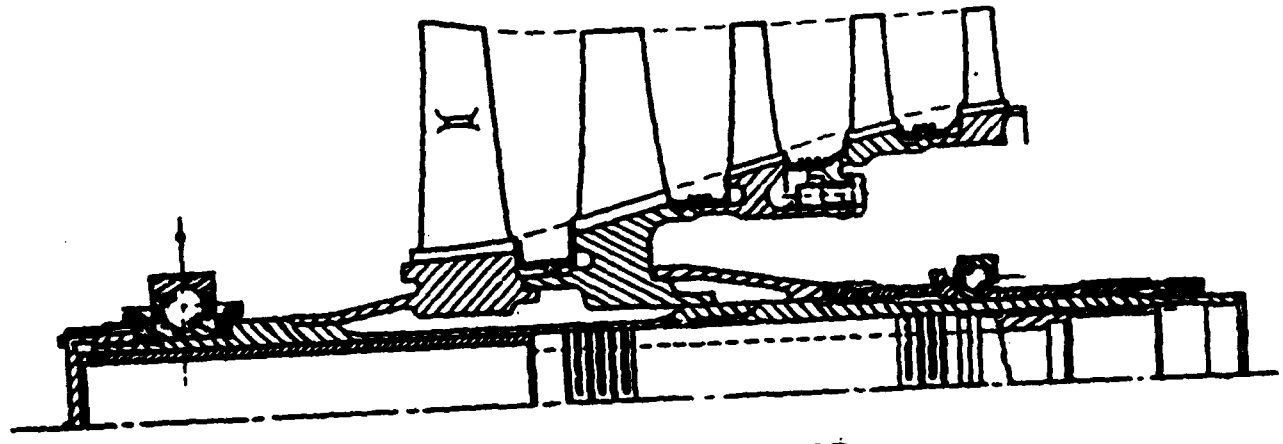

L.P. COMPRESSOR ROTOR
CURRENT PRODUCTION DESIGN (1979)

AE3016

Figure 17. Current LP Compressor Rotor Assembly Splined to the LP Turbine Rotor Assembly

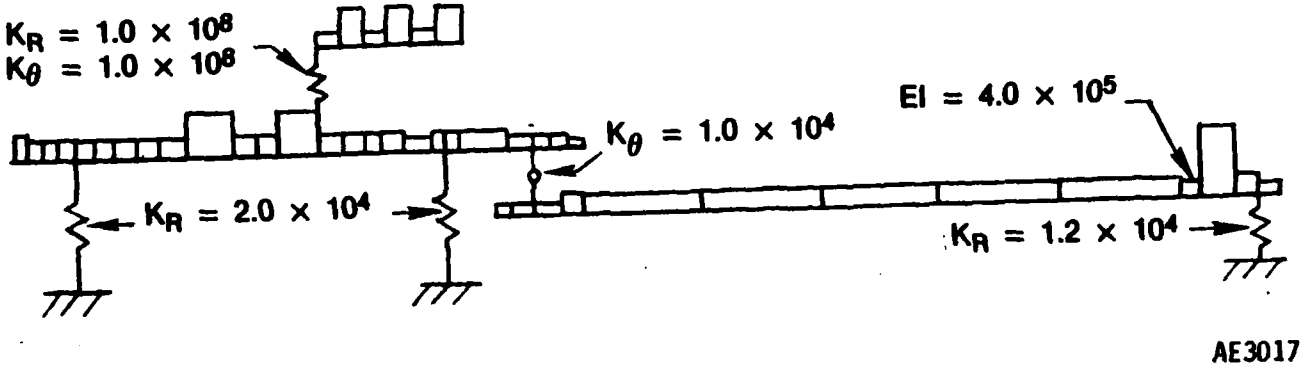

Figure 18. LP Compressor-Turbine Rotor/Shaft Lateral Vibration Model

TABLE 2. LATERAL VIBRATION NATURAL FREQUENCIES OF ALTERNATE LOW-PRESSURE COMPRESSOR FRONT BEARING CONFIGURATIONS

Mode	Design Configuration		
	Current Production	HB-1	HB-2
1st (Turbine Whirl)	5800 hertz	5800 hertz	5800 hertz
2nd (Turbine Whirl)	8350 hertz	8290 hertz	8110 hertz
3rd (Compressor Pitch)	13,730 hertz	12,970 hertz	13,170 hertz
4th (Rotor Bending)	39,970 hertz	39,840 hertz	39,640 hertz

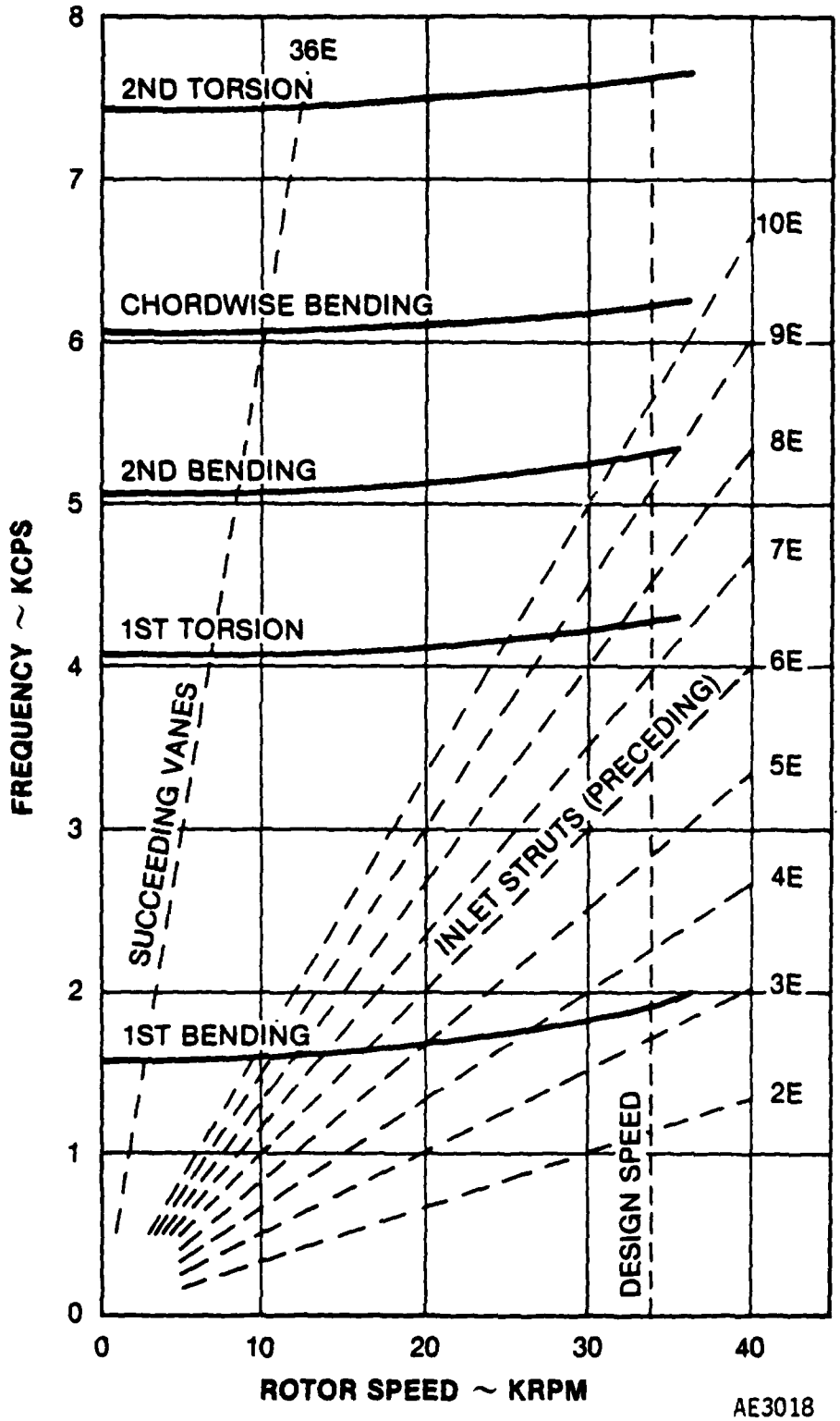

Figure 19. AGT 1500 Low Pressure Compressor First-Stage Blade Excitation Diagram

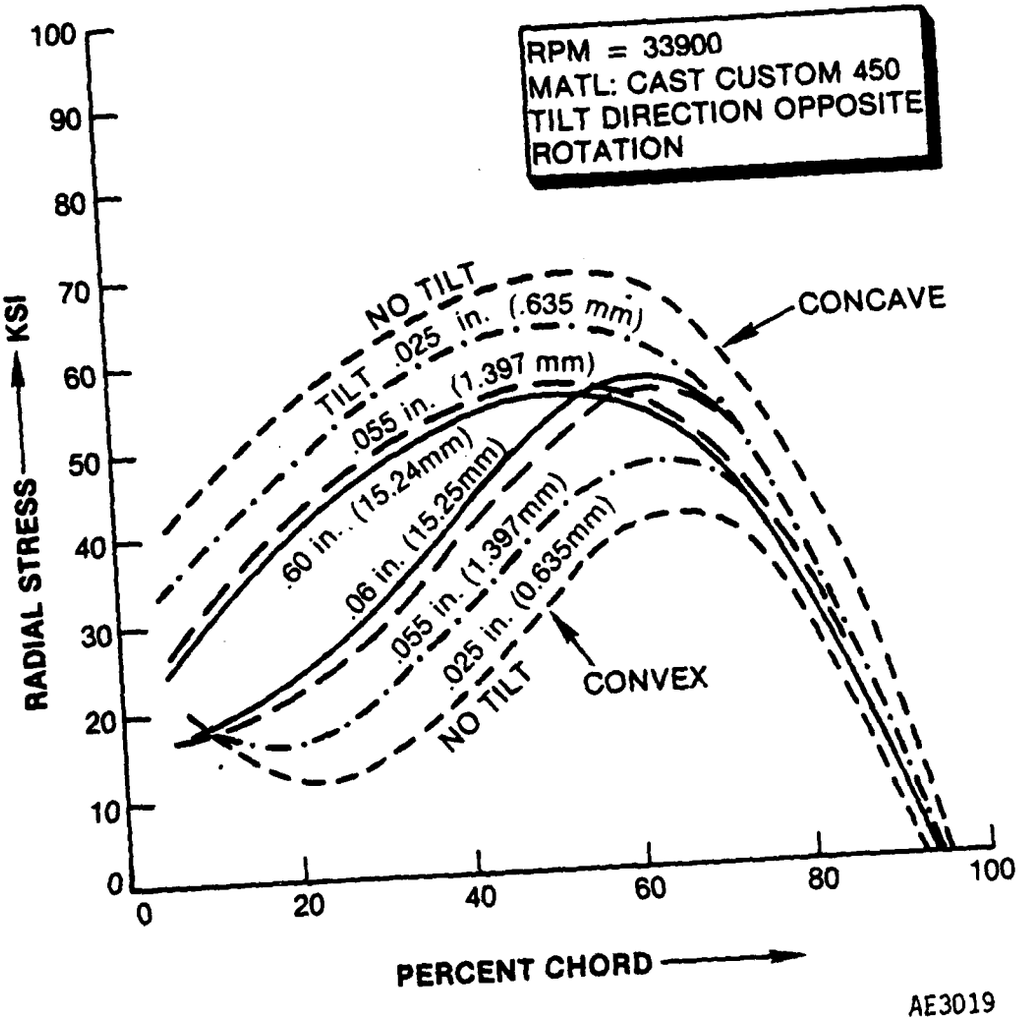

Figure 20. Steady State Stress Versus Chordal Distance for Selected Airfoil Tilts for the AGT 1500 LPC First-Stage Blade

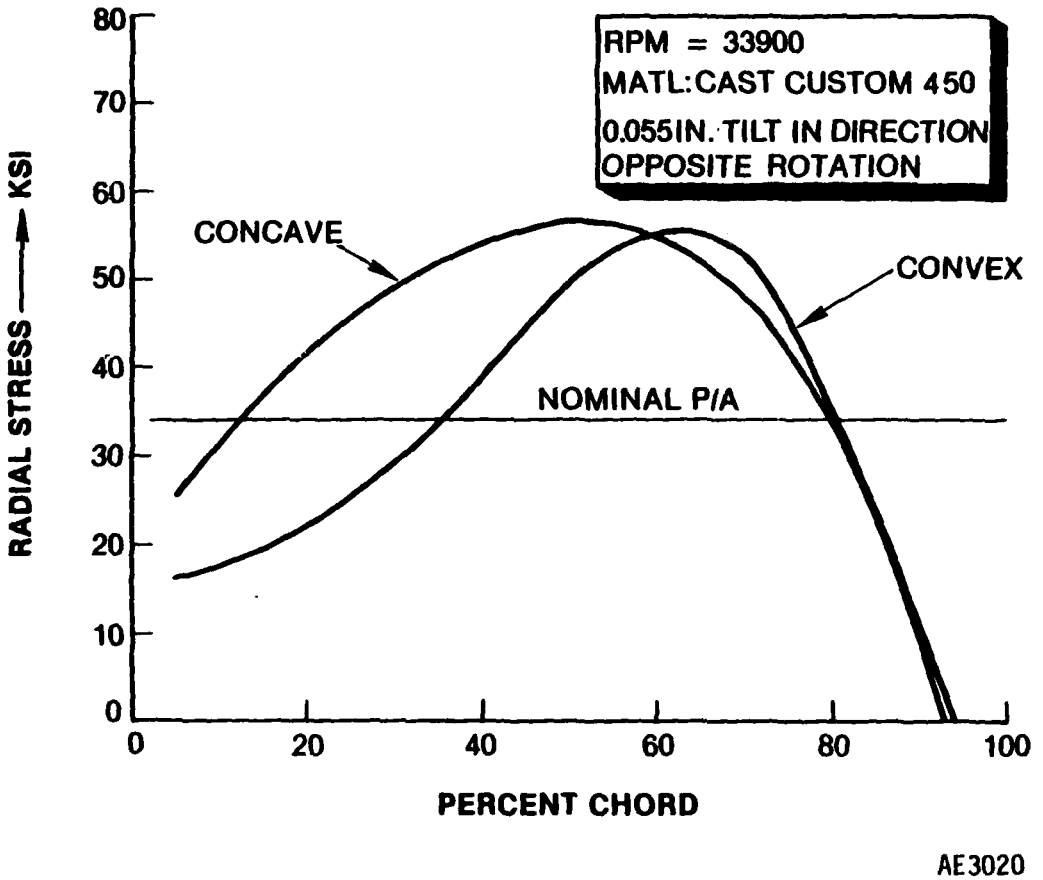

Figure 21. Steady-State Stresses Versus Chordal Distance for the AGT 1500 LPC First-Stage Blade With Optimum Tilt

The airfoil was also analyzed for vibratory stresses. A plot of normalized vibratory stresses at approximately 10 percent span from the base is shown for the primary mode (first bending) in Figure 22. This figure shows that the maximum vibratory stresses occur at the leading edge of the airfoil (concave) and at the 40 percent chordal width (convex) where the steady-state stresses were 38 KSI (262 MPa) (Figure 21).

A previously developed Goodman diagram for cast Custom 450 material is shown in Figure 23. Based upon the calculated maximum steady-state stress which exists in the first-stage blade of 56.5 KSI (389.5 MPa), at the 53 percent chordal width, the associated maximum allowable vibratory stress can be graphically found at this blade location to be +/-34.5 KSI (237.9 MPa). Based upon experience with other engines, these allowables will be well beyond the actual operating vibratory stresses of the first-stage airfoil.

4.1.3 Second-Stage Low-Pressure Compressor Rotor Airfoil Development

Analyses of the second-stage compressor blade (similar to those for the first stage) were performed and the optimum blade stacking was determined. This optimized airfoil configuration was required to be aerodynamically compatible with the new first-stage blade airfoil configuration.

The dynamic characteristics of the redesigned blade was matched to the response of the current second-stage blade whose lowest natural frequency was above second order. The excitation diagram for the final configuration is shown in Figure 24.

As was required with the first-stage blade design development, the second-stage airfoil had to have a minimum differential between the concave and convex steady-state operating stresses (i.e., the bending due to the high centrifugal and gas loads had to be minimized). This was achieved by shifting or tilting the airfoil sections to produce more efficient radial load paths. A study was conducted to evaluate airfoil stress distributions at various tilts.

Figure 25 shows the stress distribution for the evaluated tilts at approximately 10 percent span from the airfoil base. The optimum value of shifting the airfoil sections to produce minimum stresses was achieved by tilting the airfoil sections tangentially in the opposite direction to the rotation of the blade. The required airfoil section tilt for minimum stress was determined to be 0.010 in. (0.254 mm) at the blade tip.

As can be seen from Figure 25, the maximum steady-state stress level for the basic airfoil shape (without tilt) is 53 KSI (365 MPa) at 43 percent of the chord from the leading edge at the concave surface. The worst steady-state stress imbalance for this blade occurred at the 20 percent chordal width. There the diferential between the concave stress of 48 KSI (331 MPa) and the convex stress of 7 KSI (48.2 MPa) was 41 KSI (283 MPa)

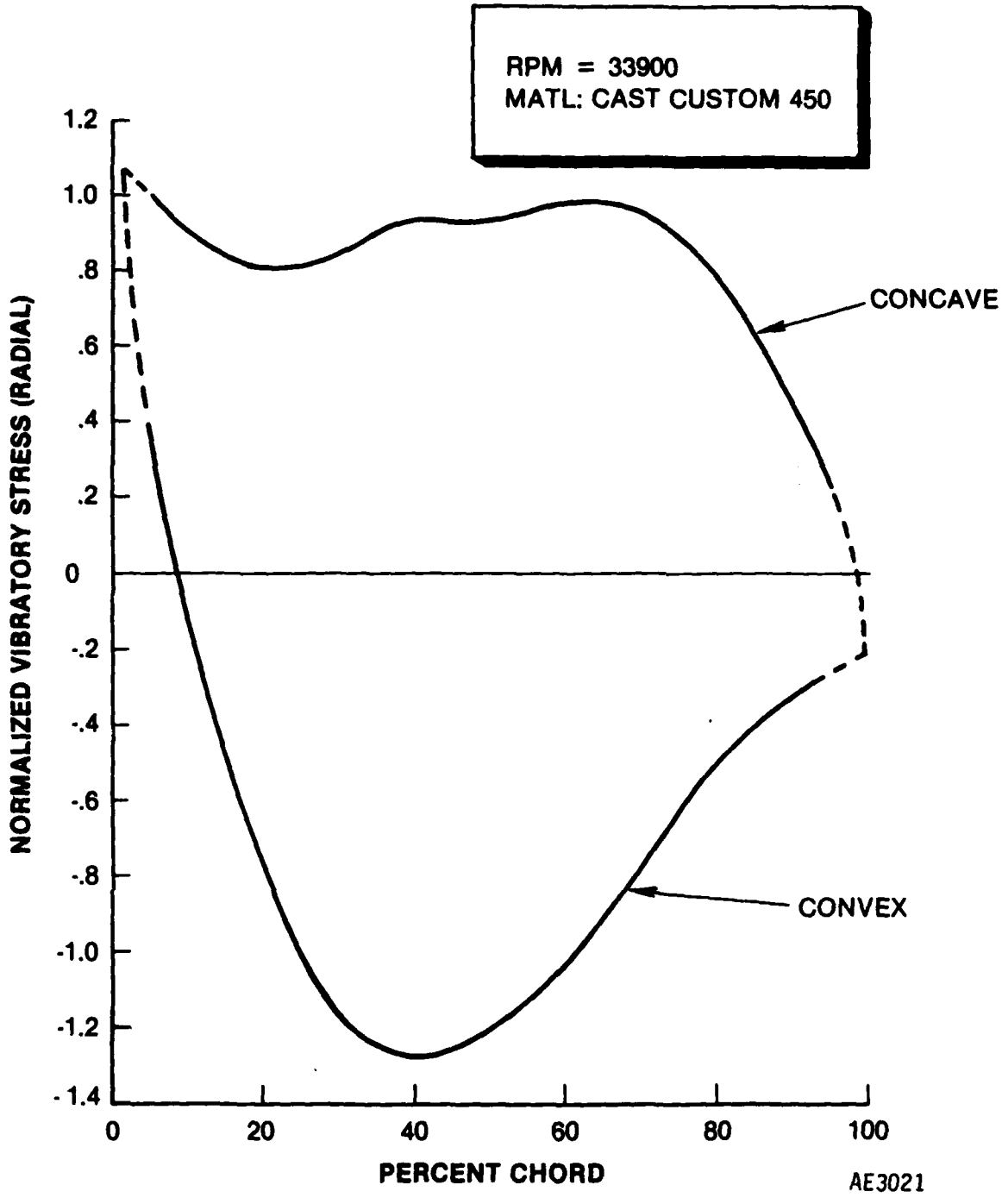

Figure 22. Normalized Vibratory Stresses Versus Chordal Distance for AGT 1500 LPC First-Stage Blade

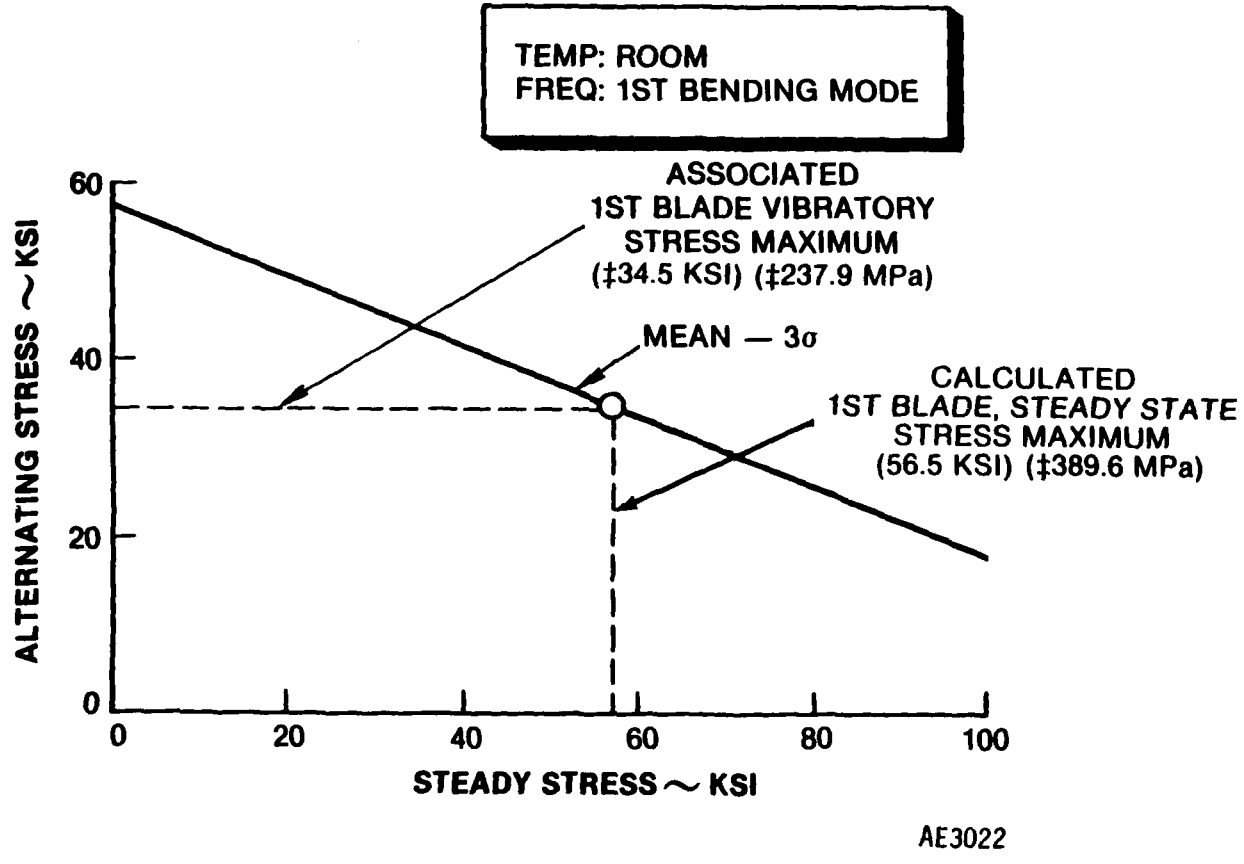

Figure 23. Goodman Diagram for Cast Custom 450 Alloy First-Stage LP Compressor Blade Calculated Maximum Allowable Stresses

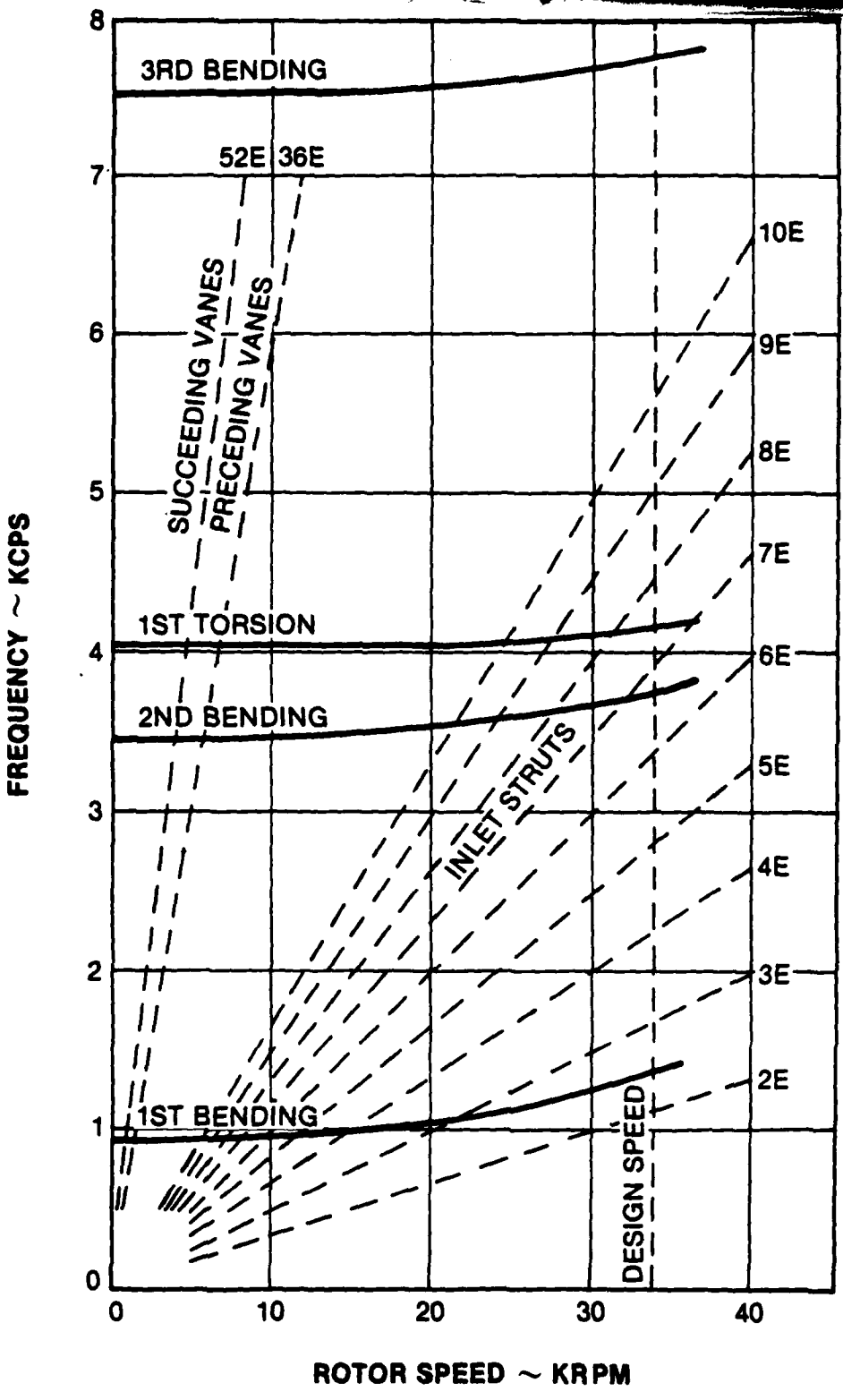

Figure 24. AGT 1500 Low-Pressure Compressor Second-Stage Blade Excitation Diagram

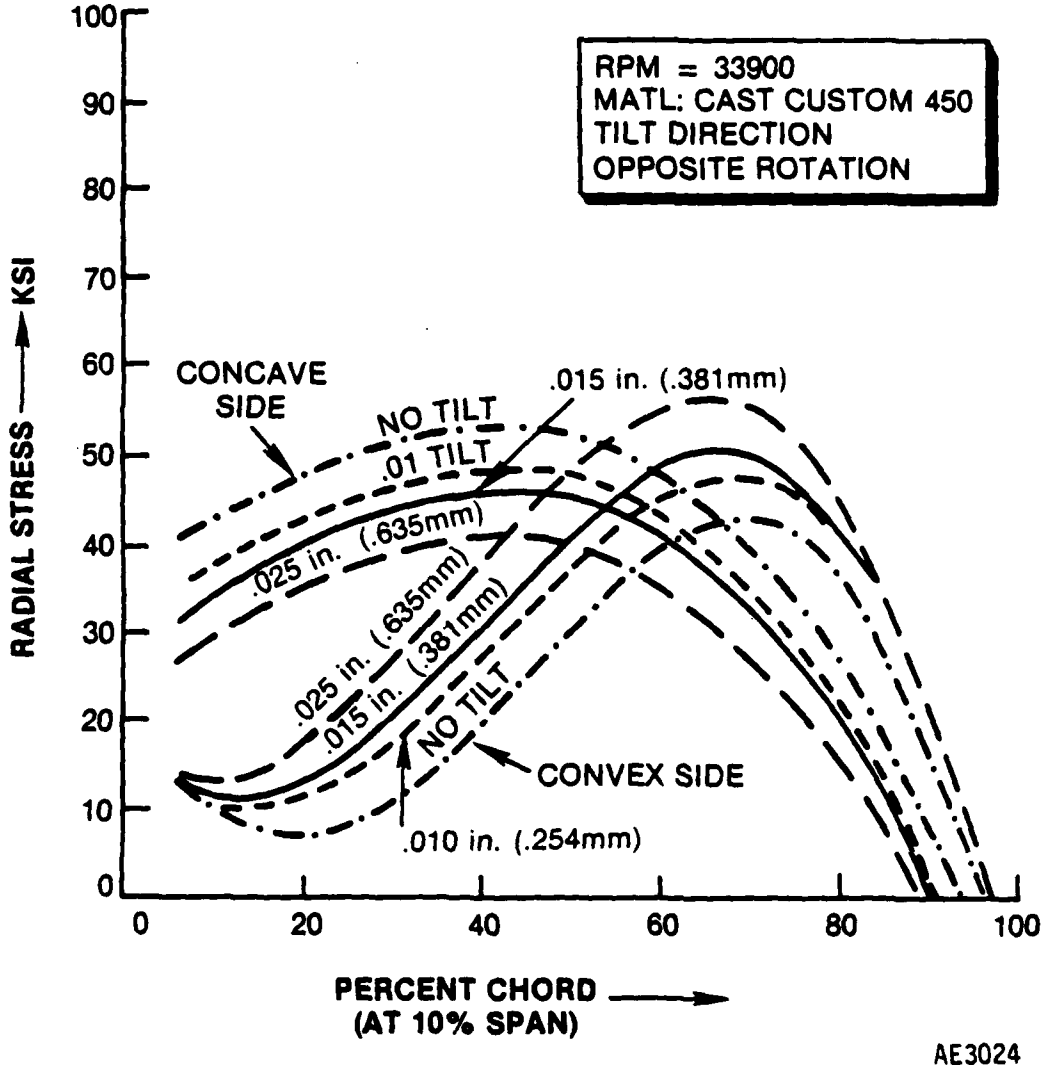

Figure 25. Steady-State Stress Versus Chordal Distance for Selected Airfoil Tilts for the AGT 1500 LPC Second-Stage Blade

Figure 26, however, shows that incorporating the optimum tilt of 0.10 in. (.254 mm) reduced the maximum steady-state stress to 47.5 KSI (327.5 MPa) (at the 43 percent chordal width, concave side) and the worst steady-state stress imbalance to 32 KSI (220.6 MPa). This imbalance is calculated based upon the 43 KSI or 296.5 MPa) at the con-cave side, and 11 KSI (75.8 MPa) at the convex side for the 20 percent chordal width. This figure shows that the application of optimized tilt not only re- duced the airfoil's tendency to bend during operational loads (i.e., reduced concave/convex stress imbalance), but also reduced the magnitude of the maxi- mum steady-state stress in the second blade by approximately 5.5 KSI (37.9 MPa)
(based on a design speed of 33,900 rpm).

The airfoil was also analyzed for vibratory stresses. A plot of normalized vibratory stresses at approximately 10 percent span from the base is shown in Figure 27 for the primary mode (first bending) at 950 hertz . This fig- ure shows that the maximum vibratory stresses occurred at the 43 percent chordal width of the convex surface where the steady-state stress was approximately 30 KSI (207 MPa). (See Figure 26.)

The previously developed Goodman diagram for cast Custom 450 material is shown in figure 23 and again in Figure 28. Based upon the calculated maximum steady-state stress which exists in the second-stage blade (47.5 KSI) at the 43 percent chordal width. The associated maximum allowable vibratory stress can be graphically found at this blade location to be +/- 38 KSI (262 MPa). Based upon experience with other engines, these allowables will be well beyond the actual operating vibratory stresses of the second-stage airfoil.

4.1.4 Fifth-Stage Low-Pressure Compressor Rotor Airfoil Evaluation

To assure that the Custom 450 integrally cast fifth-stage rotor would have sufficient mechanical property capability to allow its direct substitution for the current wrought rotor assembly (without redesigning the rotor geometry), performance studies (similar to those used for the first and the second stage) were conducted.

The steady-state stress distribution of the blade for the maximum design speed of 33,900 rpm is shown in Figure 29; these stresses were computed at approximately the 10 percent span (from the airfoil base). As can be seen from this figure, the maximum stresses were: 37 KSI (255 MPa) on the concave side of the airfoil at the 40 percent chordal width (from the leading edge), and 32 KSI (220 MPa) on the convex surface at the 65 percent chordal width. The maximum imbalance between the surfaces occurred at the 24 percent chordal width and was approximately 21 KSI (145 MPa).

Natural frequencies for the primary modes of vibration are shown in the excitation diagram in Figure 30. Strain-gage measurements were made on wrought wheels to determine the actual vibratory stresses which existed at the maximum steady-state stress location (24 percent chordal width) for selected levels of engine speed. The strain-gage tests measured a vibratory stress of +/-3.3 KSI (22.7 MPa) at 96 percent of design speed (approximately 32,500 rpm) and +/-9.7 KSI (66.9 MPa) at a reduced speed condition (approximately 19,000 rpm) in the vicinity of the location of the calculated maximum steady-state stress (37 KSI) (255 MPa) for the airfoil.

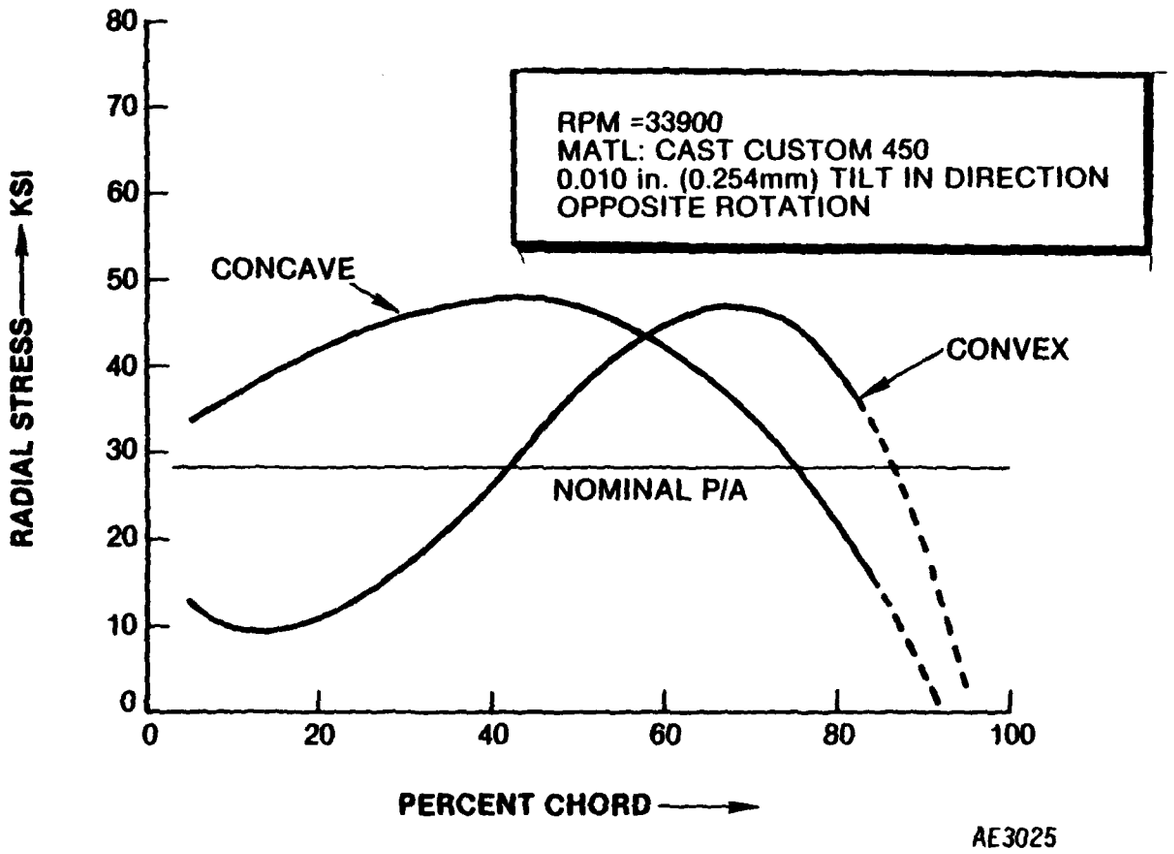

Figure 26. Steady-State Stresses Versus Chordal Distance for the AGT 1500 LPC Second-Stage Blade With Optimum Tilt

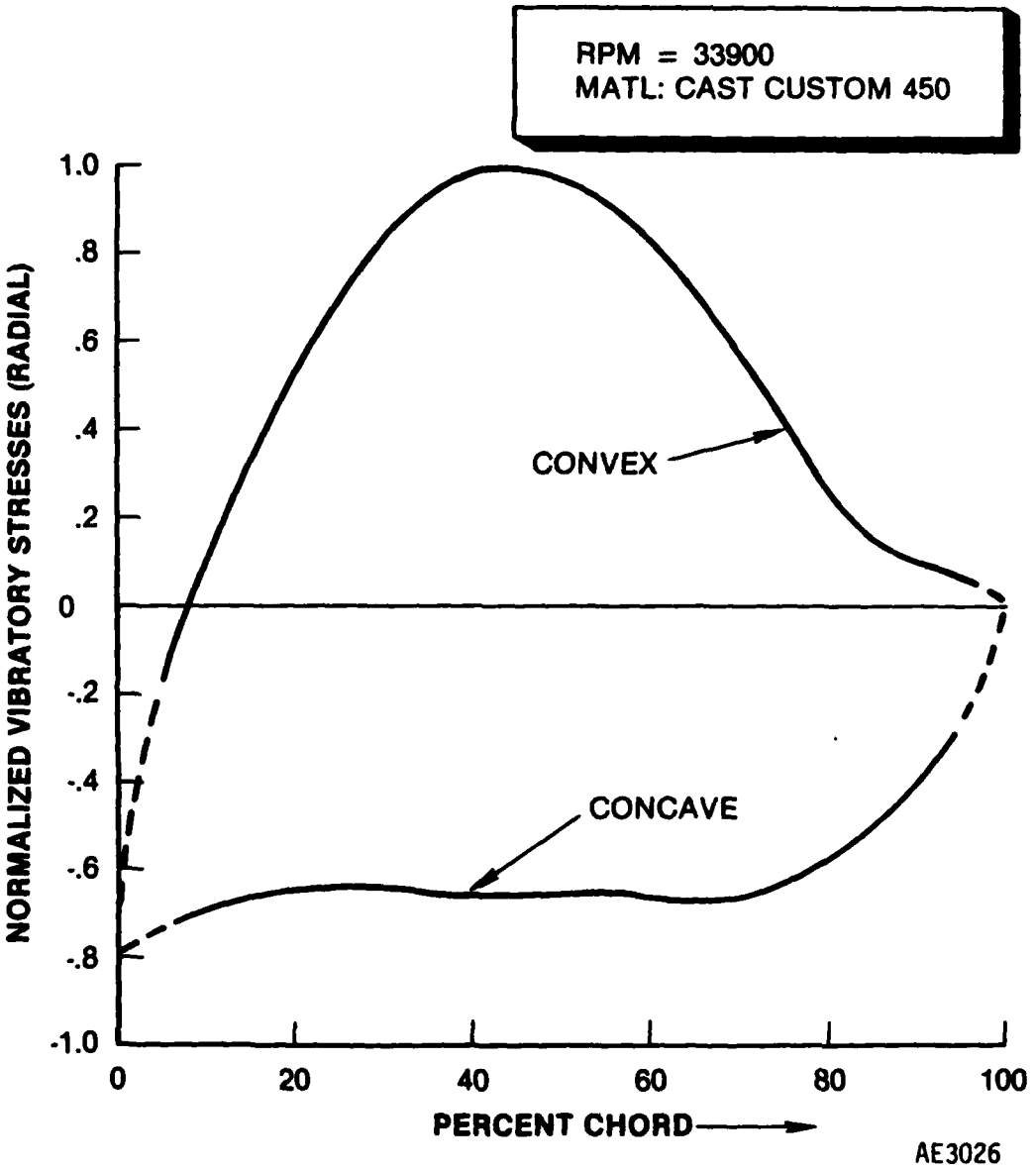

Figure 27. Normalized Vibratory Stresses Versus Chordal Distance for AGT 1500 LPC Second-Stage Blade

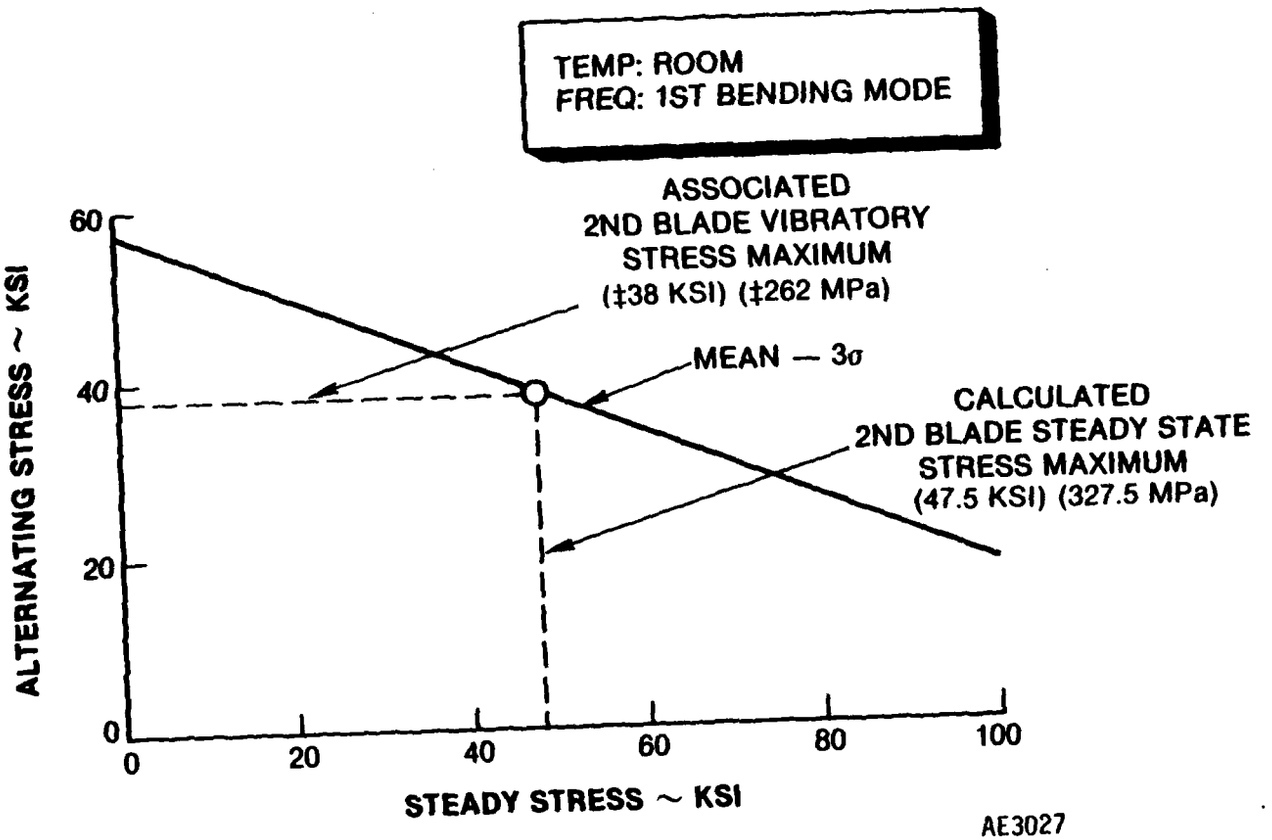

Figure 28. Goodman Diagram for Cast Custom 450 Alloy Second-Stage LP Compressor Blade Calculated Maximum Allowable Stresses

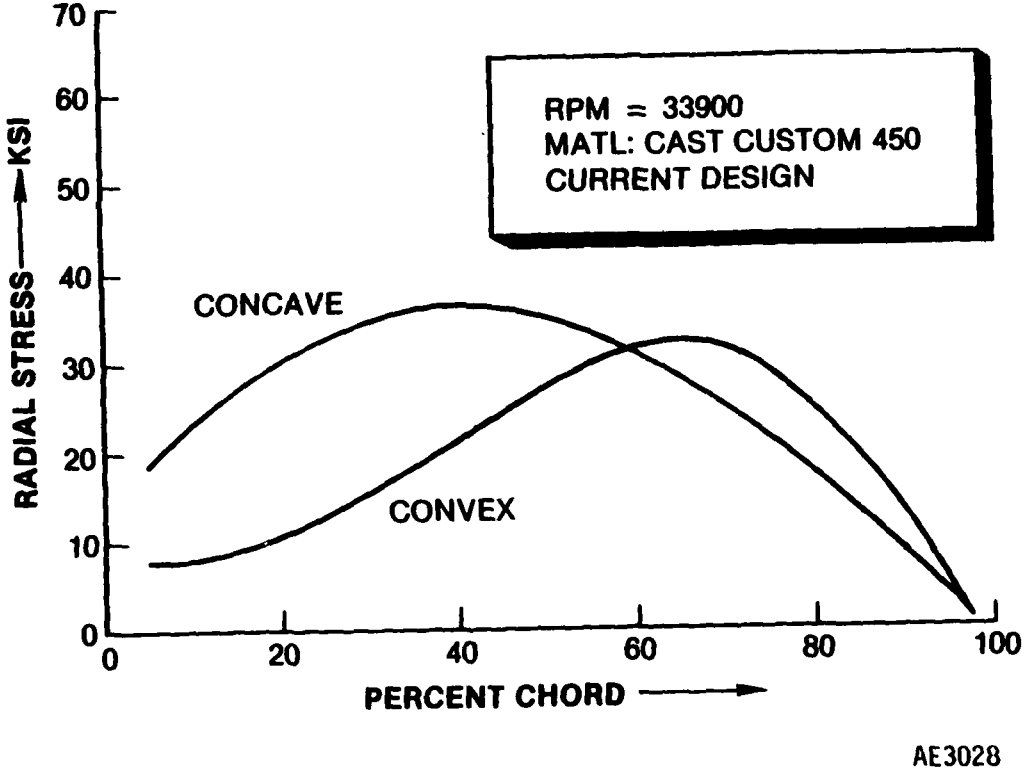

Figure 29. Steady-State Stress Versus Chordal Distance for the AGT 1500 LPC Fifth-Stage Blade

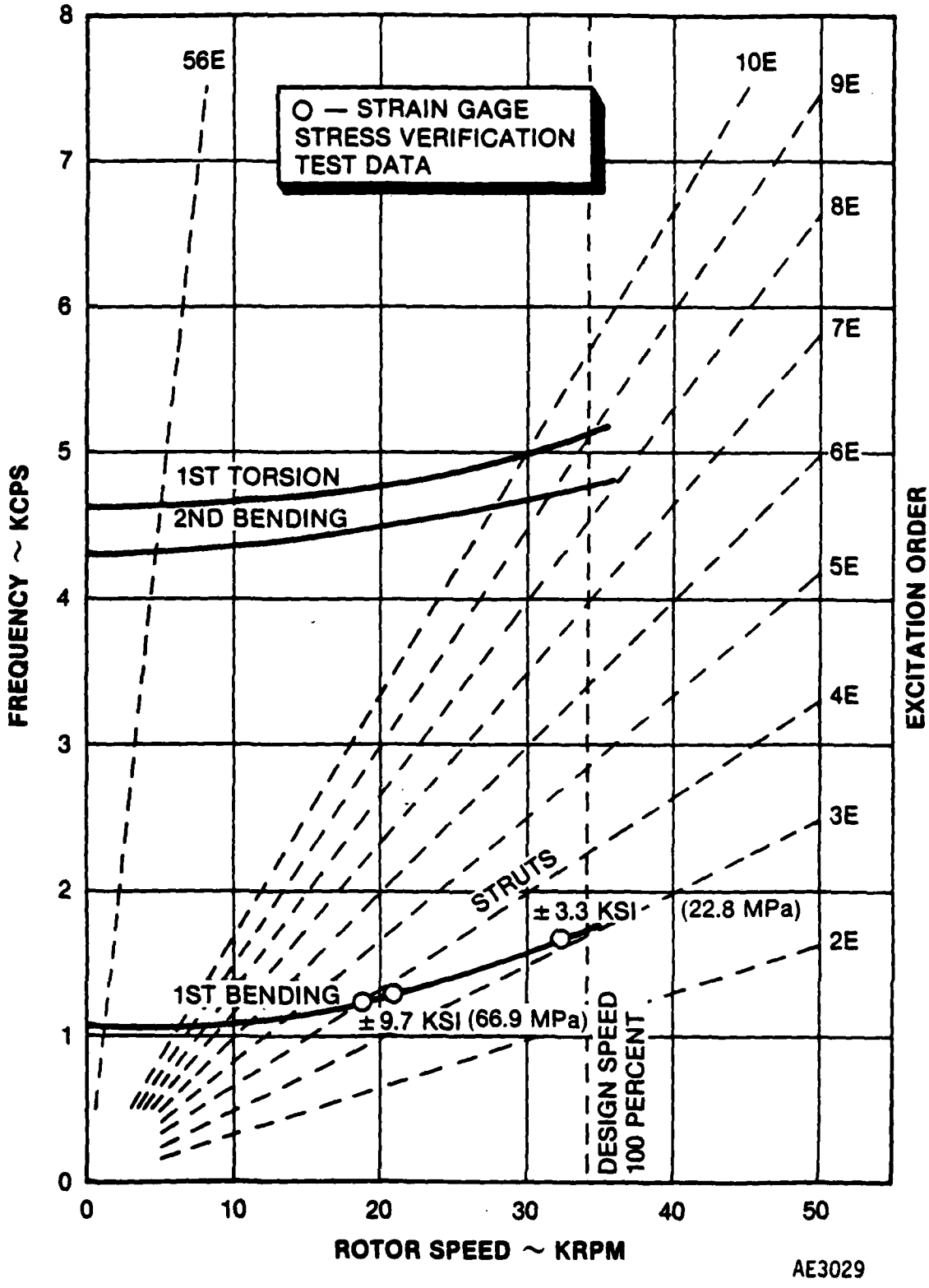

Figure 30. AGT 1500 Low-Pressure Compressor Fifth-Stage Blade Excitation Diagram

The Goodman diagram for cast Custom 450 material is shown again in Figure 31, in which the measured +/- 3.3 KSI (± 22.6 MPa) vibratory stress is plotted. The abscissa location of this point in the diagram was selected to be less than the predicted maximum steady-state stress of 37 KSI (254 MPa). The 37 KSI (254 MPa) maximum steady-state, stress was calculated at 100% of design speed (33,900 RPM). The ± 3.3 KSI (± 22.6 MPa) vibratory stress was measured at only 96% of design speed (a lower steady state stess environment). It can be seen that this ± 3.3 KSI (± 22.6 MPa) vibratory stress is well below the allowable maximum vibratory stress of +/- 43 KSI (± 295 MPa) (graphically determined) at the maximum steady-state stress location.

It should also be noted that the ± 3.3 KSI (± 22.6 MPa) was not the maximum measured vibratory stress at the maximum steady-state stress location. This maximum vibratory stress occurred not at maximum operating speed (33,900 rpm), but instead at 19,000 rpm. Although the steady-state stresses were not determined for this engine speed condition, they will be significantly lower than the 37 KSI (254 MPa) maximum calculated above.

For comparison purposes, the highest measured vibratory stress at 19,000 rpm +/- 9.7 KSI (66.9 MPa), has also been plotted on the Goodman diagram (Figure 31). As can be seen in this plot, this measured vibratory stress is also well within Custom 450 material property capabilities.

The results of the fifth-stage design/stress analyses indicate that the Custom 450 integrally cast rotor should be able to withstand the known engine conditions of steady and vibratory stresses. However, strain-gage engine testing of actual cast rotors will be required to assure that the vibratory performance of an integral wheel is similar to the conventionally assembled rotor.

4.2 PHASES I AND II TOOLING CONSTRUCTION

While the tooling for the first- and second-stage integrally cast compressor rotors was not constructed until Phase II, the fifth-stage rotor tooling was fabricated as part of the Phase I effort. This enabled the early initiation of the fifth-stage casting development under Phase II of the contract.

4.2.1 First-Stage Low-Pressure Rotor

First-stage rotor investment casting tooling was constructed in Phase II. The wax/plastic pattern produced by the first-stage investment casting tooling is shown in Figure 32. A dimensional layout of a casting produced from this tooling is shown in Table 3. (The casting used was made from a process which is considered suitable for making production quantities of hardware.) This layout indicated that the first-stage investment casting tooling was capable of producing a configuration which can be used for actual production applications.

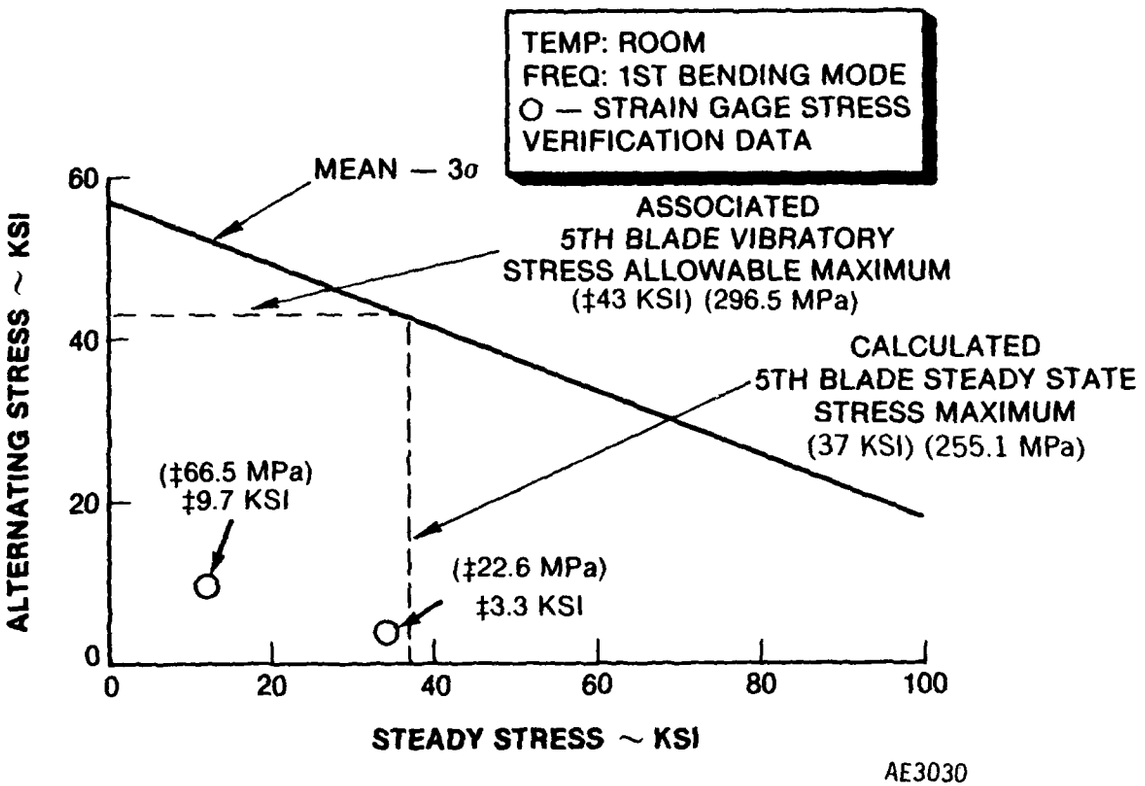

Figure 31. Goodman Diagram for Cast Custom 450 Alloy Fifth-Stage LP Compressor Blade Calculated Maximum Allowable Stresses

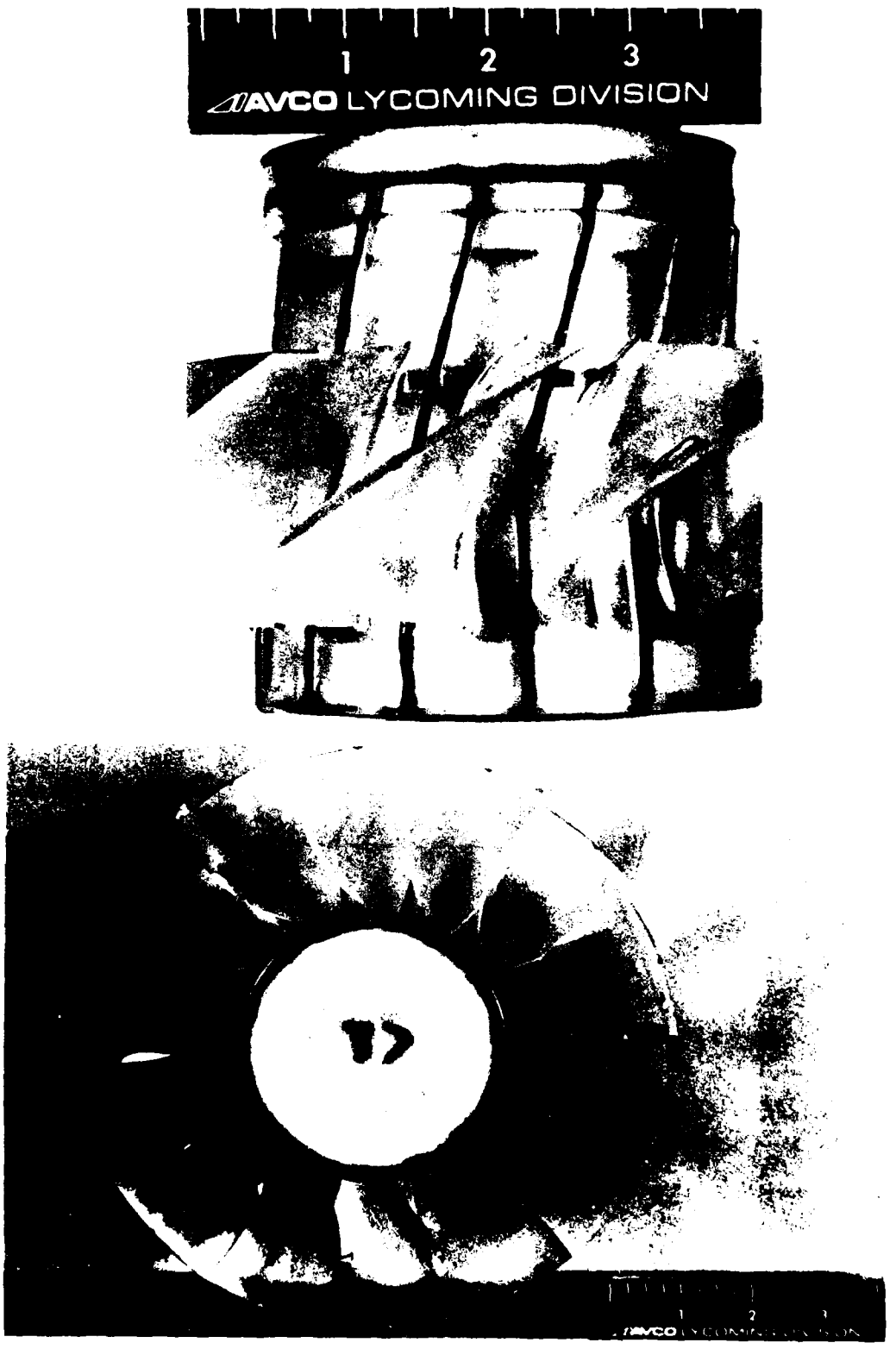

Figure 32. First-Stage Rotor Investment Casting Pattern

TABLE 3. FIRST-STAGE LOW PRESSURE COMPRESSOR ROTOR CASTING NONCONFORMING DIMENSIONS

B/P Dim.	Tol.	Zone	Actual Dim.	Code *
Airfoil Charts	+/- .002 (.0508 mm)	3-A	Nom. to +/- .006 (.1524 mm)	B
Max. Airfoil Thickness "S"	+/- .004 (.1016 mm)	2-A	.006/.008 O/Nom. (.1524/.2032 mm)	B
Chord "L"	+.005/-.015 (+ .127/- .381 mm)	2-B	.017/.025 O/Nom. (.4318/.635 mm)	B
.75	+/- .010 (.254 mm)	5-B	.730/.737 (18.542/18.720 mm)	C
3.41	+/- .015 (.381 mm)	5-B	3.435/3.417 (87.249/86.792 mm)	C
8.48 Dia.	+/- .030 (.762 mm)	4-C	8.570/8.858 (217.678/224.993 mm)	C
8.82 Dia.	+/- .030	4-C	8.882/8.892 (225.603/225.857 mm)	C
14 Blades Equally Spaced	.006 Tot. (.1524 mm)	4-C	.013 Tot. (.3302 mm)	C
.015	+/- .0075 (.1905 mm)	5-C	.003/.020 (.3302/.508)	C
"T" Angle Sect. C-C 37° 2'	+/- 0° 30'	1-B	37° 47'	C
Surface	90 RMS Max		180 RMS	F

* A - Immediate tool correction needed (part rejected for this dimension).
B - Limited approval (tool to be corrected, as instructed).
C - Accept for the life of the tool with periodic layout audits as scheduled to confirm compliance during tool life.
F - Rotor finishing operations are capable of reducing the surface roughness between 90 and 132 RMS.

4.2.2 Second-Stage Low-Pressure Rotor

Figure 33 shows the wax/platic pattern produced by the second-stage investment casting tooling. This injection tooling was fabricated in Phase II. An initial dimensional layout of the product of this tool, however, indicated that some further tooling corrections would be required prior to producing engine acceptable hardware. As can be seen from Table 4, airfoil shape and orientation corrections were required. Subsequent tooling correction and dimension rechecks performed on a rotor cast from a viable process confirmed that the tooling could produce castings acceptable for production usage. Note that the airfoil deviations listed in Table 4 are adjustable using the special gaging/correcting fixture which was designed and built for the second-stage low-pressure rotor casting subsequent to this layout. Appendix I details the use of this gage for the in-situ corrections of rotor airfoils.

4.2.3 Fifth-Stage Low-Pressure Rotor

Fifth-stage investment casting tooling was fabricated within Phase I. Figure 34 shows the wax/plastic assembly produced by the fifth-stage pattern tooling (Note that the pattern gating is not shown).

An initial dimensional layout of the product of this tool indicated that some further tooling corrections would be required prior to production of engine acceptable rotors. Table 5 indicates the airfoil shape and orientation corrections which were required. Subsequent tooling correction and dimension rechecks Table 6 were performed and confirmed the tooling's ability to produce engine hardware of acceptable dimensions. These layouts were performed on a wheel cast by the P16 process, which was the best process available at the time of the layout. Subsequently, it was determined that this process was not suitable for production use (as discussed later). The casting process (P34) which was finally determined to have the best metallurgical product yield also resulted in dimensional deviations Table 7 which will require further tooling rework if this process is to be used to produce production castings.

A gage similar to the special gage constructed for second-stage rotor inspection and in-situ corrections was built for the fifth-stage integrally cast, low-pressure compressor rotors. Appendix A outlines the use of this gage for the in-situ correction of rotor airfoils.

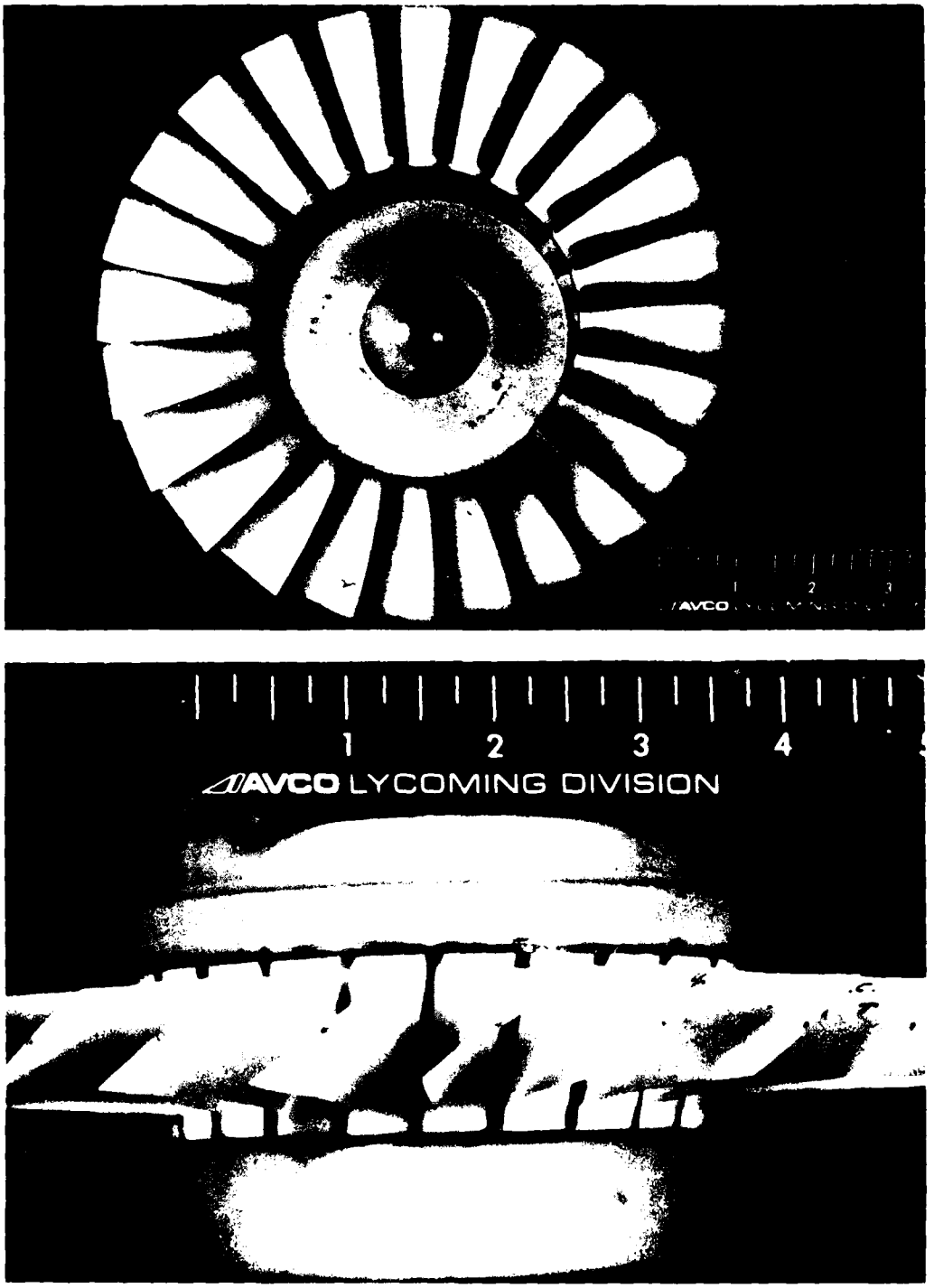

AE3035

Figure 33. Second-Stage Rotor Investment Casting Pattern

TABLE 4. SECOND-STAGE LOW-PRESSURE COMPRESSOR ROTOR CASTING NONCONFORMING DIMENSIONS

B/P Dim.	Tol.	Zone	Original Dimension	Corrected Dimension	Code *
Note 5 Bow	.005 per inch	3-A	.002 CV/.008 CC .0508/.2032 mm	.00/.009 /.2286	G
Note 5 Lean	.005 per inch	3-A	.012/.006 to LE .3048/.1524 mm	.00/.008 /.2032	G
Max Airfoil Thickness "S"	+/- .004 .1016 mm	2-B	.004/.009 O/Nom .1016/.2286 mm	To Print	
Radius "M"	+/- .001 .0254	2-B	-.006/+.005 -.1524/+.127 mm	To Print	
Airfoil Contour	+/- .001 LE	2-B	-.005/+.012 -.127/.3098 mm	-.003/+.002 -.0762/+.0508	C
Airfoil Contour	+/- .002 .0508 mm	2-B	-.0025/+.0095 -.0635/+.2413 mm	To Print	
Airfoil Contour	+/- .001 TE	3-B	-.005/+.0095 -.1397/+.2413 mm	-.003/+.002	C
4.570	+/- .015 .381 mm	4-B	4.537 115.24 mm	To Print	
2.70	+/- .015	4-A	2.776/2.791 70.510/70.891 mm	To Print	
Chord "L"	+.005/-.015 +.127/-.381 mm	2-B	.003/.010 O/Nom. .0762/.254 mm	To Print	
24 Equally Spaced Blades	+/- .001 TE .0254 mm	4-C	0.12 Tot. .3048 mm	To Print	

* A - Immediate tool correction needed (part rejected for this dimension).
B - Limited approval (tool to be corrected, as instructed).
C - Accept for the life of the tool with periodic layout audits as scheduled to confirm compliance during tool life.
G - Airfoil corrections to be made in special gaging fixture.

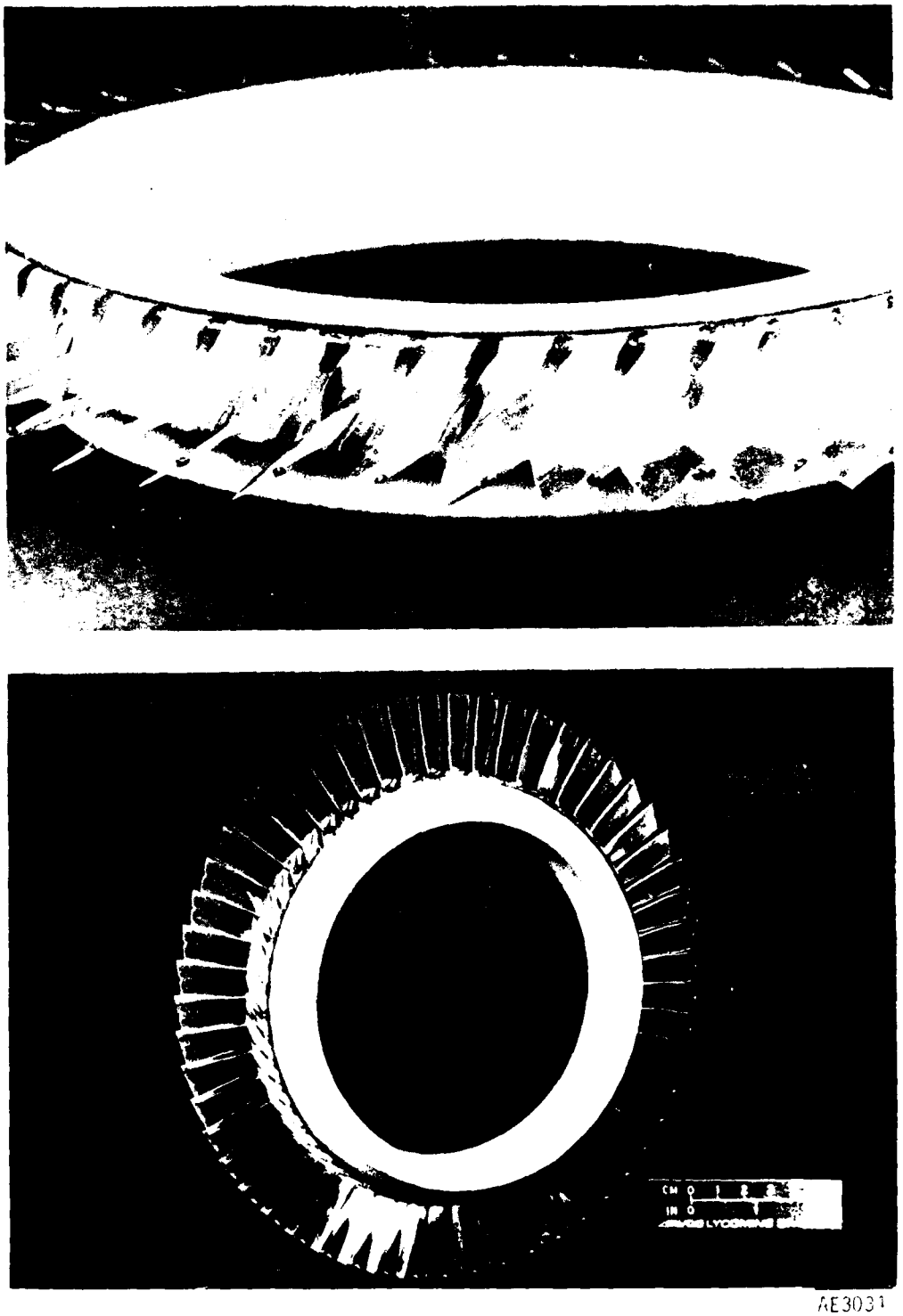

AE3031

Figure 34. Fifth-Stage Rotor Investment Casting Pattern

TABLE 5. FIFTH-STAGE LOW-PRESSURE COMPRESSOR ROTOR CASTING (P16 PROCESS) NONCONFORMING DIMENSIONS, PRIOR TO TOOL REWORK

B/P Dim.	Tol.	Zone	Actual Dim.	Code *
8.016 Dia. 203.606 mm	+/- .030 (+/- .762 mm)	4-C	8.126/8.134 (206.4/206.604 mm)	A
5.962 Dia. 151.435 mm	+/- .0075 +/- (.1905 mm)	4-B	6.002/6.003 (152.451/152.476 mm)	A
5.360 Dia. 136.144 mm	+/- .02 +/- (.508 mm)	5-B	5.395/5.410 (137.033/137.414 mm)	B
5.880 Dia. 149.352 mm	+/- .015 (.381 mm)	4-B	5.920/5.926 (150.368/150.520 mm)	A
Airfoil Charts	+/- .002 (.0508 mm)	2-B	Nom. to +/- .005 (.127 mm)	B
Max. Airfoil Thickness "S"	+/- .004 (.1016 mm)	2-B	.007 O/Nom. (.1778 mm)	B
Chord "L"	+.005/-.015 (+.127/.381 mm)	2-A	.002 O/Nom. (.0508 mm)	C
54 Blades Equally Spaced	.005 Tot. (.127 mm)	4-C	.011 Tot. (.2794 mm)	G
Surface	.015 Tot. (.381 mm)	4-C	.023 Tot. (.5842 mm)	C
"G" Angle All Sections	+/-0 Deg, 30'	2-A	To 0 Deg, 54' U/Min	G

* A - Immediate tool correction needed (part rejected for this dimension).
B - Limited approval (tool to be corrected, as instructed).
C - Accept for the life of the tool with periodic layout audits as scheduled to confirm compliance during tool life.
G - Airfoil corrections to be made in special gaging fixture.

TABLE 6. FIFTH-STAGE LOW-PRESSURE COMPRESSOR ROTOR CASTING (P16 PROCESS) NONCONFORMING DIMENSIONS, AFTER TOOL REWORK

B/P Dim.	Tol.	Zone	Actual Dim.	Code *
8.016 Dia. 203.606 mm	+/- .030 .762 mm	4-C	8.094/8.118 205.588/206.197 mm	B
5.962 Dia. 151.435 mm	+/- .0075 .1905 mm	4-B	5.963/5.985 151.460/152.019 mm	C
5.880 Dia. 149.352 mm	+/- .015 .381 mm	4-B	To Print	

* A - Immediate tool correction needed (part rejected for this dimension).
B - Limited approval (tool to be corrected, as instructed).
C - Accept for the life of the tool with periodic layout audits as scheduled to confirm compliance during tool life.

TABLE 7. FIFTH-STAGE LOW-PRESSURE COMPRESSOR ROTOR CASTING (P34 PROCESS) NONCONFORMING DIMENSIONS

B/P Dim.	Tol.	Zone	1) Previous Dim.	2) P34 Dim.	Estimated Code *
5.962 Dia. 151.435 mm	+/- .0075 .1905 mm	4-B	5.963/5.985 151.460/152.019	5.995/6.005 152.273/152.527 mm	A
8.016 Dia. 203.606 mm 3)	+/- .030 .762 mm	4-C	8.094/8.118 205.588/206.197	8.095/8.112 205.613/206.045 mm	B
4.96 Dia. 125.984 mm	+.010 Max. .254 mm	4-C	Solid Hub	4.694/4.700 119.228/119.38 mm	C

* A - Immediate tool correction needed (part rejected for this dimension).
B - Limited approval (tool to be corrected, as instructed).
C - Accept for the life of the tool with periodic layout audits as scheduled to confirm compliance during tool life.

1) Measured by layout of a P16 produced casting after tool rework (with solid hub gate).

2) Measured by layout of a P34 produced casting (hub not cast solid).

3) Machining B/P (3-100-233X02) allows a 5.080 (129.032 mm) diameter as a maximum.

4.3 PHASE II CASTING PARAMETER DEVELOPMENT

Casting parameter studies were conducted, and the casting processes for the three stages were defined to produce the thin-bladed integral rotors. The best of these processes were subsequently used to cast rotors for the mechanical properties evaluation portion of the program. Table 8 compares the casting processes developed as part of this effort. The product yield shown in this table is based on visual, radiographic, and fluorescent penetrant inspection of the rotors. In the case of the first-stage rotor, three engine runable castings were produced. Three second-stage castings which met NDT requirements were alsoproduced for future engine operation. But, metallurgical anomalies found late in the program caused concern regarding their airfoil fatigue capabilities. The process for the first-stage is considered viable from a production standpoint. However, additional second-stage casting will have to be conducted to under- stand the unexpected metallurgical phenomenon affecting fatigue life. Considerable difficulty was encountered in casting the fifth-stage, and more work is required to "productionize" the process. Since the most promising process pro- duces a dimensionally oversize fifth-stage rotor, no engine runnable castings were made.

4.3.1 First-Stage Low-Pressure Rotor

Process P1 was developed for the production of first-stage rotors (Figure 35) with a resultant product yield of 75 percent. The P1 process was capable of producing first-stage integrally cast rotors with engine acceptable metallurgical quality.

Table 9 lists the two casting processes investigated and their effects upon casting metallurgical quality, for the two general categories of "mold fill" and "surface integrity".

The ratings listed in Table 9 are subjective judgements for each of the two quality categories as determined by visual, radiographic, and fluorescent penetrant-inspection techniques. A rating of "poor" indicates that the level of misruns or surface defects are far below acceptable standards. Ratings of "fair" describe surface integrity or mold fill which approach but are below the quality which is usually accepted for engine hardware. When some of the evulated castings from a specific process achieve "good" ratings; while others are "poor", the term "fair" was used to describe these results. A "good" rating was given in either category when a process achieved at least a 50 per- cent level of acceptable product (i.e., half of the castings produced by the process were able to meet minimal engine acceptance requirements) for that category. "Good" ratings in both quality categories indicated that the cast- ings could be machined for engine usage, but it does not mean that the rotor was entirely free of surface defects or misruns.

TABLE 8. SELECTED CASTING PROCESSES FOR AGT 1500 FIRST-, SECOND-, AND FIFTH-STAGE ROTOR PRODUCTION

Rotor Stage	Process No.	Qty Cast	(1) Mold Type	(2) Insulation Thickness	Mold Preheat	(3) Metal Temp.	(4) Estimated Product Yield
1	P1	12	E	1/2" All Over 12.7 mm	2150°F 1177°C	P+450°F P+232°C	75%
2	P4	16	CC	1" (25.4 mm) - Mold 1/2" Pour Cup	2000°F 1093°C	P+325°F P+163°C	75%
5	P16 5)	24	A	1/4" (6.35 mm) - Mold 1/2" Pour Cup	2150°F	P+400°F P+204°C	10%
5	P34 5)	10	A	1/4" - Mold 1/2" Pour Cup	2150°F	P+450°F	50%

(1) Exact mold compositions are proprietry to the casting vendor; mold systems have been designated above as: E, CC, and A. An investment mold consists of fine grained face coat layers backed by coarser layers of "stucco" sand. These layers are composed of zircon, alumina, and silica refractories.

(2) Insulating blankets are composed of "KAOWOOL" (alumina-silica fibers).

(3) "P" is the melting plateau (i.e., liquidus) temperature of the alloy. For example, the P+400°F (204°C) refers to a 400°F (204°C) melt superheat.

(4) Product yield is a measure of the ability of a casting process to produce usable product (i.e., castings free from cracks or rejectable levels of airfoil misruns, surface pitting, or negative troughs). Radiographic, visual, and penetration inspection NDI techniques form the basis for this judgement. Product yield data excludes inclusion defects which are more related to general melting and casting practices than to the individual rotor casting configuration.

(5) P16 process casts the rotor hub solid. The P34 process casts the rotor hollow using eight gate runners which extend from the central pouring cup to the ID of the rotor platform.

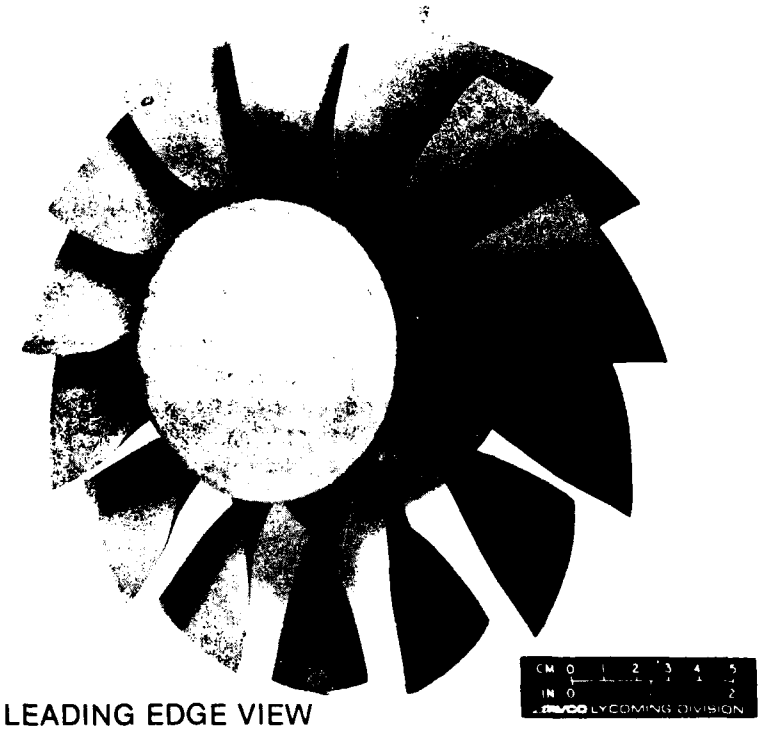

LEADING EDGE VIEW

AE3001

Figure 35. First-Stage Integrally Cast Rotor

TABLE 9. DETAILS OF THE FIRST-STAGE CASTING PARAMETER STUDY

Process No.	Qty. Cast	(1) Mold Type	(2) Insulation Thickness	Mold Preheat	(3) Metal Temp.	Rating (4) Mold Fill	Rating (4) Surface Integrity
P1	12	E	1/2" All Over 12.7 mm	2150°F 1177°C	P+450°F P+232°C	Good	Fair
P2	2	E	1/2" All Over 12.7 mm	2000°F 1093°C	P+325°F P+163°C	Fair	Poor

(1) Exact mold compositions are priprietary to the casting vendor; the mold system used for this wheel has been designated as "E." An investment mold consists of fine grained face coat layers backed by coarser layers of "stucco" sand. These layers are composed of zircon, alumina, and silica refractories.

(2) Insulating blankets are composed of "KAOWOOL" (alumina-silica fibers).

(3) "P" is the melting plateau (i.e., liquidus) temperature of the alloy. For example, the P+450°F (232°C) refers to a 450°F (232°C) melt superheat.

(4) Ratings are subjective judgements. Mold fill refers to misruns (or lack of same) on the thin leading and trailing edges of the airfoils. Surface integrity refers to the airfoil surface only; rating is principally based on the presence or absence of surface troughs, cracks and/or pits as determined by visual and penetrant inspection.

The selected process (P1) demonstrated its ability to produce rotors with a minimum of misruns. Misruns are produced when the molten alloy solidifies prematurely during pouring and does not completely fill portions of airfoil edges and corners. Because the P1 process did not have a misrun problem the process received a "good" rating in the category of mold fill. The process was also capable of providing castings with a minimum of surface pitting and hot-tear cracks. Normally this would have been sufficient for it to earn a "good" rating for its surface integrity. However, the occasional appearance of rough surface finishes (up to 180 rms instead of 90 rms on the airfoil and flow channel surfaces) reduced the overall rating to "fair". However, it was found that by using hand blending and abrasive flow finishing, acceptable surface finishes can be achieved on the majority of the castings.

The second process (P2) which was attempted was aimed at reducing the tendency of the alloy to react with the mold material and thereby, improve the overall surface finish. This process used a lower mold preheat temperature and a lower metal pouring temperature. But results were not encouraging. A greater number of airfoil misruns, surface pits, and hot tear cracks were observed, compared with the P1 process. The ratings of this process reflected the degradation of the cast product ("fair" - mold fill and "poor" - surface integrity). For this reason, the P1 process was selected to produce the remaining rotors for the contract, relying on post-casting surface conditioning to provide acceptable surfaces.

4.3.2 Second-Stage Low-Pressure Rotor

Process P4 was selected to produce the second-stage integrally cast rotors (Figure 36). The P4 process was able to produce castings of engine acceptable quality, approximately 75 percent of the time. This judgement was based on conventional visual, radiographic, and penetrant inspection techniques. However, late in the program, subsurface metallurgical anomalies were discovered which could detrimentally affect airfoil fatigue life and will require some adjustments in future casting processes.

Table 10 lists the parameters associated with the four casting processes evaluated for second-stage rotor casting development. Early processing trials using mold system "AA" (processes P1 and P2) indicated that that mold material was too weak. Although a low strength mold helps minimize the occurrence of hot-tear cracking, other casting problems such as mold splits, mold breakage, and inclusions did result. In order to eliminate these casting problems without incurring hot-tear cracking, two other mold materials were investigated. In addition, the P1 and P2 trials indicated that a too low metal-pouring temperature results in excessive misruns, while at too high a temperature cast surface degradation occurs. A pouring temperature of P+325^{o}F (163^{o}C) was, therefore, selected for the remaining casting trials.

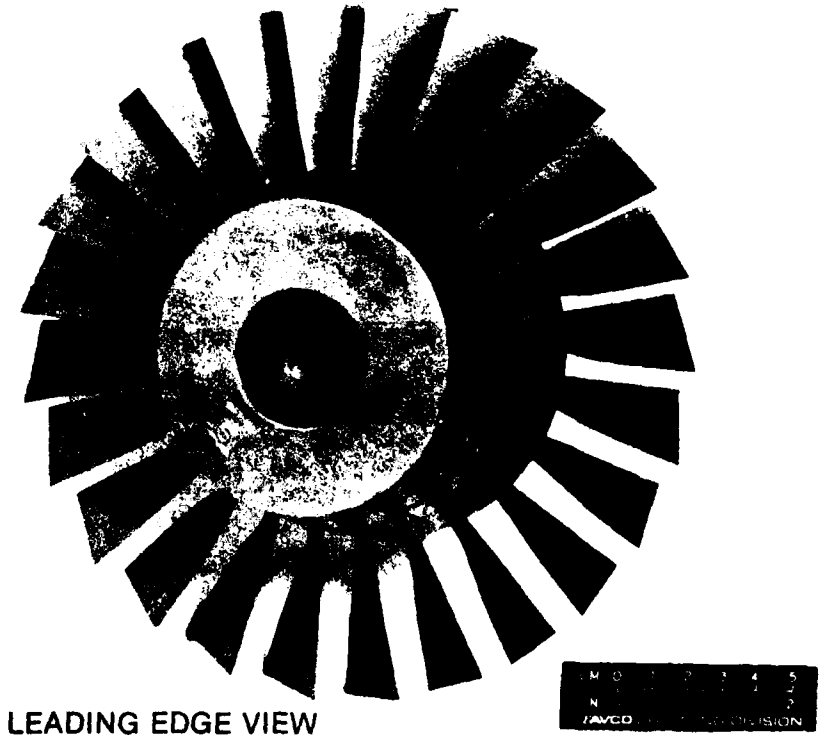

Figure 36. Second-Stage Integrally Cast Rotor

TABLE 10. DETAILS OF THE SECOND-STAGE CASTING PARAMETER STUDY

Process No.	Qty. Cast	(1) Mold Type	(2) Insulation Thickness	Mold Preheat	(3) Metal Temp.	Rating (4) Mold Fill	Rating (4) Surface Integrity
P1	2	AA	1" (25.4 mm) on mold only	2000°F 1093°C	P275°F P+135°C	Poor	Poor
P2	2	AA	1" (25.4 mm) on mold only	2000°F	P375°F P+191°C	Poor	Poor
P3	4	BB	1" (25.4 mm) on mold only	2000°F	P325°F P+163°C	Fair	Fair
P4	13	CC	1/2" (12.7 mm) - mold 1/2" (12.7 mm) - pour cup	2000°F	P325°F P+163°C	Good	Good

(1) Exact mold compositions are proprietary to the casting vendor; mold systems have been designated above as: AA, BB, and CC. An investment mold consists of fine grained face coat layers backed by coarse layers of "stucco" sand. These layers are composed of zircon, alumina, and silica.

(2) Insulating blankets are composed of "KAOWOOL" (alumina-silica fibers).

(3) "P" is the melting plateau (i.e., liquidus) temperature of the alloy. For example the P+275°F (135°C) refers to a 275°F)204°C) melt superheat.

(4) Ratings are subjective judgements. Mold fill refers to misruns (or lack of same) on the thin leading and trailing edges of the airfoils. Surface integrity refers to the airfoil surface only; rating is principally based on the presence or absence of surface troughs, cracks and/or pits as determined by visual and penetrant inspection.

The P3 process appeared to be an improvement over the P1 and P2 processes. Some of the rotors produced still exhibited misruns on isolated airfoils. The P4 process again modified the mold material (which affects the thermal conductivity of the mold system) and included the addition of mold insulation on the pouring cup. This process produced rotors relatively free of misruns. The "good" rating for the surface integrity of the P4 rotors was given in spite of the existence of occasional mold splits which required post-casting finishing for removal of the resultant defects. These mold splits did not reduce the number of acceptable rotors to below 50 percent and, therefore, did not reduce the rating for surface integrity. The mold splits occurred in the airfoils rather than in the airfoil fillet and platform as described below for the fifth-stage rotors.

4.3.3 Fifth-Stage Low-Pressure Rotor

While first-stage and second-stage casting processes showed promising results, the P16 process initially developed for fifth-stage rotor (Figure 37) production exhibited a product yield of less than 10 percent. This outcome was not surprising because of the level of difficulty associated with casting the extremely thin airfoils of this configuration. Therefore, although the P16 process was used to cast fifth-stage rotors for mechanical testing, rotor casting development continued for nearly the duration of this contract. Casting feasibility was finally demonstrated by the promising results of the P34 process. This process appeared capable of producing metallurgically acceptable rotors at a product yield of 50 percent based upon a sampling of 10 rotors and initially excluding inclusion scrap, which is related to general melting/casting practices rather than to the individual rotor configuration.

Table 11 lists the various casting processes investigated and their effects upon casting metallurgical quality (for the two general categories of mold fill and surface integrity).

Originally it was thought that the main difficulty in casting fifth-stage rotors would be filling the narrow airfoil passages without incurring excessive misruns. Figure 38 shows an example of a fifth-stage airfoil misrun. Because of the concern over misruns, a decision was made to cast the rotor hub as a solid section. This was accomplished by filling the 4.96 in. (126 mm) diameter of the wax pattern ID was filled in with wax prior to mold fabrication. Casting a solid hub was expected to provide a massive, continuous, central gate for enhanced feeding of the airfoils. This gating system is illustrated through comparison of the original wax pattern (Figure 34) without the center gate to the actual casting (Figure 37) with the gate cast and still in position.

Although a few misruns were encountered in some of the castings within the development effort, these defects did not occur as frequently as originally expected. Hot-tear cracking (Figures 38 and 39) and surface pitting (Figure 40) were also found in castings, but were later eliminated through process parameter adjustments. The most difficult and frequent obstacle to the casting of engine quality fifth stage rotors was, however, due to mold splitting which resulted in the scrapping of rotors when manifested as visual, negative defects

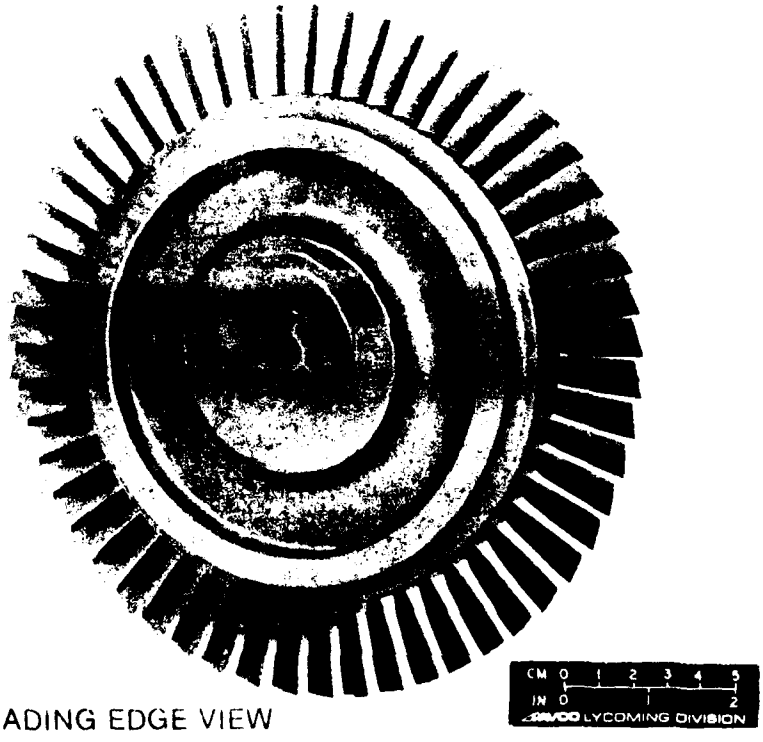

Figure 37. Fifth-Stage Integrally Cast Rotor

TABLE 11. DETAILS OF THE FIFTH-STAGE CASTING PARAMETER STUDY (Sheet 1 of 4)

Process No.	Qty. Cast	(1) Mold Type	(2) Insulation Thickness	Mold Preheat	(3) Metal Temp.	Gating System	Rating (4) Mold Fill	Rating (4) Surface Integrity
P1	2	A	1" - pour cup 1/2" - mold	2300°F 1260°C	P+500°F P+260°C	Convex Full Hub	Poor	Poor
P2	1	B	1" - pour cup 1/2" - mold	2300°F	P+400°F P+204°C	Convex Full Hub	Poor	Poor
P3	1	A	1" - pour cup 1/2" - mold	2300°F	P+400°F P+204°C	Convex Full Hub	Fair	Poor
P4	1	A	1" - pour cup 1/2" - mold	2300°F	P+375°F P+191°C	Convex Full Hub	Fair	Poor
P5	1	B	1" - pour cup 1/2" - mold	2300°F	P+500°F P+260°C	Convex Full Hub	Poor	Poor
P6	1	A	1" - pour cup 1/4" - mold	2100°F 1149°C	P+375°F P+191°C	Convex Full Hub	Poor	Fair
P7	1	C	1" - pour cup 1/4" - mold	2100°F	P+375°F P+191°C	Convex Full Hub	Poor	Poor
P8	1	C	1" - pour cup 1/4" - mold	2100°F	P+450°F P+232°C	Convex Full Hub	Poor	Poor
P9	2	A	1" - pour cup 1/4" - mold	2100°F	P+375°F P+191°C	Convex Full Hub	Fair	Poor
P10	4	D	1" - pour cup 1/4" - mold	2100°F	P+375°F P+191°C	Convex Full Hub	Fair	Poor
P11	2	D	1" - pour cup 1/2" - mold	2150°F 1177°C	P+425°F P+218°C	Convex Full Hub	Poor	Poor
P12	2	D	1" - pour cup 1/4" - mold	2100°F 1149°C	P+400°F P+204°C	Convex Full Hub	Poor	Fair

TABLE 11. DETAILS OF THE FIFTH-STAGE CASTING PARAMETER STUDY (Sheet 2 of 4)

Process No.	Qty. Cast	(1) Mold Type	(2) Insulation Thickness	Mold Preheat	(3) Metal Temp.	Gating System	Rating (4) Mold Fill	Rating (4) Surface Integrity
P13	2	A	1" - pour cup 1/4" - mold	2100°F	P+400°F P+204°C	Convex Full Hub	Poor	Fair
P14	2	A	1" - pour cup 1/4" - mold	2150°F 1177°C	P+375°F P+191°C	Convex Full Hub	Poor	Fair
P15	2	D	1" - pour cup 1/4" - mold	2150°F 1177°C	P+375°F P+191°C	Convex Full Hub	Poor	Poor
5) P16	6	A	1/2" Pour Cup 1/4" - Mold	2150°F 1177°C	P+400°F P+204°C	Convex Full Hub	Fair	Fair
P17	1	E	1/2" Pour Cup 1/4" - Mold	2150°F	P+400°F	Convex Full Hub	Good	Poor
P18	1	F	1/2" Pour Cup 1/4" - Mold	2150°F	P+400°F	Convex Full Hub	Good	Poor
P19	2	F	1/2" Pour Cup 1/4" - Mold	2150°F	P+400°F	Convex Full Hub	Fair	Poor
P20	2	A	1/2" Pour Cup 1/4" - Mold	2150°F	P+400°F	Added 4 Vent Tubes	Fair	Poor
P21	2	A	1/2" Pour Cup 1/4" - Mold	2150°F	P+400°F	Added 4 Vent Tubes	Fair	Poor
P22	2	A	1/2" Pour Cup 1/4" - Mold	2150°F	P+400°F	Full Hub (Hollowed) + 4 Vents	Fair	Poor
P23	2	A	1/2" Pour Cup 1/4" - Mold	2150°F	P+450°F P+232°C	Full Hub (Hollowed) + 4 Vents	Fair	Poor
P24	2	A	1/2" Pour Cup 1/4" - Mold	2150°F	P+375°F P+191°C	Full Hub (Hollowed) + 4 Vents	Fair	Poor

TABLE 11. DETAILS OF THE FIFTH-STAGE CASTING PARAMETER STUDY (Sheet 3 of 4)

Process No.	Qty. Cast	(1) Mold Type	(2) Insulation Thickness	Mold Preheat	(3) Metal Temp.	Gating System	Rating (4) Mold Fill	Rating (4) Surface Integrity
P25	2	A	1/2" Pour Cup 1/4" - Mold	2150°F	P+300°F P+149°C	Full Hub (Hollowed) + 4 Vents	Fair	Poor
6) P26	2	A	1/2" Pour Cup 1/4" - Mold	2100°F 1149°C	P+400°F P+204°C	Full Hub (Hollowed) + 4 Vents	Fair	Poor
P27	2	A	1/2" Pour Cup 1/4" - Mold	2100°F	P+375°F P+191°C	Full Hub (Hollowed) + 4 Vents	Fair	Poor
6) P28	2	A	1/2" Pour Cup 1/4" - Mold	2100°F	P+400°F P+204°C	Full Hub (Hollowed) + 4 Vents	Fair	Poor
P29	2	A	1/2" Pour Cup 1/4" - Mold	2200°F 1204°C	P+400°F	Full Hub (Hollowed) + 4 Vents	Fair	Poor
P30	2	A	1/2" Pour Cup 1/4" - Mold	2250°F 1232°C	P+450°F P+232°C	Full Hub (Hollowed) + 4 Vents	Fair	Poor
P31	2	A	1/2" Pour Cup 1/4" - Mold	2150°F 1177°C	P+450°F	Ring Gate + 4 Vents	Poor	Fair
P32	2	A	1/2" Pour Cup 1/4" - Mold	2150°F 1177°C	P+450°F	Intermittent Ring Gate + 4 Vents	Poor	Fair
P33	4	A	1/2" Pour Cup 1/4" - Mold	2150°F	P+450°F	Intermittent Ring Gate + 6 Spokes + 4 Vents	Poor	Fair

TABLE 11. DETAILS OF THE FIFTH-STAGE CASTING PARAMETER STUDY (Sheet 4 of 4)

Process No.	Qty. Cast	(1) Mold Type	(2) Insulation Thickness	Mold Preheat	(3) Metal Temp.	Gating System	Rating (4) Mold Fill	Rating (4) Surface Integrity
P34	10	A	1/2" Pour Cup 1/4" - Mold	2150°F	P+450°F	+ 8 Spokes + 4 Vents	Fair	Good

(1) Exact mold compositions are proprietary to the casting vendor; mold systems have been designated above as: A, B, C, D, etc. An investment mold consists of fine grained face coat layers backed by coarser layers of "stucco" sand. These layers are composed of zircon, alumina, and silica refractories.

(2) Insulating blankets are composed of "KAOWOOL" (alumina-silica fibers).

(3) "P" is the melting plateau (i.e., liquidus) temperature of the alloy. For example the P+500°F (260°C) refers to a 500°F (260°)melt superheat.

(4) Ratings are subjective judgements. Mold fill refers to misruns (or lack of same) on the thin leading and trailing edges of the airfoils. Surface integrity refers to the airfoil surface only; rating is principally based on the presence or absence of surface troughs, cracks and/or pits as determined by visual and penetrant inspection.

(5) P16, having given the best results up to the time mechanical test specimens were needed, was selected to produce the fifth-stage rotor castings for the contact's mechanical property evaluation.

(6) Vendor proprietary, post-casting cooling environmental changes.

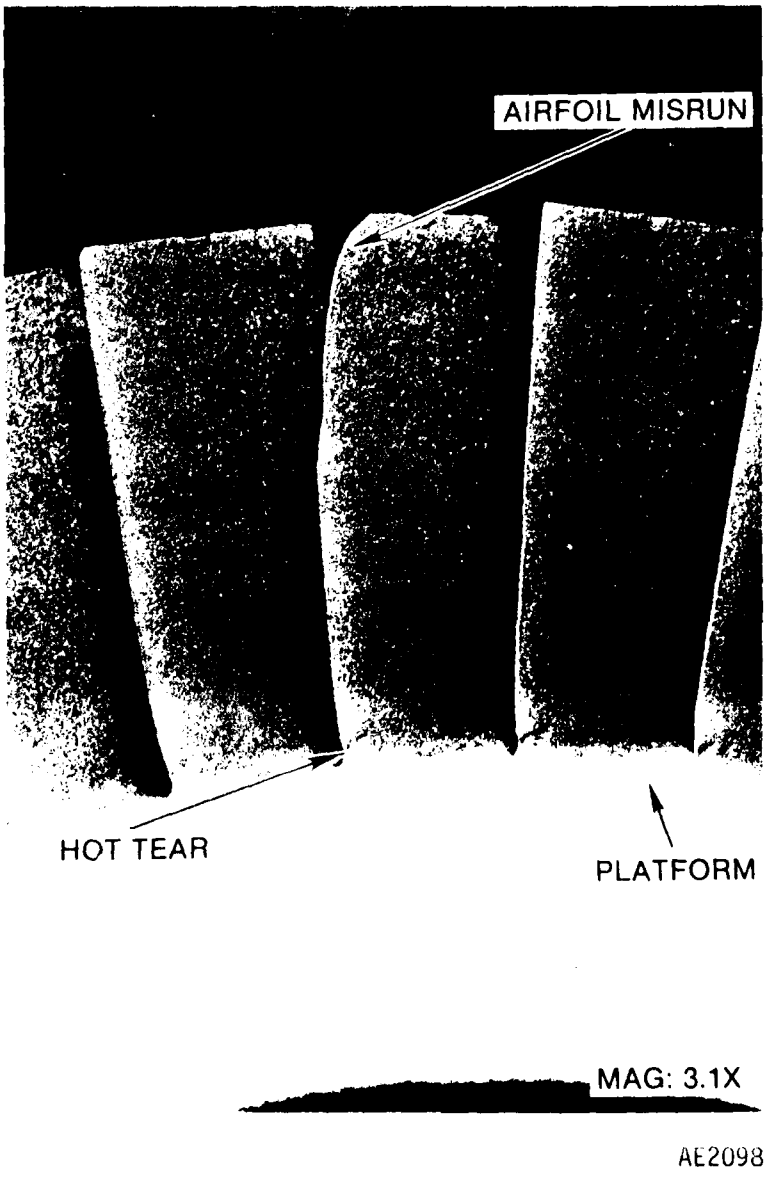

Figure 38. Example of Airfoil Misrun and Hot Tear Cracking in Fifth-Stage As-Cast (Unfinished) Rotor

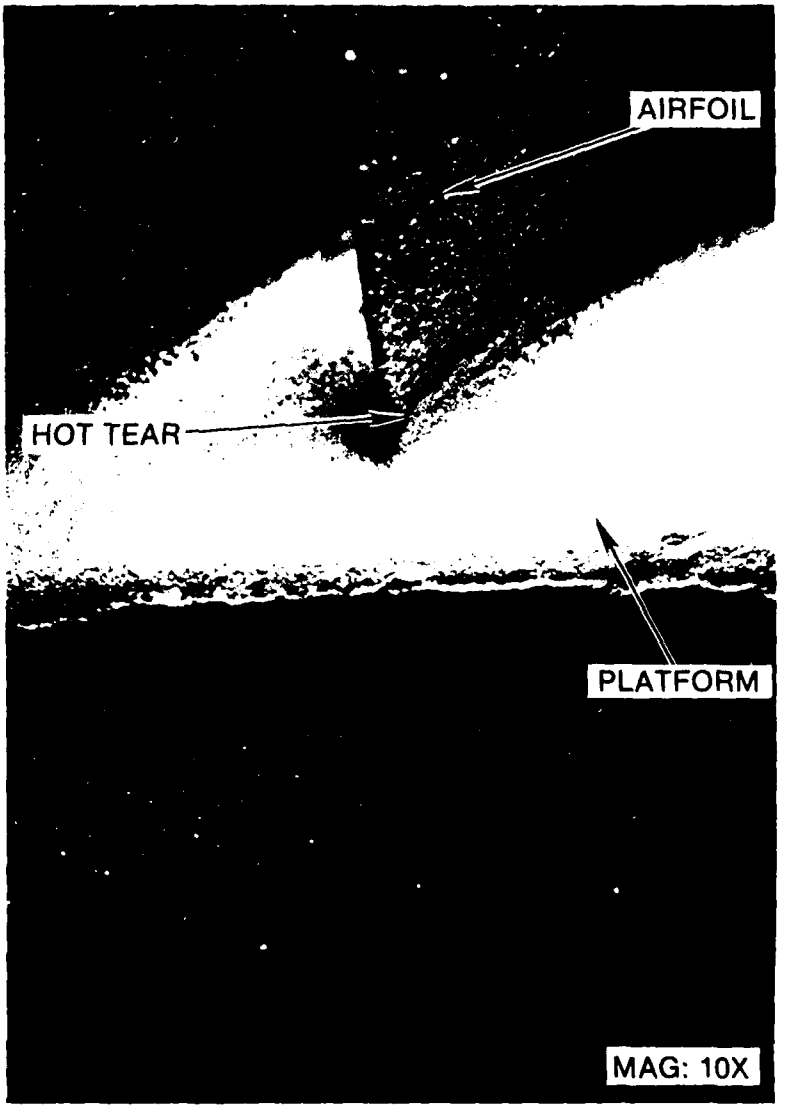

Figure 39. Magnified View of a Hot Tear at the Trailing Edge Fillet Radius of Fifth-Stage Rotor

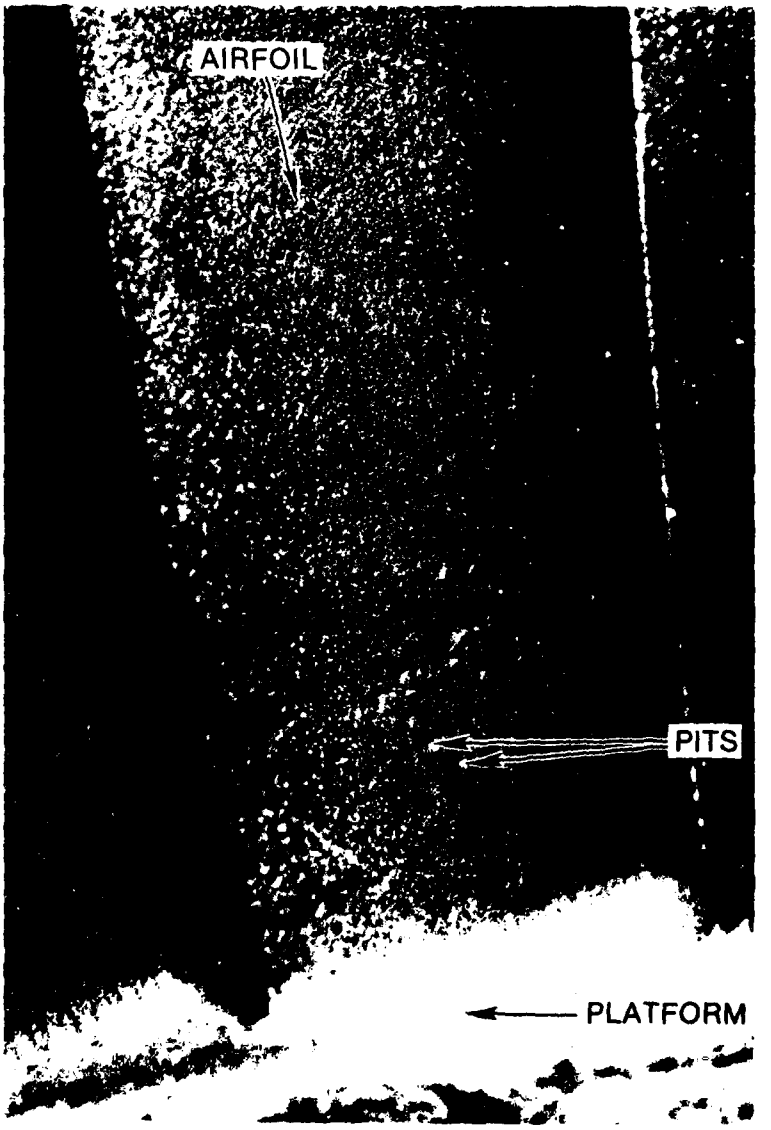

Figure 40. Example of Surface Pitting Found on Some Fifth-Stage Rotors

on the airfoil or fillet radii surfaces. While a positive metal fin can usually be removed by subsequent casting finishing operations, the negative trough cannot, and when this defect occurs on airfoil or blade fillet regions the casting (in most cases) has to be scrapped. This prompted an intensive study of this type of defect.

Mold splits commonly occur in investment castings and are due to cracks which develop in the mold during mold build-up or dewax. A comparison of Figures 41, 42, and 43 show the correspondance of cracks in the mold and the manifestation of these mold defects on the cast rotor surface. Normally, the molten metal fills these mold cracks and leaves a fin of positive metal in the solidified casting. Occasionally, however, a negative trough is produced. The positive metal is removable by post-casting finishing operations, but a negative trough is not reworkable.

Figure 44 shows a typical cross section through a negative trough. SEM, EDAX (energy dispersive analysis of X-rays) analysis of the fine micro-constituent (located in the bottom of the trough) indicated that it was probably a fine, complex metallic carbide. This region seemed enriched in alloy solute (i.e., chromium, silicon, and to some extent, nickel). This phase was visible only in the etched condition.

The relationship of this locally anomalous microstructure and chemistry to the occurrence of negative troughs is not well understood. It has been hypothesized that this phenomenon may have been caused by some residual carboneous material in the mold which reacted with the molten alloy during solidification (probably as a gas/mold/metal reaction). Carbon monoxide gas may have concentrated within some of the mold splits faster than the vacuum system and mold permeability could dissipate it. Subsequent chemical reduction of CO to carbon and its local diffusion into the solidifying metal (at the mold/metal interface) may have occurred. This local carbon pickup could have resulted in isolated areas of high carbon and solute concentrations, which in ferrous alloys could locally depress the alloy's melting point. A negative trough may have been produced by some combination of final solidification contractions and locally high carbon monoxide vapor presures.

In the absence of a fundamental understanding of the cause of mold splits, process development was continued in an effort to eliminate these defects. The results of the parametric variations (re. P1-P19) used up to this point in the program were carefully reviewed. During this unsuccessful attempt to develop a viable production process, the mold system thermal parameters (mold temp., metal pour temp., and the thickness of insulating material) were systematically modified to try to improve the overall casting quality. The review showed that hot-tear cracking, misruns, and surface pitting were influenced by these changes. However, these process variations seemed to have little effect in alleviating mold splits. After exhausting other alternatives, fifth-stage rotor process development was redirected towards gating changes. This step was taken reluctantly because the gating configuration used produced a minimum of mis-run problems and changes could affect the rotor dimensions. As is listed in Table 11 (P20-P34), a series of trials were conducted to determine the effects of alternate gating schemes on casting quality and in particular the occurrence of mold splits. Modified gating was ultimately successful in the reduction of mold splitting (using the P34 casting process), while incurring only a minor increase in airfoil misruns.

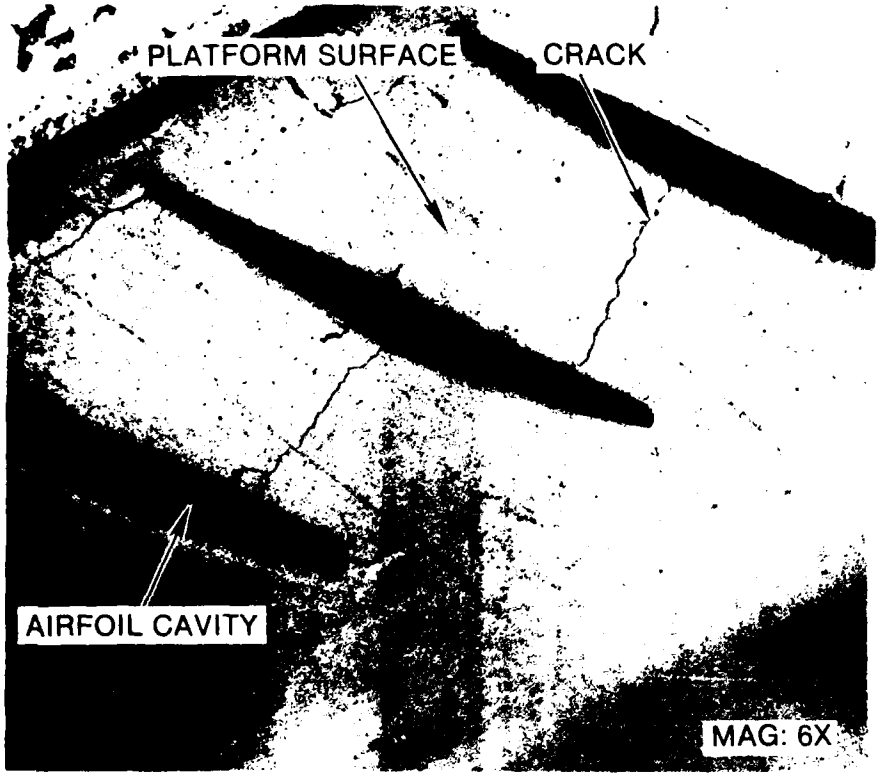

Figure 41. Interior of Fifth-Stage Mold Showing Cracks After Dewax, Burnout, and Firing

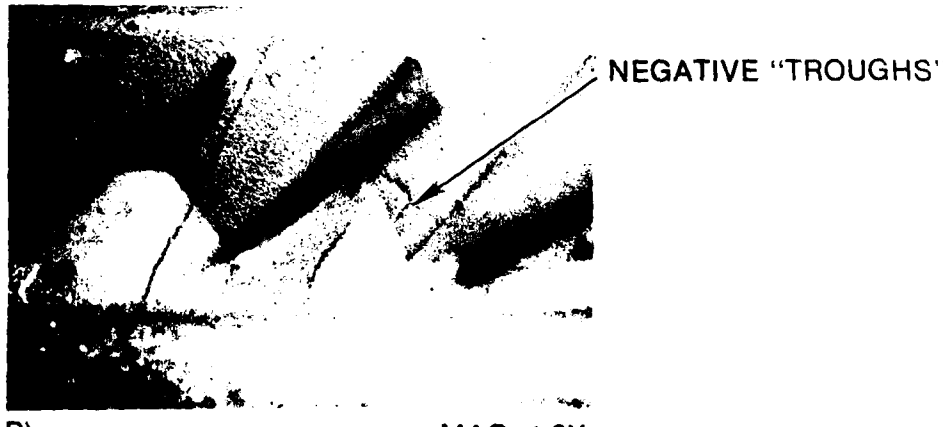

Figure 42. Examples of Fifth-Stage Rotor Fins and Troughs

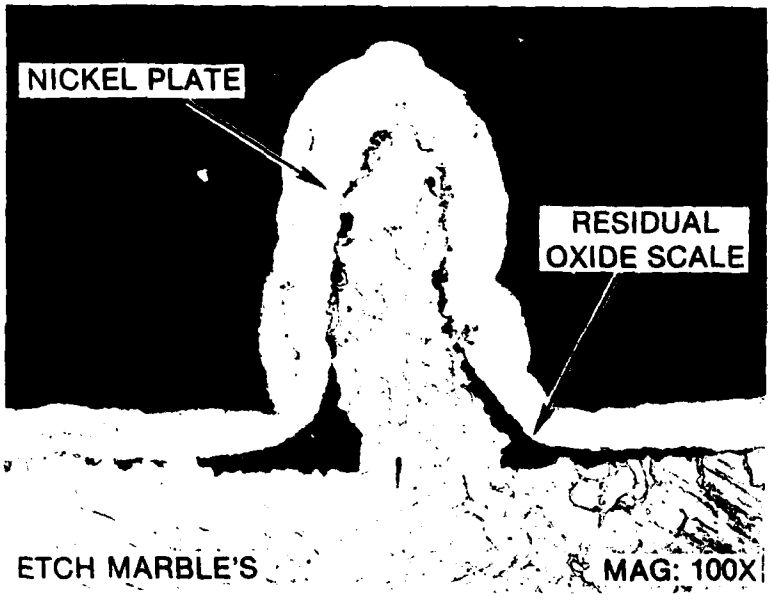

AE2093

Figure 43. Microstructure of a Metal Fin (Produced by the Intrusion of Molten Alloy Into a Mold Split)

AD-A127 663 INTEGRALLY CAST LOW-COST COMPRESSOR(U) AVCO LYCOMING DIV STRATFORD CT B H HESSLER ET AL. 03 JAN 83 TACOM-TR-1273 DAAK30-78-C-0039 2/2

UNCLASSIFIED F/G 11/6 NL

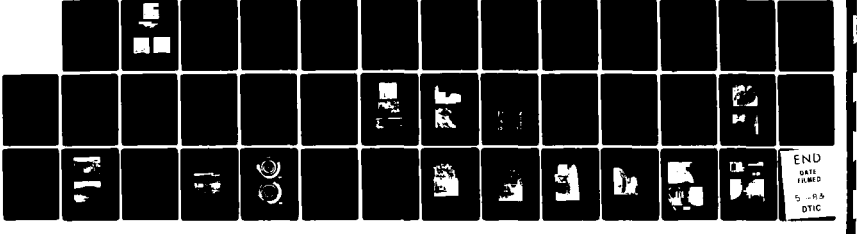

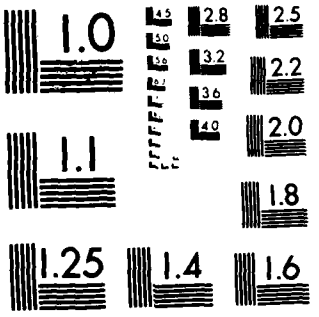

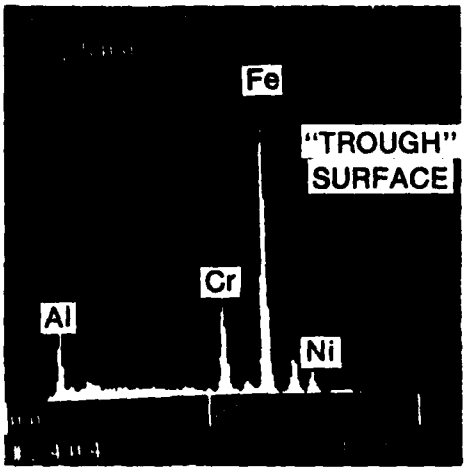

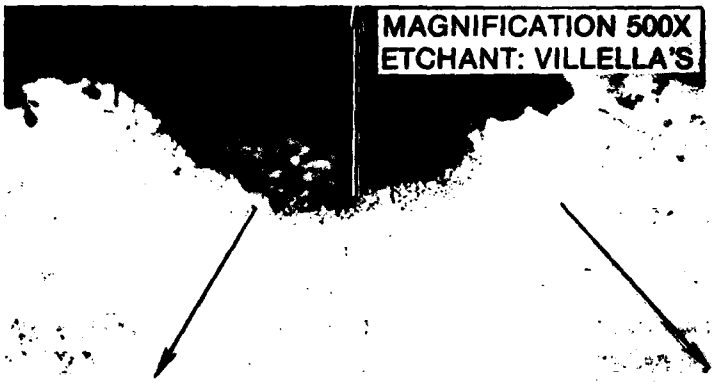

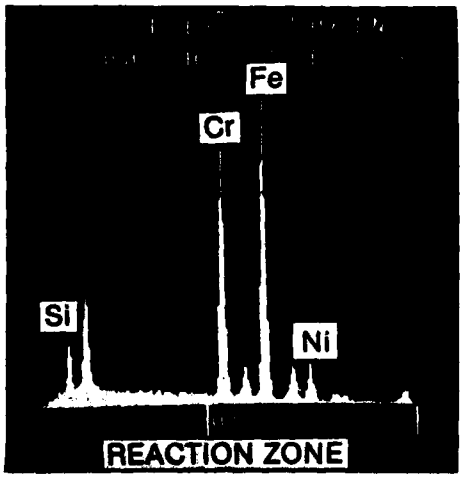

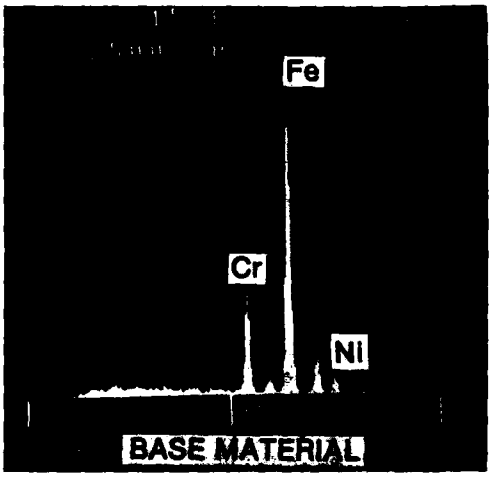

Figure 44. Microstructure and EDAX Analysis of a Trough
(Produced by a Mold Split)

A sketch of the P34 casting process gating is shown in Figure 45. The gating consists of eight interrupted gates (called "spoke gates) which extend radially out from the center sprue and intersect the hub (at approximately the 4.96 in. diameter)
across from the mold airfoil passages.

The probable explanation as to why the gating change reduced the occurrence of mold splits and mitigated the occurrence of negative troughs is improved and more efficient "dewaxing." Dewaxing is the process by which the wax and plastic pattern is melted and/or burned out of the mold. Several techniques such as high temperature "flash fire", low temperature steam autoclaves, etc., are used. But each heats the wax/plastic assembly causing it to expand within the ceramic mold. Since the thermal expansion coefficients of wax and plastic are greater than that of the ceramic mold, it is possible to develop high pattern/mold stresses before the wax/plastic material softens sufficiently to plastically yield and flow out of the mold cavity. In the fifth-stage rotor with its massive hub gate, enough wax remained solid within the pouring cup/hub region to cause stresses to build up on the outer hub and fillet surfaces. The pattern of mold splits induced was a result of the wax expansion stresses that had built-up within the mold.

Initial gating modifications (P20-P21) were unsuccessful in an attempt to "vent" (i.e., provide better exiting paths for the wax as it tried to flow from the mold) the pattern. This method employed auxiliary vent runners which attached to the hub from the pouring cup, passing over the center hub gate. This method was not effective and other more drastic (with respect to final casting dimensions as well as gating efficiency) methods were tried. Hollowing the center hub gate (P22-P30) seemed to help by reducing the volume of wax which had to soften and flow from the mold; but the small improvement in product yield did not justify adoption of this technique as the final process solution. The only gating method which seemed to solve the mold splitting problem was to remove the central hub gate entirely (P31-P34). The thinner gate runners in P34, with their high surface-to-volume ratios, offered a more uniform mold and pattern heating. As a result, enough of the pattern was able to flow from the mold to prevent significant splitting damage and result in approximately a 50 percent product yield. The reason that the resulting product yield was only 50 percent was due to a combination of defects which, although they had been minimized, were still fatal to the casting when they occurred. The defects encountered included: misruns, hot tears, and inclusions, as well as an occasional negative trough. Additional process modifications will be required to further reduce the occurrence of these casting defects.

The discussion above was concerned with mold splits and the elimination of the resulting defects through gating changes. However, other process variables such as mold composition and thermal parameters also have an influence on casting quality. The effects of these parameters are discussed below.

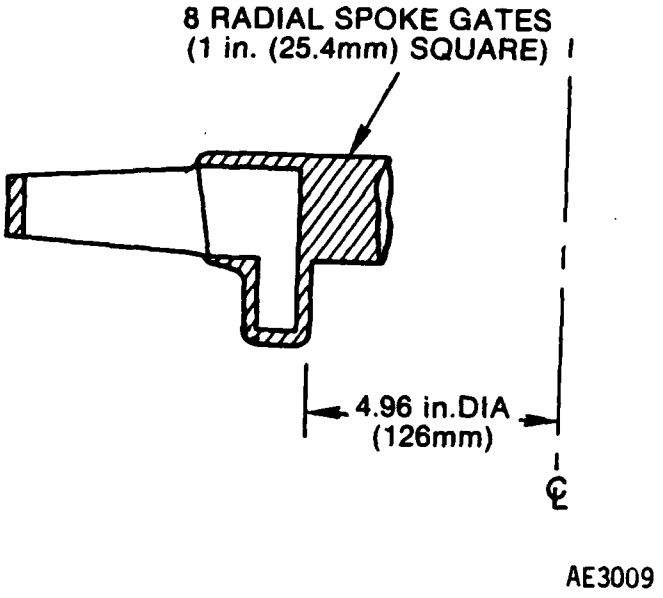

Figure 45. Sketch of the P34, Fifth-Stage Gating System

The effects of mold composition, with respect to mold fill, was significant because composition can influence the freezing and the post-solidification cooling rates of castings (due to thermal mass and heat transfer characteristics) and can disrupt normal alloy fluidity due to mold/metal surface tension and interactions. In addition, mold composition affects the propensity of the castings to hot tear crack. This is directly related to mold versus casting strength at elevated temperatures. Finally, changes in mold composition seem to correspond to changes in casting surface integrity (mold/metal reactions at elevated temperatures). The effect of mold changes is shown in Table 11 (processes P1-P20). Finally, mold system "A" was selected as an optimum for fifth-stage rotor casting. This mold system was used for both the P16 process (used to cast fifth-stage rotors for the mechanical testing portion of the contract) and the P34 process (best process to date).

Thermal parameters were used to help "fine tune" the casting processes; these parameters (i.e., mold temperature, metal pouring temperature, and insulation thickness) were varied in an effort to understand their effect on mold fill and surface integrity. The initial values of casting parameters were selected based upon practical experience with similar parts cast in Custom 450 alloy.

Contrary to what might have been expected, higher temperatures did not consistently benefit mold fill. However, higher temperatures and/or slower cooling rates did seem to impair surface quality. The small volume of molten alloy required to fill the thin airfoil section and the high surface-to-volume ratio of the mold's airfoil cavity, caused heat extraction from the molten alloy into the mold walls to be extremely efficient and rapid. Solidification under these conditions is so quick that further raising the mold temperature to reduce heat extraction or raising the pouring temperature to increase fluidity did not seem to appreciably reduce misruns. However, the higher temperatures provided more favorable conditions for mold/metal re- actions (i.e., mold pitting). Although the thermodynamics affecting mold pit- ting is poorly understood, pits are thought by some investigators to result from a reduction of oxides. Oxide stabilities decrease with increasing tem- peratures and elements such as carbon can begin reducing less stable oxides of chromium, silicon, and iron. Elemental diffusion also increases with higher temperatures, accelerating the rates of reactions which are thermodynamically possible at the particular temperature.

Mold insulation thickness did not affect alloy freezing rate and misruns because the solidification rate in the airfoil cavity was too rapid to be controlled by heat loss from the mold to the surrounding environment. Increasing insulation thickness did, however, seem to foster pitting by slowing the casting post-solidification cooling rate, thereby allowing a longer time at higher temperature to promote mold/metal reaction.

At the point in time when a casting process had to be selected to produce rotors for the mechanical property evaluation in accordance with the contract, the P16 process offered the best chance of producing rotors with sufficient quality for mechanical testing. As indicated in Table 11, the P16 process used mold system "A", a mold preheat of 2150°F (1177°C), a metal pouring tem- perature of P+400°F (204°C) (i.e., a superheat of 400°F above the alloy's liquidus), and a center hub gate. Subsequently, the P34 process (which proved to be the best process developed within the program) used the same casting process as P16 with the exception of a P+450°F (232°C) pouring temperature (slightly higher than in P16) and the runner gating system.

As stated above, the P34 casting process successfully reduced the occurrence of mold-split defects in fifth-stage rotor castings. However, due to the elimination of the massive amount of metal in the hub gate, casting solidification contractions were changed. This affected final casting dimensions. The deviant dimensions listed in Table VII will have to be corrected by tooling rework prior to the use of fifth-stage castings in any engine qualification program. Also, a 50-percent product yield is not in concert with the concept of a "production" process. More castings will have to be made, and the process will have to be "fine tuned" further to reduce scrap. It is not certain that this goal can be achieved.

4.4 PHASE II MECHANICAL PROPERTIES EVALUATION

The mechanical property testing of first-, second-, and fifth-stage rotors was completed. Tables 12-19 list the tensile LCF (low cycle fatigue), and HCF (high cycle fatigue) test data for all three stages, with the exception that first-stage HCF testing could not be performed because the airfoils were too rigid to test with the available equipment. The data were evaluated to determine the effects of HIP parameters, alloy chemistry, and configuration on integrally cast, Custom 450 rotor mechanical properties. The results of this evaluation follows:

4.4.1 Hot-Isostatic Press (HIP) Parameter Optimization

The HIP parameter study evaluated the mechanical property test results from fifth-stage cast rotors HIP'd at either 2050°F (1121°C) or 2165°F (1185°C). In general, the results of this study indicated that while tensile properties were comparable, the rotors HIP at 2165°F had better LCF and HCF properties than did rotors HIP at 2050°F. This led to the selection of the 2165°F HIP'd temperature for processing the balance of the rotors in the program. Table 20 summarizes the average mechanical properties of HIP'd 2165° (1185°C) and 2050°F (1121°C).

Although tensile ductility of 2165°F (1185°C) HIP'd rotors appeared to be slightly lower than that of material HIP'd at 2050°F (1121°C), the observed differences were not statistically significant. It can be concluded that the tensile properties of the alloy are insensitive to the range of HIP temperatures evaluated. Fatigue tests, however, were more discriminating.

As can be seen from Table 20, for both LCF and HCF, the mean life and mean -3 Sigma life of 2165°F HIP'd rotors were higher than those HIP'd at 2050°F (1121°C). Not included in Table 20 were the HCF test results from S/N 24 (re., Table 19) Figures 46 and 47 show the inordinate degree of S/N 24 data scatter, as well as its lower HCF values.

Scanning Electron Microscope (SEM) and Energy Dispersive Analysis by Xray (EDAX) evaluations were performed using six (6) S/N 24 airfoils which exhibited low HCF lives and six S/N 32 airfoils which exhibited good HCF lives. Both rotors (S/N24 and 32) were cast from the same heat of material (heat "SZN") and were HIP and heat treated together using the 2165°F (1185°C) HIP temperature and the standard Lycoming P6000 specification heat treatment. The evaluation of the airfoil fracture surfaces indicated that only one of the S/N 24 fatigue failures was the result of basic metallurgical anomalies; this

TABLE 12. TENSILE TEST RESULTS FOR FIRST-STAGE INTEGRALLY CAST ROTORS

	UTS		2% YS		% ELONG	% RA
	(MPa)	(KSI)	(MPa)	(KSI)		
	1141.8	165.6	1067.3	154.8	11.6	54.7
	1128	163.6	1059.03	153.6	13.0	53.0
	1124.5	163.1	1056.3	153.2	11.0	46.5
	1134.2	164.5	1061.1	153.9	12.9	52.3
	1110.06	161.0	1012.8	146.9	13.9	55.4
Mean:	1128	163.6	1051.5	152.5	12.5	52.4
Std Dev: (+/-)	11.72	1.7	22.06	3.2	1.2	3.5
Specification Requirements:						
		145.0 KSI	135.0 KSI		8.0	35.0
		999.74 MPa	930.79 MPa			

Material: Custom 450
Heat #: TAS
Test Temp: Room
HIP: 2165°F, (1185°C) 4 hrs, 25 KSI (172.4 MPa)
Heat Treatment: Per Lycoming Specification as follows:
Solution: 1904°F (1040°C), 1 hr, air cool to < 200°F (93°C), water quench to < 70°F (21°C).
Age: At a temperature up to 1058°F (570°C) max., 4 hrs, to achieve HRC 33-37.

TABLE 13. LOW-CYCLE FATIGUE RESULTS FOR FIRST-STAGE INTEGRALLY CAST ROTORS

Cycles to Failure:	11760
	16305
	23280
	97542
Mean Cycle Life:	16400
-3 Sigma Cycle Life:	6200

Material:	Custom 450
Heat #:	TAS
Test Temp:	500°F (260°C)
Strain Range:	0.006
Freq:	0.4 Hz
A Ratio:	1:1
Wave Form:	Sine
HIP:	2165°F (1185°C), 4 hrs, 25 KSI (172.4 MPa)
Heat Treatment:	Per Lycoming Specification as follows:
Solution:	1904°F (1040°C), 1 hr, air cool to < 200°F (93°C), water quench to < 70°F (21°C).
Age:	At a temp up to 1058°F (570°C) max, 4 hrs, to achieve HRC 33-37.

Mean cycle life was determined from a Weibull plot at the 50 percent confidence level; the -3 Sigma value was the 97 percent confidence life.

TABLE 14. TENSILE TEST RESULTS FOR SECOND-STAGE INTEGRALLY CAST ROTORS

Heat No.	UTS		2% YS		% ELONG	(%)RA
	(KSI)	(MPa)	(KSI)	(MPa)		
1485	169.4	1168.0	164.2	1132.1	4.8	13.6
	165.5	1141.1	162.3	1119.0	3.1	7.0
	168.9	1164.5	165.4	1140.4	5.2	13.6
	163.3	1125.9	161.9	1116.3	1.8	9.4
	170.6	1176.2	167.1	1152.1	6.4	19.4
	173.1	1193.5	170.0	1172.1	3.3	10.8
	170.7	1176.9	167.5	1154.9	4.1	12.9
	169.5	1168.7	168.4	1161.1	2.9	10.9
Mean:	168.9	1164.5	165.8	1143.3	4.0	12.2
Std Dev (+/-):	3.1	21.37	2.9	20.	1.5	3.7
1543	171.7	1183.8	167.2	1152.8	10.2	39.6
	173.7	1197.6	168.4	1116.1	12.2	51.3
	172.6	1190.0	168.4	1161.1	8.5	31.8
	172.0	1185.9	168.8	1163.8	4.1	15.7
	173.5	1196.2	168.9	1164.5	7.3	28.2
	173.5	1196.2	168.2	1159.7	10.3	41.9
	172.6	1190.0	164.9	1136.9	11.2	46.8
	172.4	1188.7	167.2	1152.8	8.0	27.5
Mean:	172.7	1190.7	167.7	1156.2	9.0	35.4
Std Dev (+/-)	1.0	6.89	1.3	8.96	2.6	11.7
Specification Requirements:						
	145.0	999.74	135.0	930.8	8.0	35.0

Material: Custom 450
Test Temp: Room
HIP: 2165°F (1185°C), 4 hrs, 15 KSI (103 MPa)
Heat Treatment: Per Lycoming specification as follows:
Solution: 1904°F (1040°C), 1 hr, air cool to < 200°F (93°C), water quench to < 70°F (21°C).
Age: At a temp up to 1058°F (570°C) max, 4 hrs, to achieve HRC 33-37.

TABLE 15. LOW-CYCLE FATIGUE RESULTS FOR SECOND STAGE INTEGRALLY CAST ROTORS

Heat No.	1485	1543
Cycles to Failure:	475	8792
	983	9295
	1103	9422
	1381	9549
	1391	10163
	1764	10780
	2193	10799
	2627	19012
Mean Cycle Life:	1080	9900
-3 Sigma Cycle Life:	355	8400

Material:	Custom 450
Test Temp:	500°F (260°C)
Strain Range:	0.006
Freq:	0.4 Hz
A Ratio:	1:1
Wave Form:	Sine
HIP:	(1185°C), 4 hrs, 15 KSI (103 MPa)
Heat Treatment:	Per Lycoming specification as follows:
Solution:	1904°F, (1040°C), 1 hr, air cool to < 200°F (93°C), water quench to < 70°F (21°C).
Age:	At a temp up to 1058°F (570°C) max, 4 hrs, to achieve HRC 33-37.

Mean cycle life was determined from a Weibull plot at the 50 percent confidence level; the -3 Sigma value was the 97 percent confidence life.

TABLE 16. HIGH-CYCLE FATIGUE RESULTS FOR SECOND-STAGE INTEGRALLY CAST ROTORS

Rotor S/N	Heat No.	No. of Airfoils Per Rotor Tested	Mean Fatigue Limit (+/-)		-3 Sigma Limit (+/-)	
			KSI	MPa	KSI	MPa
26	1485	9	61.0	420.6	42.3	291.6
21		9	73.8	508.3	52.8	364.0
17	1543	11	48.3	333.0	37.3	257.2
25		9	70.6	486.8	54.7	377.1

Frequency:	870-940Hz (function of blade natural frequency)
Material:	Custom 450
Test Temp:	Room
HIP:	2165°F (1185°C), 4 hrs, 15 KSI (103 MPa)
Heat Treatment:	Per Lycoming specification as follows:
Solution:	1904°F (1040°C), 1 hr, air cool to < 200°F (93°C), water quench to < 70°F (21°C).
Age:	At a temp up to 1058°F (570°C) max, 4 hrs, to achieve HRC 33-37.

All tests conducted by exciting airfoils with air. Tip deflections are controlled by regulation of air pressure. Tip deflection was related to the stress at failure locations by strain gaging techniques.

TABLE 17. TENSILE TEST RESULTS FOR FIFTH-STAGE INTEGRALLY CAST ROTORS
(Sheet 1 of 2)

Heat No.	HIP Temp	HIP Pressure	TENSILE RESULTS UTS (KSI)	UTS (MPa)	2% YS (KSI)	2% YS (MPa)	% ELONG	% RA
SZN	2050°F	15 KSI	157.9	1088.7	148.6	1024.6	13.8	64.1
	1121°C	103.4 MPa	155.6	1072.8	143.9	992.2	15.1	62.9
			155.9	1072.8	145.3	1001.8	15.5	60.4
			156.3	1074.9	145.0	999.7	14.6	63.7
			157.8	1088.	147.9	1019.7	12.8	60.2
			156.1	1076.3	145.3	1001.8	14.3	58.9
			156.3	1077.7	145.0	999.7	15.8	61.5
			156.4	1078.3	146.4	1009.4	19.5	54.1
			155.8	1074.2	143.9	992.2	19.5	54.1
			156.3	1077.7	143.2	987.3	20.4	58.5
			155.0	1068.7	143.2	987.3	20.1	56.7
			155.0	1068.7	142.9	985.3		
Mean:			156.2	1077.	145.0	999.7	16.5	60.2
Std Dev (+/-)			1.0	6.89	1.9	13.1	3.0	3.0
SZN	2165°F	25 KSI	156.5	1079.0	143.2	987.3	15.2	56.5
	1185°C	172.4 MPa	156.8	1081.0	145.0	999.7	15.8	58.5
			156.6	1079.7	145.4	1002.5	14.7	57.8
			158.0	1089.4	146.0	1006.6	16.7	58.5
			157.1	1083.2	146.0	1006.6	14.6	59.4
			158.3	1091.4	147.9	1019.7	13.2	54.4
			155.7	1073.5	143.9	992.2	13.1	54.6
			157.2	1083.9	147.8	1019.0	12.0	49.1
			156.7	1080.4	143.9	992.2	12.5	48.4
			155.9	1074.9	144.2	994.2	14.2	52.9
			158.1	1090.1	147.5	1017.	12.1	52.9
			155.7	1073.5	143.9	992.2	14.4	55.2
Mean:			156.9	1081.8	145.4	1002.5	14.0	54.8
Std Dev (+/-)			1.0	6.89	1.7	11.72	1.5	3.6
TAS	2165°F	25 KSI	161.9	1116.3	152.7	1052.8	14.2	53.7
	1185°C	172.4 MPa	162.0	1116.95	153.0	1054.9	13.9	53.2
			162.1	1117.6	153.7	1059.7	13.8	51.5
			161.8	1115.6	152.5	1051.5	16.4	59.5
Mean:			161.9	1116.3	153.0	1054.9	14.6	54.5
Std Dev (+/-)			0.2	1.38	0.5	3.45	1.2	3.5

TABLE 17. TENSILE TEST RESULTS FOR FIFTH-STAGE INTEGRALLY CAST ROTORS
(Sheet 2 of 2)

	HIP		TENSILE RESULTS					
Heat No.	Temp	Pres-sure	UTS (KSI)	UTS (MPa)	2% YS (KSI)	2% YS (MPa)	% ELONG	% RA
TWA	2165	25 KSI	160.3	1105.2	149.6	1031.5	13.9	55.9
		172.4 MPa	159.8	1101.8	146.4	1009.4	15.1	58.2
			159.3	1098.3	148.1	1021.1	14.8	57.0
			159.5	1099.7	147.4	1016.3	18.5	60.7
Mean:			159.7	1101.1	147.9	1019.7	15.6	58.0
Std Dev (+/-)			0.5	3.45	1.3	8.97	2.0	3.6
Specification Requirements:			145.0	999.7	135.0	930.8	8.0	35.0

Material: Custom 450
Test Temp: Room
HIP: At temperature and pressure indicated above for 4 hrs.
Heat Treatment: Per Lycoming specification as follows:
Solution: 1904°F (1040°C), 1 hr, air cool to < 200°F (93°C), water quench to < 70°F (21°C).
Age: At a temp up to 1058°F (570°C) max, 4 hrs, to achieve HRC 33-37.

TABLE 18. LOW-CYCLE FATIGUE RESULTS FOR FIFTH-STAGE INTEGRALLY CAST ROTORS

Heat No.	SZN	SZN	TAS	TWA
HIP Temp:	2050°F(1121°C)	2165°F(1185°C)	2165°F(1185°C)	2165°F(1185°C)
HIP Pres:	15 KSI 103.42 MPa	25 KSI 172.4 MPa	25 KSI 172.4 MPa	25 KSI 172.4 MPa
Cycles to Failure:	8792	11800	10305	17218
	10318	12031	10473	19425
	10758	13493	10653	25180
	14544	23030	10879	31607
Mean Cycle Life:	9900	12300	10400	20000
-3 Sigma Cycle Life:	7400	10100	10200	1190

Material:	Custom 450
Test Temp:	500°F (260°C)
Strain Range:	0.006
Freq:	0.4 Hz
A Ratio:	1:1
Wave Form:	Sine
HIP:	At temperature and pressure indicated above for 4 hrs.
Heat Treatment:	Per Lycoming specification as follows:
Solution:	1904°F (1040°C), 1 hr, air cool to < 200°F (93°C), water quench to < 70°F (21°C).
Age:	At a temp up to 1058°F (570°C) max, 4 hrs, to achieve HRC 33-37.

Mean cycle life was determined from a Weibull plot at the 50 percent confidence level; the -3 Sigma value was the 97 percent confidence life.

TABLE 19. HIGH-CYCLE FATIGUE RESUTS FOR FIFTH-STAGE INTEGRALLY CAST ROTORS

		HIP			Test Results			
Rotor S/N	Heat No.	Temp	Pres-sure	Airfoils Per Rotor Tested	Mean Fatigue Limit (+/-) KSI	MPa	-3 Sigma Limit (+/-) KSI	MPa
26*	SZN	2050°F	15 KSI	10	74.2	511.6	64.0	441.3
29		1121°C	103.42 MPa	11	78.6	541.9	65.2	449.5
30				10	72.8	501.9	64.3	443.3
24	SZN	2050°F	25 KSI	13	65.3	450.2	38.5	265.4
25*		1185°C	172.4 MPa	12	82.8	570.9	74.2	511.6
32				12	82.6	569.5	75.3	519.2
22	TAS	2165°F	25 KSI	12	87.3	601.9	70.9	488.8
35		1185°C	172.4 MPa	13	83.8	577.8	62.4	430.2
77	TWA	2165°F	25 KSI	16	75.0	517.1	49.7	342.7
79		1185°C	172.4 MPa	12	81.4	561.2	52.8	364.0

Frequency: 1020-1130HZ
Material: Custom 450
Test Temp: Room
HIP: At temperature and pressure indicated above for 4 hrs.
Heat Treatment: Per Lycoming specification as follows:
Solution: 1904°F (1040°C), 1 hr, air cool to < 200°F (93°C), water quench to < 70°F (21°C).
Age: At a temp up to 1058°F (570°C) max, 4 hrs, to achieve HRC 33-37.

* - S/N 25 and 26 were glass-bead peened (refer to para. 4.4.4 for details).

All tests conducted by exciting airfoils with air. Tip deflections are controlled by regulation of air pressure. Tip deflection was related to the stress at failure locations by strain gaging techniques.

TABLE 20. SUMMARY OF MECHANICAL PROPERTY DATA FOR HIP PARAMETER EVALUATION

A. Tensile Test

HIP		Mean Test Results					
Temp °F	Pressure	UTS (KSI)	MPa	2% YS (KSI)	MPa	% Elong	% RA
2050 (1121°C)	15 KSI (103 MPa)	156.2 +/- 1.0	1077. 6.89	145.0 1.9	999.7 13.1	16.5 3.0	60.2 3.0
2165 (1185°C)	25 KSI (172.4 MPa)	156.9 +/- 1.0	1081.8 6.89	145.4 1.7	1002.5 11.7	14.0 1.5	54.8 3.6

B. Low Cycle Fatigue

HIP		Cycles to Failure	
Temp °F	Pressure	Mean Life	-3 Sigma Life
2050(1121°C)	15 KSI (103 MPa)	9900	7400
2165(1185°C)	25 KSI (172.4 MPa)	12300 2), 3)	10100

C. High Cycle Fatigue

Rotor S/N	HIP Temp °F	HIP Pressure	Airfoils Per Rotor Tested	Test Results: Mean Fatigue Limit (+/-)		-3 Sigma Limit (+/-)	
26	2050°F	15 KSI	10	74.2 KSI	511.6 MPa	64.0 KSI	441.3 MPa
29	(1121°C)	(103 MPa)	11	78.6	541.9	65.2	449.5
20			10	72.8	501.9	64.3	443.3
25	2165°F	25 KSI	12	82.8	570.9	74.2	511.6
32	(1185°C)	(172.4 MPa)	12	82.6	569.5	75.3	519.2

Material: Custom 450 integrally cast fifth-stage rotors
Heat: SZN
Test Temp: Tensile - Room; LCF - 500°F (260°C); HCF - Room
HIP: At temperature and pressure indicated above for 4 hrs.
Heat Treatment: Per Lycoming specification as follows:
Solution: 1904°F (1040°C), 1 hr, air cool to < 200°F (93°C), water quench to < 70°F (21°C).
Age: At a temp up to 1058°F (570°C) max, 4 hrs, to achieve HRC 33-37.

1) LCF test parameters; refer to Table 18.
2) "Beehive"; see text.
3) S/N 24 HCF data not included due to anomalous surface finish; for data Refer to Table 19.

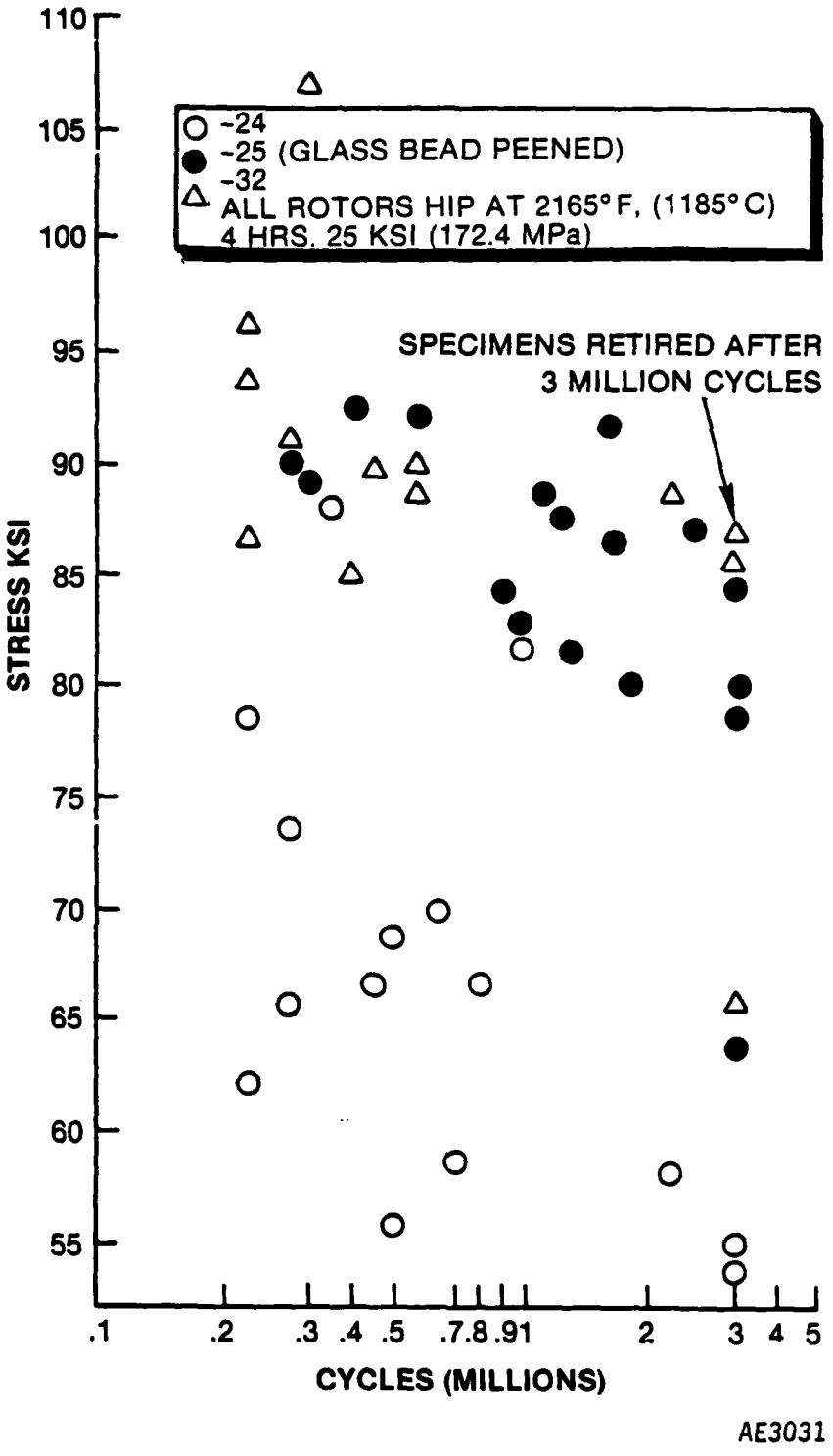

Figure 46. High-Cycle Fatigue Comparison of Fifth-Stage Wheels HIP'D at 2165°F (1185°C)

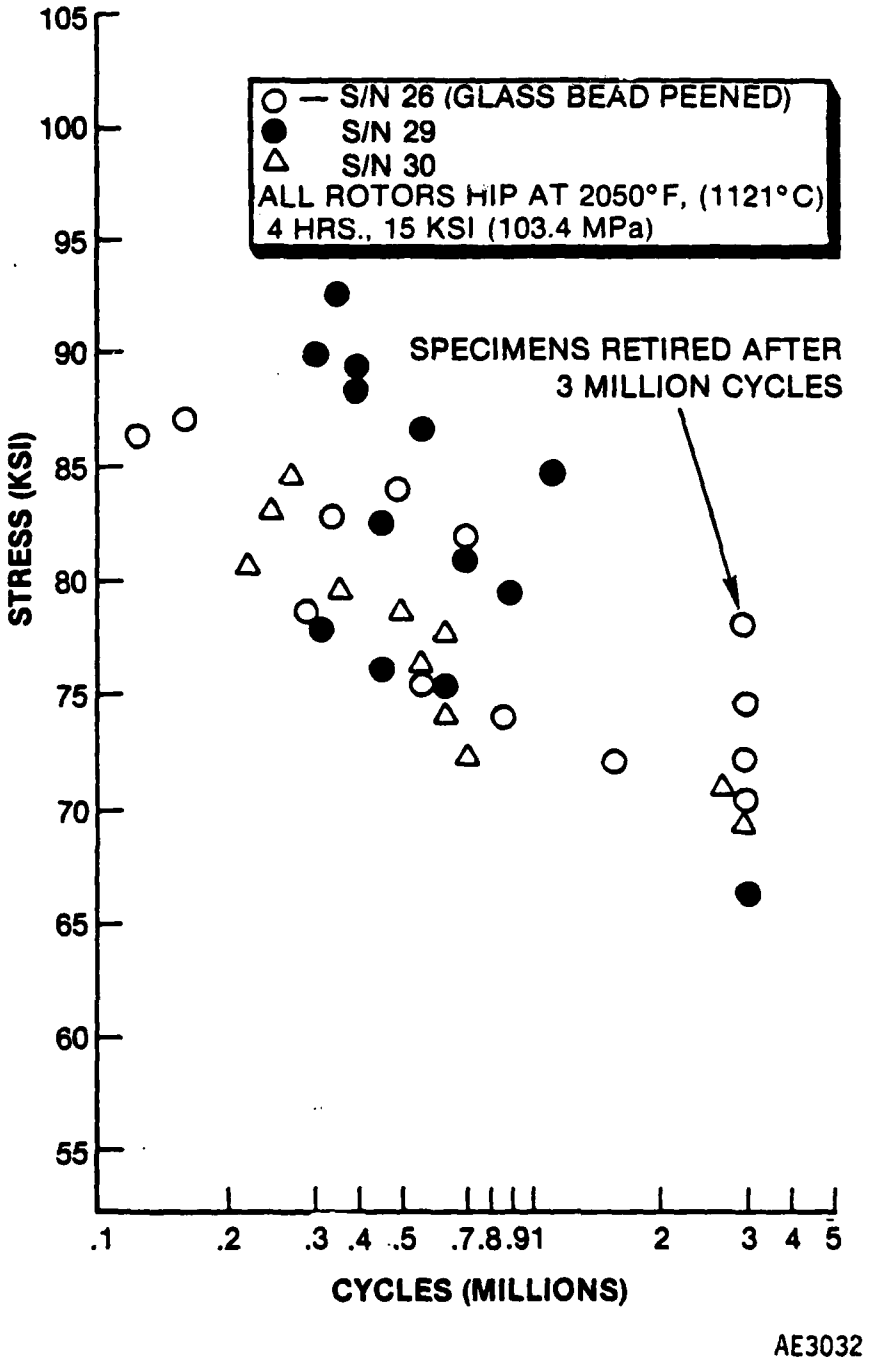

Figure 47. High-Cycle Fatigue Comparison of Fifth-Stage Wheels HIP'D a 2050°F (1121°C)

specimen had an aluminum-oxide inclusion at the fatigue origin (Figure 48). The remainder of the low S/N 24 results are believed to have been caused by rough as-cast surfaces which, although tested, would not have been acceptable for production hardware (Figure 49). The study of the S/N 32 fractures did not reveal any surface or metallurgical anomalies.

Excluding S/N 24 HCF data, the LCF and HCF properties of rotors HIP at 2165°F (1185°C) were better than those HIP'd at 2050°F (1121°C); this is probably due to the homogenization/solutionizing effects. Figure 50 compares the microstructure of test specimens HIP at these two temperatures. The specimen HIP'd at 2165°F (1185°C) has a more homogeneous structure.

4.4.2 Effects of Heat Chemistry

In order to evaluate the effects of alloy chemistry variations on the mechanical properties of integrally cast Custom 450 rotors, second- and fifth-stage rotors were cast in multiple heats. All rotors were HIP'd at 2165°F (1185°C) for 4 hours. The second-stage rotors were HIP'd at 15 KSI (103 MPa) because of the IMT, INC. (HIP vendor) equipment limitations. The fifth-stage rotors were HIP'd by Howmet Corp. at a pressure of 25 KSI (172.4 MPa). This difference in pressure is not considered to be a significant variable because of the very low strength of the Custom 450 alloy at the HIP temperature (i.e., either pressure is sufficient to deform the alloy and close internal voids).

Chemical analyses were performed for each heat of alloy used for casting rotors for the program. Table 21 lists the results of these heat analyses.

The effects of heat chemistry on the mechanical properties of cast Custom 450 rotors was initially evaluated using the second-stage rotors (heats 1485 and 1543). The test results listed in Table 22 indicated that heat 1485 (which had a higher than usual columbium content) had lower tensile ductility and poorer LCF life than did the rotors cast from heat 1543. In order to expand the study, fifth-stage rotors cast from multiple heats (SZN, TAS, and TWA) were evaluated in a similar manner (but in a separate evaluation not including second-stage rotors due to the configuration diffrences between the two stages). No significant mechanical property differences were observed among the fifth-stage rotors tested. (Refer to Table 22.)

From the results of this study, it appears that control of Custom 450 alloy columbium content may be important to optimize tensile ductility and LCF life. Metallographic and SEM fractography of several of the lower life (LCF) test specimens was conducted confirming the fact that a greater than normal amount and size of columbium carbides existed in the microstructure at the failure origins of many of the test specimens from heat 1485 (Figure 51).

Within the second-stage rotor group, the high columbium heat did not seem to have an adverse effect on airfoil HCF properties. Solidification is rapid in the airfoils, microconstituants are small, and no large columbium carbides were found. However, heat chemistry in general may have influenced the relatively low second-stage HCF properties.

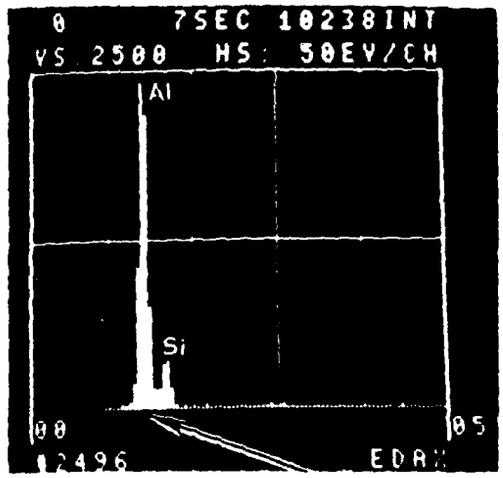

ALUMINUM OXIDE INCLUSION

FATIGUE ORIGIN

AIRFOIL SURFACE

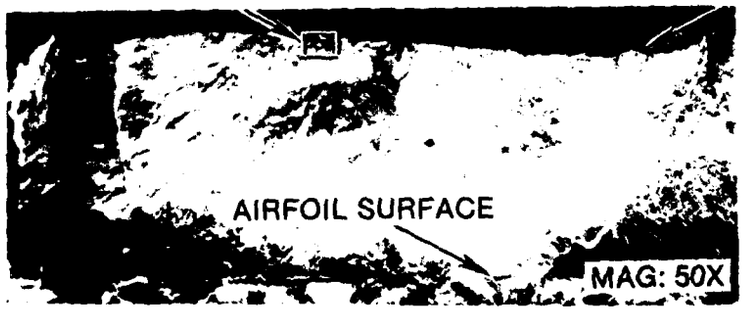

AE2091

Figure 48. SEM and EDAX Examination of a Fatigue Failure of an Airfoil from Rotor S/N 24

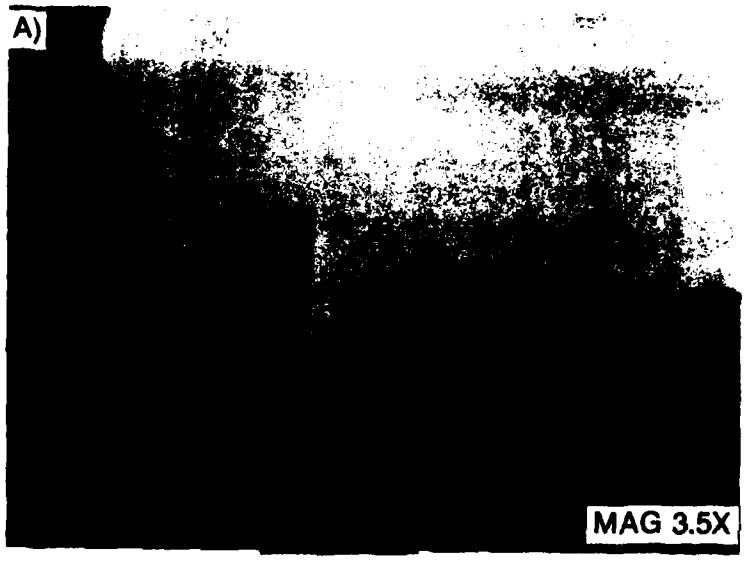

(a) S/N 24

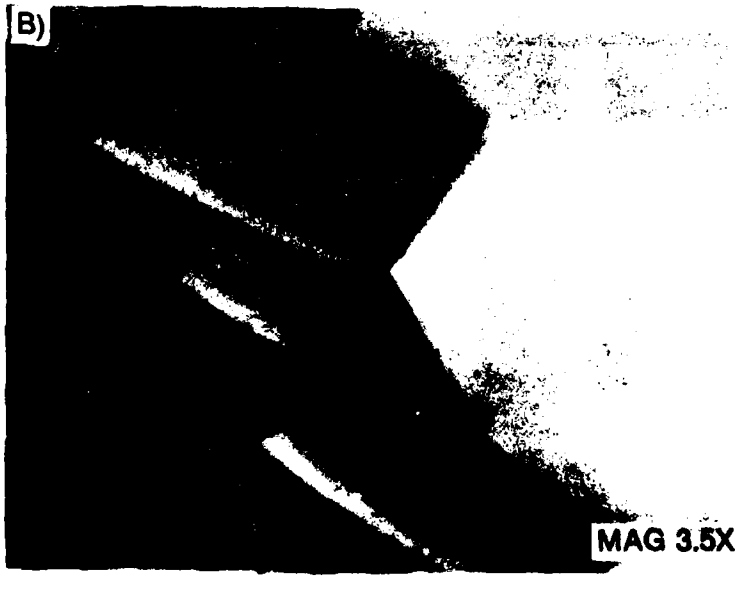

(b) S/N 32

AE2090

Figure 49. Surface Condition of Fifth-Stage Wheels S/N 24 and S/N 32

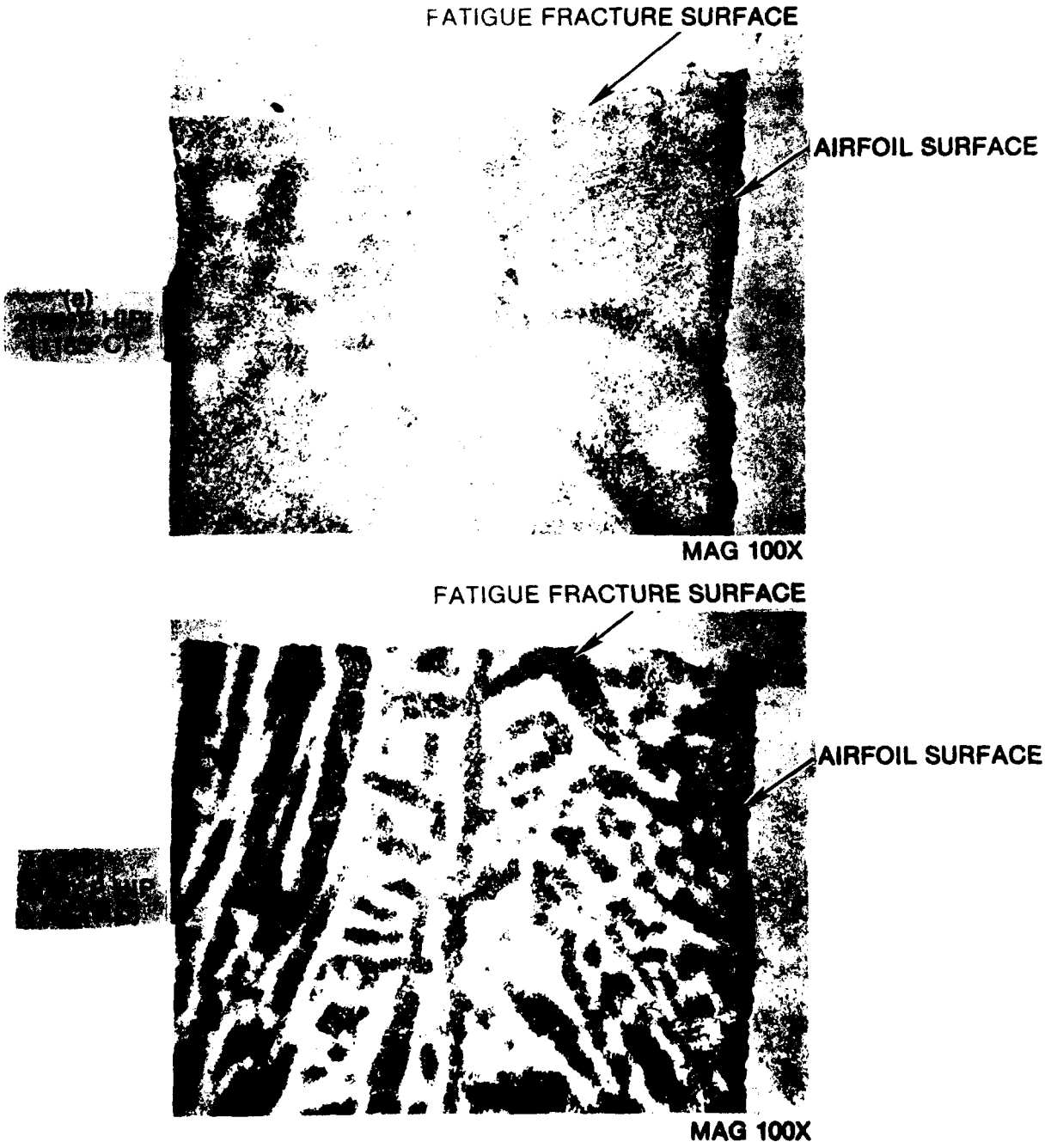

Figure 50. Microstructures of Rotors HIP'D at 2050°F (1121°C) and 2165°F (1185°C)

TABLE 21. CHEMICAL ANALYSIS OF CUSTOM 450 HEATS

Element	Specification Typical (%)	Heat No. 1485	1543	1711	SZN	TAS	TWA
Carbon	0.03	0.026	0.022	0.031	0.034	0.025	0.023
Manganese	0.10	0.30	0.28	0.22	0.30	0.30	0.32
Silicon	1.00 Max	0.34	0.36	0.47	0.40	0.34	1.0
Chromium	14.75	14.65	14.69	14.75	14.97	14.54	14.93
Nickel	6.50	6.64	6.38	6.48	6.58	6.51	6.60
Molybdenum	0.75	0.66	0.64	0.81	0.75	0.73	0.72
Copper	1.50	1.53	1.28	1.52	1.49	1.53	1.41
N2	2000 PPM Max	162	122	130	104	80	90
Columbium	8 x C +0.5 Min	0.76	0.60	0.42	0.65	0.70	0.67
Iron	Remainder						
Alloy Source:		(1)	(1)	(1)	(1)	(2)	(3)

(1) Carpenter Technology Corp., electric arc air melt/AOD (argon, oxygen decarburization.
(2) Howmet Corp., Dover Alloy Div., vacuum induction melt.
(3) Carpenter Technology Corp., electric arc air melt/AOD/electroslag remelt.

TABLE 22. SUMMARY OF MECHANICAL PROPERTY DATA FOR MULTIPLE HEAT EVALUATION (Sheet 1 of 2)

A. Tensile Test

Stage	Heat No.	Mean Test Results UTS (KSI)	UTS (MPa)	2% YRS (KSI)	2% YRS (MPa)	% Elong	% RA
2	1485	168.9	1164.5	165.8	1143.2	4.0	12.2
		+/- 3.1	21.37	2.9	20.	1.5	3.7
2	1543	172.7	1190.7	167.7	1156.2	9.0	35.4
		+/- 1.0	6.89	1.3	8.96	2.6	11.7
5	SZN	156.9	1081.8	145.4	1002.5	14.0	54.8
		+/- 1.0	6.89	1.7	11.72	1.5	3.6
5	TAS	161.9	1116.3	153.0	1054.9	14.6	54.5
		+/- 0.2	1.38	0.5	3.45	1.2	3.5
5	TWA	159.7	1101.1	147.9	1019.7	15.6	58.0
		+/- 0.5	3.45	1.3	8.96	2.0	3.6

B. Low Cycle Fatigue

Stage	Heat No.	Cycles to Failure Mean Life	-3 Sigma Life
2	1485	1080	355
2	1543	9900	8400
5	SZN	12300	10100
5	TAS	10400	10200
5	TWA	20000	11900

C. High Cycle Fatigue 2)

Stage	Heat No.	Rotor S/N	Airfoils Per Rotor Tested	Test Results Mean Fatigue Limit (+/-)		-3 Sigma Limit (+/-)	
2	1485	21	9	73.8 KSI	508.8 MPa	52.8 KSI	364.0 MPa
2		26	9	61.0	420.6	42.3	291.6
2	1543	17	11	48.3	333.0	37.3	257.2
2		25	9	70.6	486.8	54.7	377.1

TABLE 22. SUMMARY OF MECHANICAL PROPERTY DATA FOR MULTIPLE HEAT EVALUATION (Sheet 2 of 2)

Stage	Heat No.	Rotor S/N	Airfoils Per Rotor Tested	Test Results: Mean Fatigue Limit (+/-)		Test Results: -3 Sigma Limit (+/-)	
5	SZN	25	12	82.8 KSI	570.9 MPa	74.2 KSI	511.6 MPa
5		32	12	82.6	569.5	75.3	519.2
5	TAS	22	12	87.3	601.9	70.9	488.8
5		35	13	83.8	577.8	62.4	430.2
5	TWA	77	16	75.0	517.1	49.7	342.7
5		79	12	81.4	561.2	52.8	364.0

Material: Custom 450 integrally cast rotors
Test Temp: Tensile - 70°F; LCF - 500°F (260°C); HCF - 70°F
HIP: At 2165°F (1185°C) and at either 15 KSI (103 MPa) (second stage) or 25 KSI (172.4 mPa) (fifth stage), 4 hrs.
Heat Treatment: Per Lycoming specification as follows:
Solution: 1904°F (1040°C), 1 hr, air cool to 200°F (93°C), water quench to 70°F (21°C).
Age: At a temp up to 1058°F (570°C) max, 4 hrs, to achieve HRC 33-37.

1) LCF test parameters; refer to Tablex 15 and 18.

2) "Beehive"; see text.

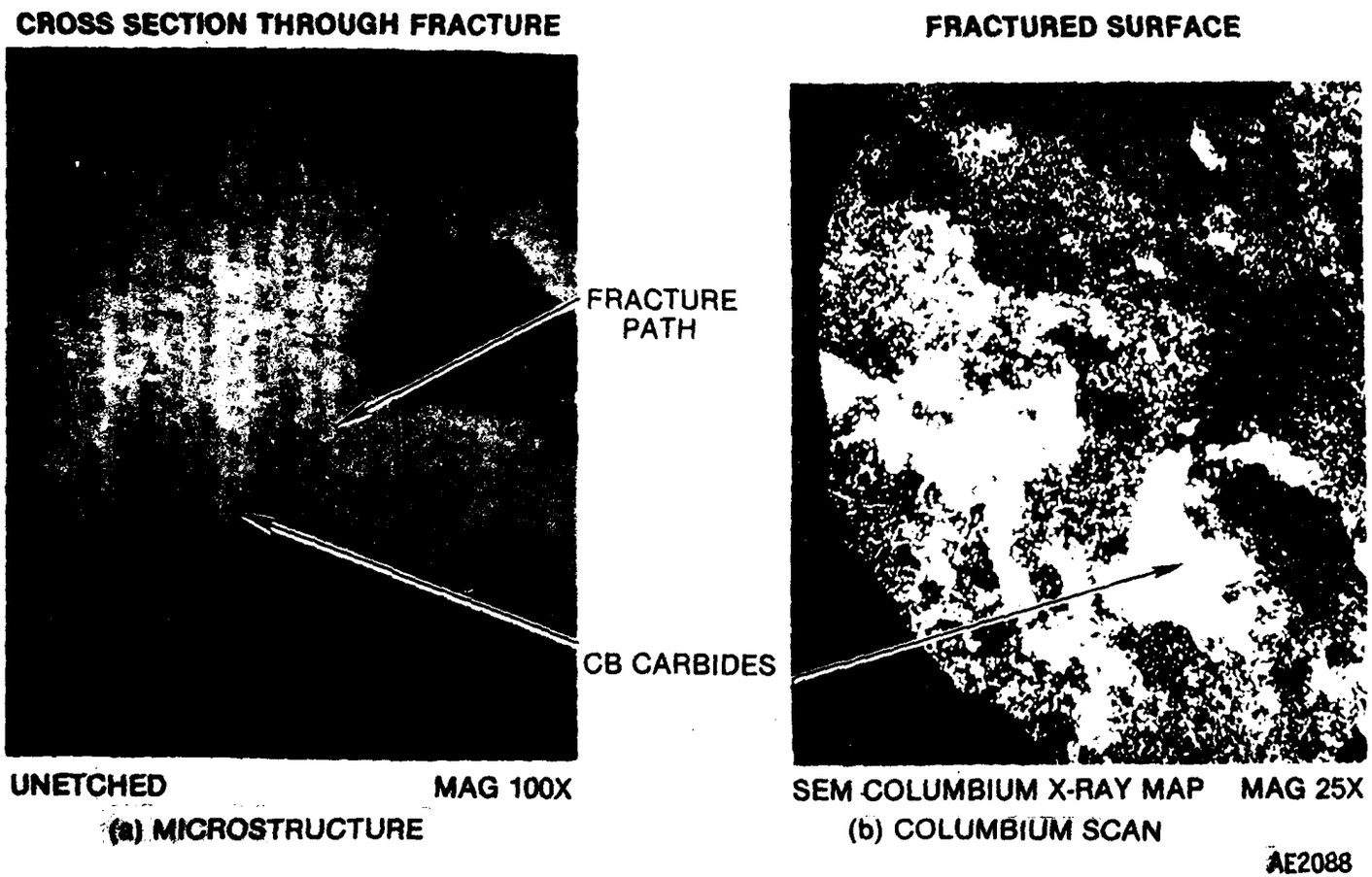

Figure 51. Microstructure and Columbium Scan of LCF Specimen From Heat 1485 Which Fractured After Only 1381 Cycles

4.4.3 Effects of Configuration

In order to evaluate the effects of rotor configuration (shape and size) on mechanical properties, test data from first and fifth-stage rotors Table 23 was evaluated. To eliminate heat chemistry influences, the first- and fifth-stage rotors for this comparison were produced from the same heat of master alloy (TAS), HIP'd at 2165°F (1185°C), and heat treated to equivalent hardness (HRC 34-35).

Usually, the mechanical properties of the heat-treatable stainless steels are relatively insensitive to casting size. This is primarily due to the extensive homogenization (during HIP at 2165°F, 4 hours) and the aged martensitic transformation which is a prime determinant of final casting properties. Theoretically, these factors should help minimize the effects of different solidification and cooling rates on the as-cast rotor microstructure. In fact, all rotors exhibited acceptable mechanical properties, and it was concluded that configuration did not have a significant influence on tensile properties.

However, there was some variation in LCF properties between the two stages. Although first-stage rotor data showed a higher mean LCF life than the fifth-stage, the high degree of scatter in first stage LCF test data also caused this stage to have a lower mean -3 Sigma life (Refer to Tables 13 and 18). The extraordinarily high life (97542 cycles) of one first-stage test specimen, coupled with the small sample size, distorts the standard deviation. Accordingly, it is felt that the differences between the two stages are not really significant.

The second-stage rotors were not included within the aforementioned comparison because they were produced from different heats. However, if one discounts the data from the high columbium heat (1485), the second-stage LCF properties are in the same range as the first and fifth stages. (Refer to Table 15).

Second-stage airfoil HCF properties are however, generally lower than those exhibited by the fifth-stage Table 22. In an attempt to understand this reduction, fractography and metallographic studies were performed on fatigued second and fifth-stage airfoils. This study determined that the second-stage fatigue origins were on the convex side of the airfoil near mid- chord. This location was predicted by the vibration analyses described in paragraph 4.1.3. Second-stage rotor S/N 26 was examined in detail; the airfoils
which exhibited the lowest fatigue life were found to have subsurface defects at the fracture origin. An example of such a defect is shown in Figure 52. This defect is probably a gas pore; the reason the defect was not healed by HIP is that it was surface-connected (possibly by a passage small enough to elude detection by penetrant inspection). The highest life airfoils from S/N 26 did not exhibit these defects and neither did airfoils from second-stage rotor S/N 25 (better HCF properties) or any fifth-stage airfoils; all these higher fatigue life airfoils had surface origins.

TABLE 23. SUMMARY OF MECHANICAL PROPERTY DATA FOR CONFIGURATION EVALUATION

A. Tensile Test

	Mean Test Results					
	UTS		2% YS		% Elong	% RA
Stage	(KSI)	(MPa)	(KSI)	(MPa)		
1	163.6	1128.	152.5	1051.5	12.5	52.4
	+/- 1.7	11.72	3.2	22.1	1.2	3.5
5	161.9	1116.3	153.0	1054.9	14.6	54.5
	+/- 0.2	1.38	0.5	3.45	1.2	3.5

B. Low Cycle Fatigue

	Cycles to Failure	
Stage	Mean Life	-3 Sigma Life
1	16400	6200
5	10400	10200

Material:	Custom 450 integrally cast rotors
Heat:	TAS
Test Temp:	Tensile - Room; LCF - 500°F (260°C); HCF - Room
HIP:	At 2165°F (1185°C), 25 KSI (172.4 mPa), 4 hrs.
Heat Treatment:	Per Lycoming specification as follows:
Solution:	1904°F (1040°C), 1 hr, air cool to < 200°F (93°C), water quench to < 70°F (21°C).
Age:	At a temp up to 1058°F (570°C) max, 4 hrs, to achiev. HRC 33-37.

1) LCF test parameters; refer to Tables 13 and 18.

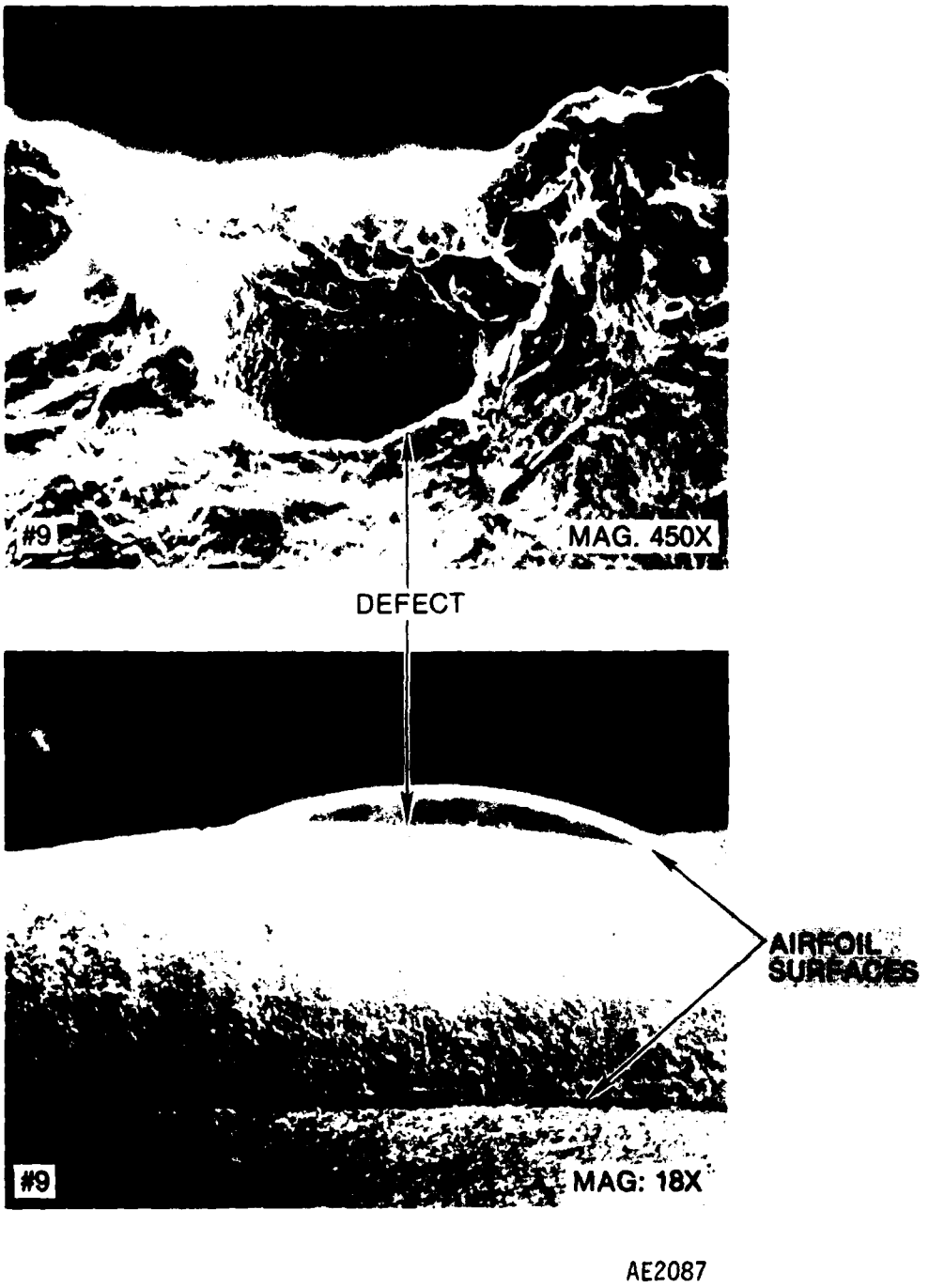

Figure 52. SEM Fractograph of Second-Stage Airfoil With Low HCF Fatigue Life Showing a Subsurface Defect

Another microstructural anomaly was observed on S/N 26 airfoils (Figure 53). This is known as "white layer" and is austenite which did not transform to martensite after solution anneal. "White layer" is not uncommon in many precipitation-hardening stainless steels. It is usually caused by carbon pickup from the atmosphere used to protect the casting during cooling after pouring. Since it is caused by diffusion into the surface, its presence is normally detectable by etching. Subsurface white layer is unusual. It is hypothesized that it was caused in the normal manner, but that carbon was removed during heat treatment, allowing the surface to transform to martensite. Other metallographic examinations did not reveal any white layer on first- and fifth-stage wheels. "White layer", being lower strength austenite, certainly is not beneficial to fatigue strength although its exact quantitative effect is not known. Obviously it must be eliminated along with the other subsurface defects. Additional second-stage casting efforts will be required to finetune the melting/heat treating practices used by the second-stage vendor (Aerocast, Inc.). However, the probability of success is high since none of the first- or fifth-stage rotors (cast by Howmet Corp.) exhibit such defects.

4.4.4 Effects of Glass Bead Peening

As reported above, poor surface condition was responsible for premature HCF failures in rotor S/N 24. In order to evaluate the effect of surface on HCF properties, two fifth-stage rotors (one from each HIP group) were glass-bead peened per AMS 2430H, using #13,0.0025 inch B glass shot (MIL-G-9954) at an intensity of 2.5N. All airfoils were covered 200 percent (i.e., complete cov- erage twice), and airfoil edges were masked to prevent edge rollover.

The results of the evaluation (Table 19) indicated that, in either HIP group, glass-bead peening of rotor airfoils did not seem to significantly improve rotor HCF properties, although a more consistent failure location was observed. (See Figure 54.) The lack of HCF improvement in the peened rotors may be due to the fact that only low peening intensities could be used on the ultra-thin fifth-stage airfoils. Higher peening intensities, which could be used on thicker airfoils, could produce more noticeable HCF improvements.

4.5 PHASE II PRODUCTION OF ENGINE-RUNABLE CASTINGS

Tooling and casting processes were adequately developed to produce dimensionally acceptable first- and second-stage rotors. "Engine runable" castings were produced for the first stage, and these castings are available for use in any follow-on component and engine qualification program. Second-stage castings were also produced, but metallurgical anomalies found late in the program cause concern regarding the fatigue capability of these wheels in the engine environment. Although these second-stage castings can be used for rig performance testing, further casting trials and metallurgical evaluations to refine the process should be accomplished prior to engine testing second-stage rotors. This could be accomplished early in any future follow-on program. As mentioned previously, the detailed redesign of the mating LP compressor components for the first- and second-stage rotors will also have to be incorporated into this future effort.

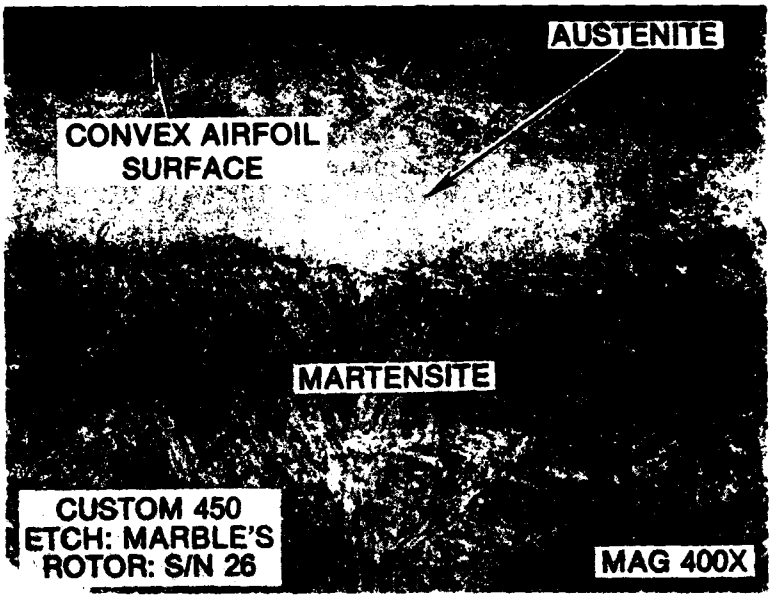

AE2086

Figure 53. Microstructure of Second-Stage Airfoil Exhibiting Subsurface "White Layer" (Untransformed Austenite) Near the Convex Surface

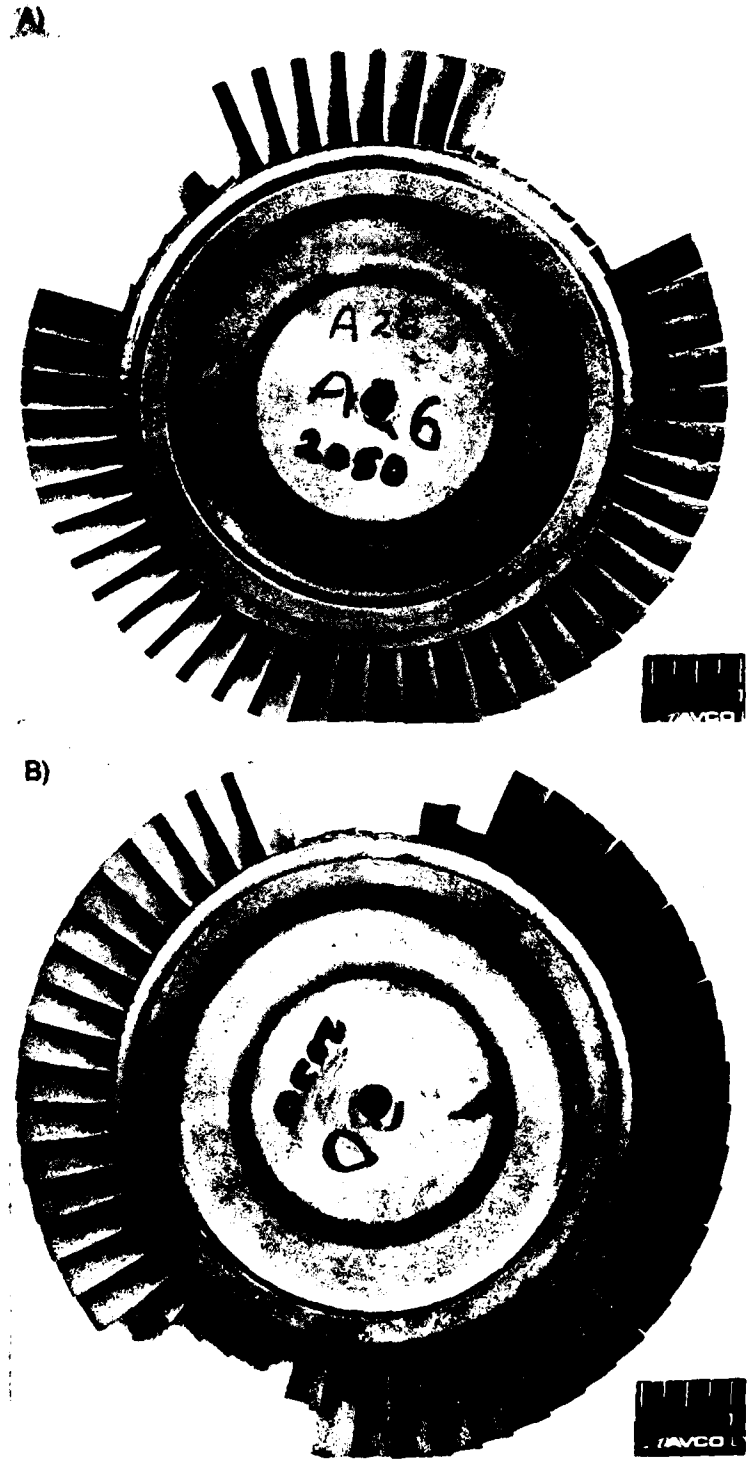

Figure 54. HCF Failure Location of Fifth-Stage Wheels: A) With Glass Bead Peened Surfaces and B) Without Peened Surfaces

Although no engine runable fifth-stage castings were produced for use within any follow-on effort, casting feasibility has at least been demonstrated. However, more rotors will have to be cast to determine if the process is viable from a production standpoint. The proposed follow-on TACOM, support cost reduction program ("SCORE", compressor improvement program) could incorporate fifth-stage rotor castings; however, investment casting tool rework will be required before engine runable castings could be produced.

APPENDIX A. OPERATION OF THE SPECIAL AIRFOIL GAGING AND *CORRECTING FIXTURES*

Special gaging fixtures for the second and the fifth stage rotors were designed and constructed for the in-situ inspection and correction of airfoils (Figure A-1). The gaging checked the airfoils for B/P deviations with respect to contour, blade-to-blade spacing, tangent angle, and tangential and axial lean.

Operation of the special gaging fixtures were essentially the same for both the second and the fifth stage rotors, and as follows:

1. The casting is placed into the gage fixture with the chuck open (Figure A-2).

2. The casting is rotated until it contacts the base section contour detail at the proper airfoil section (Figure A-3).

Figure A-6. Axial Lean Inspection

3. The three jaw chuck is then pneumatically closed and proper positioning of the No. 1 airfoil is secured. This insures the proper timing of each airfoil for subsequent processing steps. The part is now ready for inspection.

4. The tip section contour slide (Figure A-4) is moved into its inspection position (Figure A-5) and an adjustable thumb screw with a dial indicator determines the blade tangential lean. The blade tangent angle and contour are also checked. This process is repeated for the mid-section of the airfoil using a second contour slide.

5. If a dimension is found to be out of tolerance, a mechanical adjustment to the airfoil is made at that point.

6. After this check is completed, the base section contour slide is withdrawn and a second airfoil is indexed using the splined gear wheel (the initial set-up of the No. 1 airfoil establishes the "timing" of the airfoil positions with respect to the gear teeth.

7. The base section slide is again positioned for this new airfoil, and the above steps repeated.

8. After the required mechanical adjustments have been made, and all of the airfoils have been inspected for position, tangent angle, contour, and tangential lean, the blades are then inspected for axial lean. This is accomplished with the base section contour slide retracted. Each airfoil is rotated past an axial lean pin whose dial indicator registers the axial lean of each airfoil (Figure A-6). If a mechanical adjustment is required on any of the individual airfoils at that point, that airfoil then has to be completely re-inspected for orientation (steps 1-7 above).

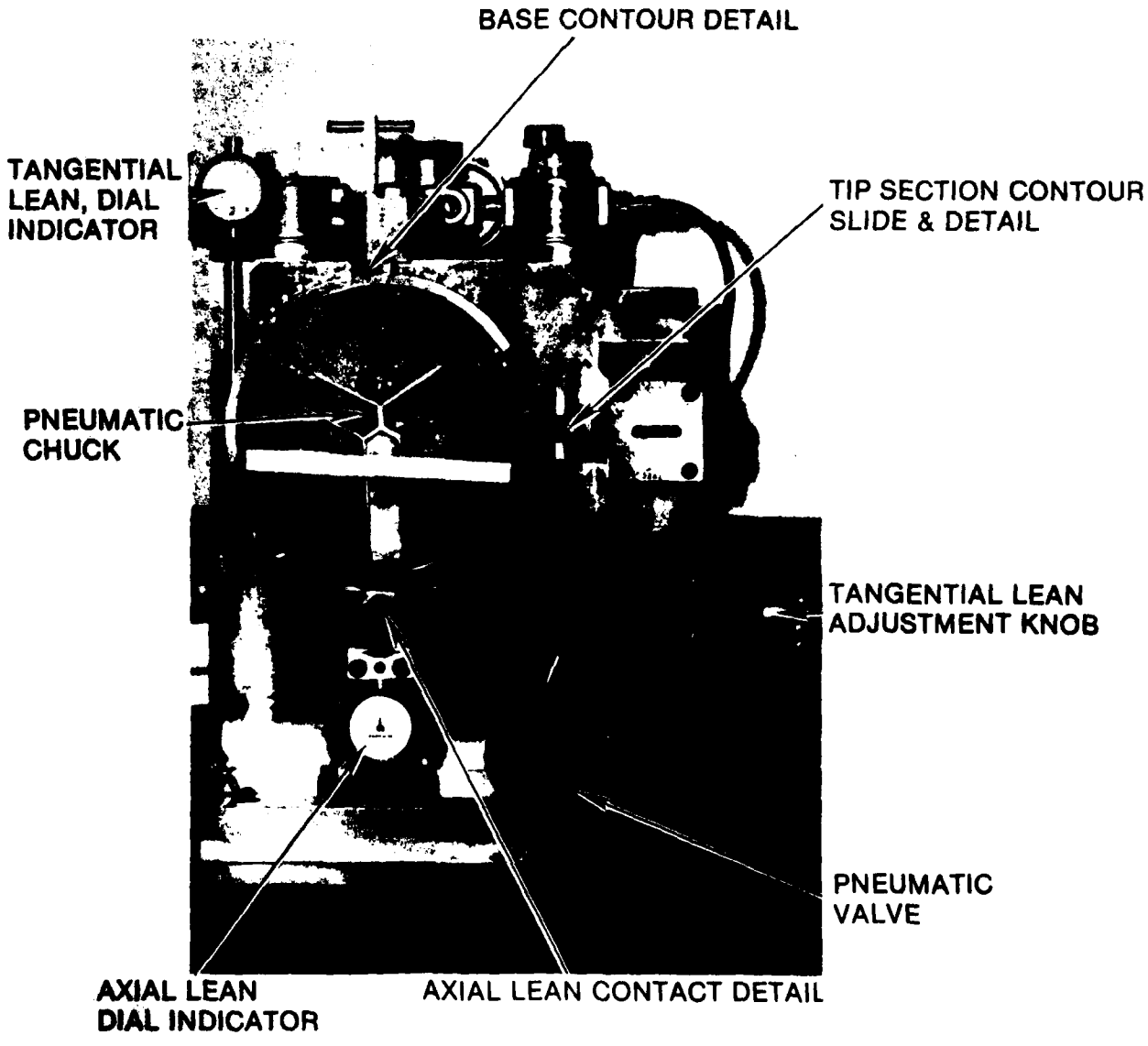

Figure A-1. Fifth-Stage Blade Angle Contour Gage (Ready for Rotor Positioning)

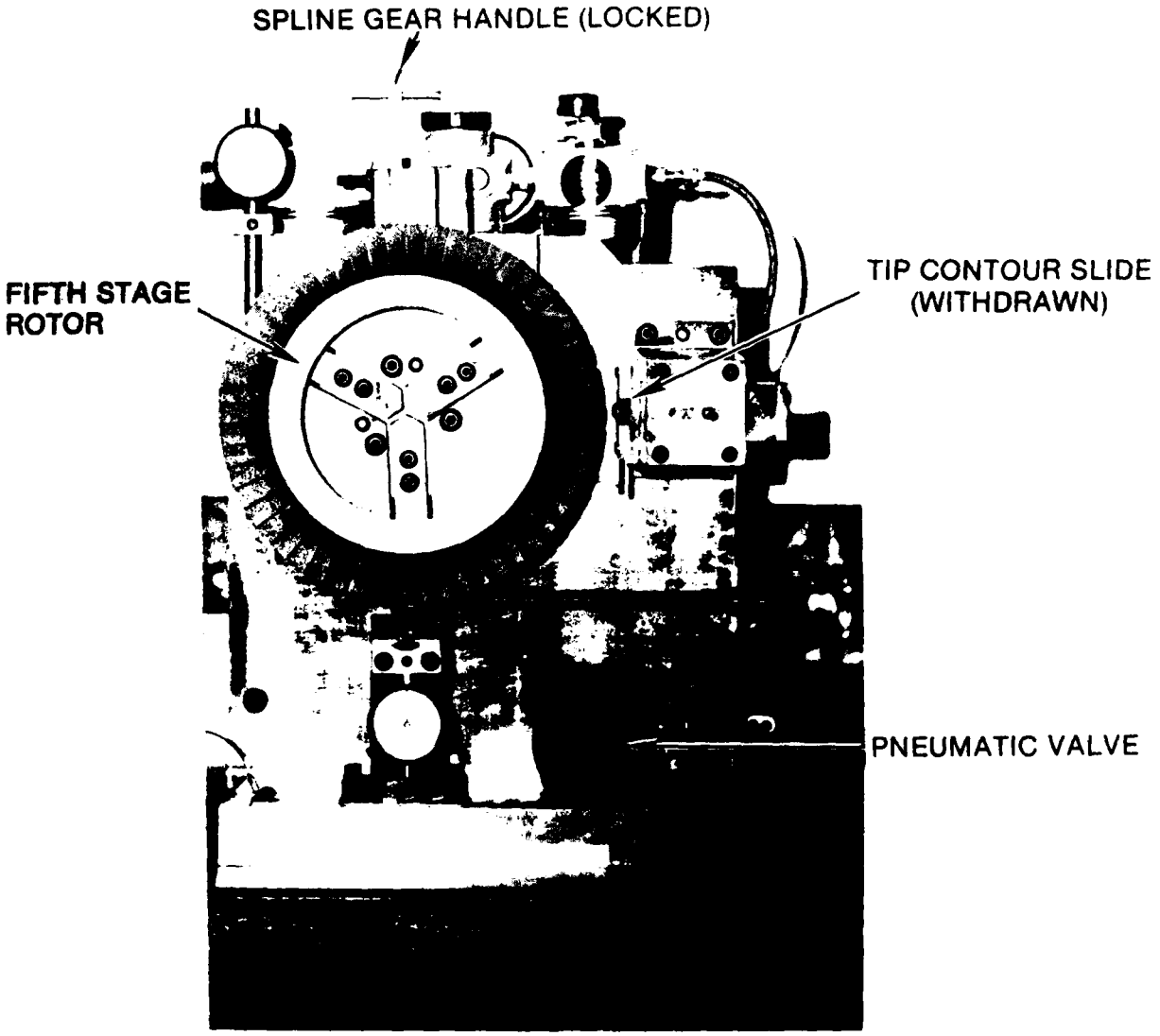

Figure A-2. Rotor Placed Into Gage

Figure A-3. Rotor Positioned

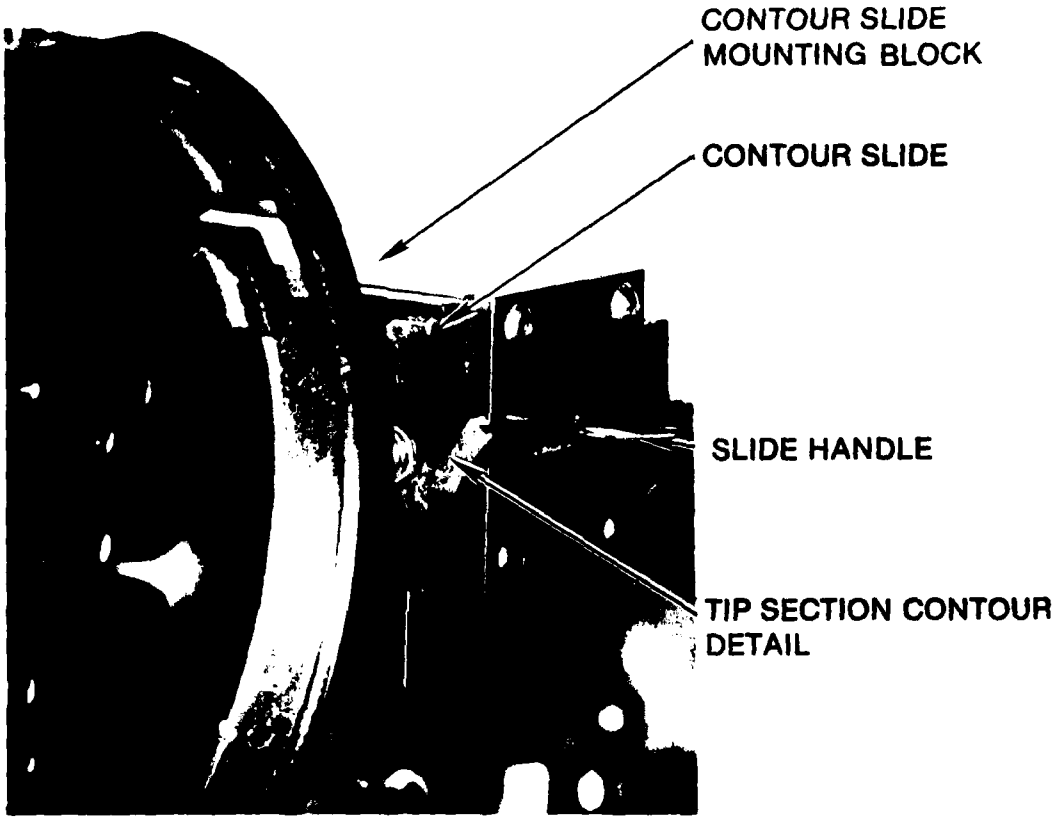

Figure A-4. Tip Section Contour Slide and Detail

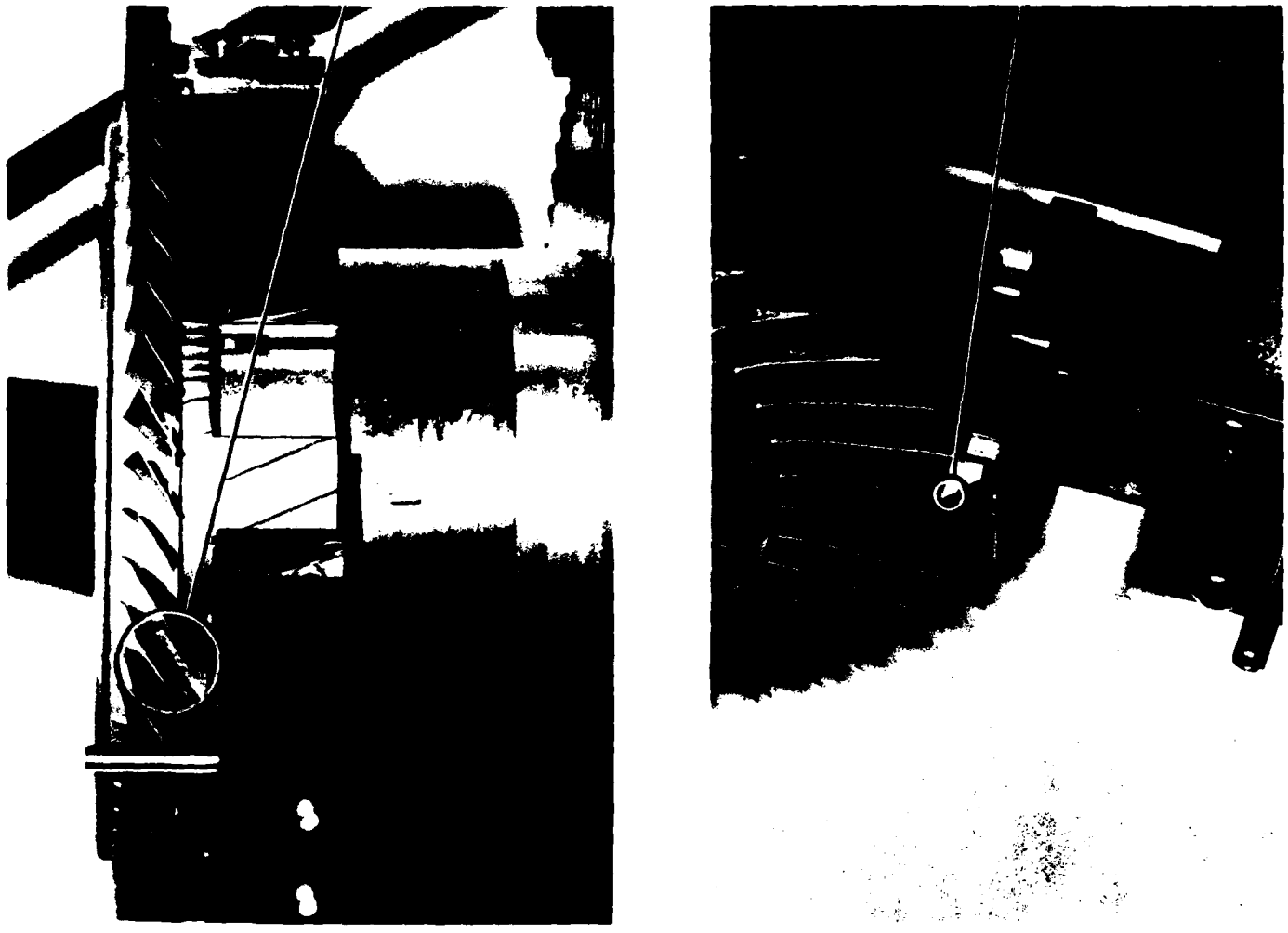

Figure A-5. Tangential Lean, Blade Contour, and Tangent Angle Inspection of Fifth-Stage Rotor

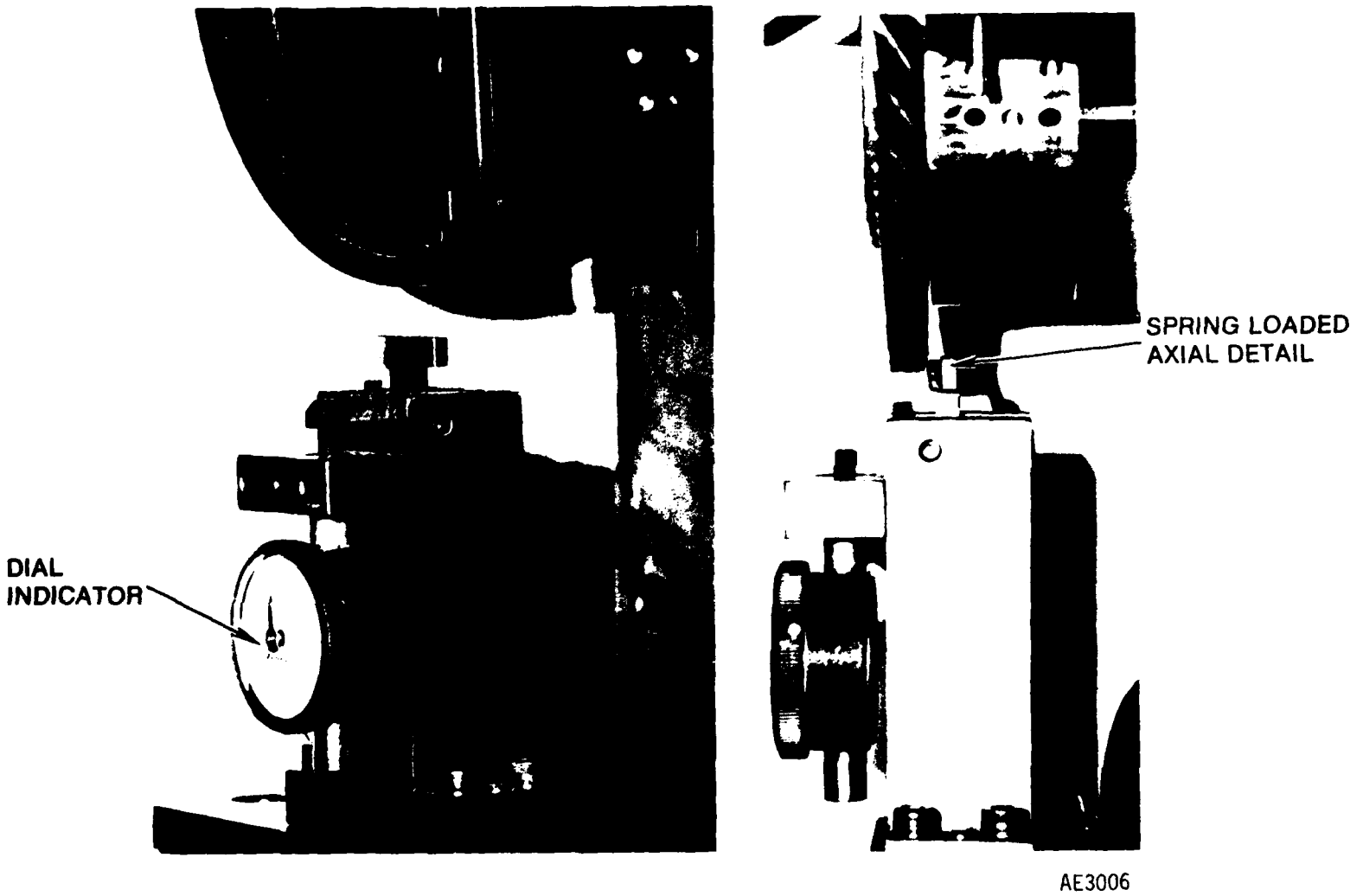

Figure A-6. Axial Lean Inspection

E

D

FI

5